# Physicochemical Characterization of Immortal Strand DNA

by

Janice A. Lansita

B.A., Biochemistry
Barnard College, Columbia University, 1997

SUBMITTED TO THE BIOLOGICAL ENGINEERING DIVISION IN PARTIAL FULFILLMENT OF THE REQUIREMENTS FOR THE DEGREE OF

DOCTOR OF PHILOSOPHY
AT THE
MASSACHUSETTS INSTITUTE OF TECHNOLOGY

JUNE 2004



Signature of Author:_____
Biological Engineering Division
May 20, 2004

Certified by:_____
James L. Sherley
Associate Professor of Biological Engineering
Thesis Supervisor

Accepted by:_____
Alan J. Grodzinksy
Professor of Electrical, Mechanical, and Biological Engineering

# Physicochemical Characterization of Immortal Strand DNA

by

Janice A. Lansita

B.A., Biochemistry
Barnard College, Columbia University, 1997

SUBMITTED TO THE BIOLOGICAL ENGINEERING DIVISION IN PARTIAL FULFILLMENT OF THE REQUIREMENTS FOR THE DEGREE OF

DOCTOR OF PHILOSOPHY
AT THE
MASSACHUSETTS INSTITUTE OF TECHNOLOGY

JUNE 2004



Signature of Committee Chair:_____

Peter C. Dedon
Professor of Toxicology and Biological Engineering

Signatures of Committee Members:

_____

Terry Orr-Weaver
Professor of Biology

_____

William G. Thilly
Professor of Biological Engineering

_____

Steven R. Tannenbaum
Professor of Biological Engineering, Chemistry, and Toxicology

## Table of Contents

## Table of Contents (continued)

**Abstract:**

Adult tissue differentiation involves the generation of distinct cell types from adult stem cells (ASCs). Current understanding of tissue differentiation mechanisms is based on studies of protein and RNAs that asymmetrically segregate between daughter cells during embryogenesis. Whether or not other types of biomolecules segregate asymmetrically has not been widely studied. In 1975, John Cairns proposed that ASCs preferentially segregate the oldest parental template DNA strands to themselves and pass on newly replicated DNA strands to their differentiating progeny in order to protect the stem cell from inheriting DNA replication mutations.

This laboratory has shown non-random chromosome segregation in murine fetal fibroblasts that model asymmetric self-renewal like ASCs. In these cells, chromosomes that contain the oldest DNA strands co-segregate to the cycling daughter stem-like cells, while chromosomes with more recently replicated DNA segregate to the non-stem cell daughters. Previously, cytological methods were reported to elucidate non-random segregation in these cells. This dissertation research provides additional confirmation of the mechanism using physicochemical methods. Specifically, buoyant density-shift experiments in equilibrium CsCl density gradients were used to detect co-segregated "immortal DNA strands" based on incorporation of the thymidine base analogue bromodeoxyuridine. In addition, DNA from cells undergoing non-random mitotic chromosome segregation was analyzed for unique DNA base modifications and global structural modifications (by HPLC and melting temperature analyses). To date, these studies show no significant differences compared to control randomly segregated DNA.

Components of the mitotic chromosome separation apparatus that might play a role in the co-segregation mechanism were also evaluated. Two homologous proteins, essential for proper chromosome segregation and cytokinesis, Aurora A kinase and Aurora B kinase, were highly reduced in expression in cells retaining immortal DNA strands and may indicate a role for them in the immortal strand mechanism.

These studies independently confirm the immortal strand mechanism and provide methods for its detection in other cell lines. In addition, observed changes in chromosome segregation proteins that are potential candidates for involvement in the mechanism have revealed a new area of investigation in the laboratory. These findings are relevant to understanding normal tissue development, cancer, and aging.

## Introduction

Adult stem cells divide asymmetrically into two daughter cells with different division capacities: one daughter divides to produce mature differentiated cells, and the other daughter maintains the division capacity of the parent without differentiation. This pattern is known as asymmetric cell kinetics. In 1975, John Cairns hypothesized that adult stem cells divide with a DNA segregation pattern distinct from differentiating cells. Cairns' theory is known as the immortal strand hypothesis and postulates that adult stem cells segregate replicated DNA and retain parental template DNA in order to minimize retention of unrepaired replication errors (which can lead to mutations). Prior to this time, Cairns' hypothesis could not be tested directly. However, this laboratory developed cell lines regulated to divide with the asymmetric cell kinetics of adult tissue stem cells. The asymmetric cell kinetics properties of these cells enable us to investigate the immortal strand hypothesis *in vitro*. Studies in the lab demonstrate an "immortal strand" mechanism does in fact function in laboratory cells that divide with asymmetric cell kinetics. This thesis aims to independently confirm the existence of an immortal strand mechanism in cultured cells, develop new methods for its detection in other cultured cell types, and investigate its molecular basis. These studies have important implications in stem cell biology.

### Historical Perspective and Biological Significance

The immortal strand hypothesis, first proposed in 1975 by John Cairns, described a unique mechanism by which adult stem cells divide to permanently retain an "old" parental DNA template strand for all chromosomes. This mechanism allows an adult

stem cell to eliminate the accumulation of mutations from replication errors and protects its ability to replenish the stem cell compartment with mutation free clonal descendants. Cairns argued that humans undergo $10^{16}$ cell divisions over a life time with an estimated spontaneous mutation rate of $10^{-6}$ per gene per cell division. This high mutation rate predicts that the prevalence of cancers should be greater than the observed rate (Cairns, 2002). The discrepancy in expected cancer prevalence versus observed prevalence led Cairns to hypothesize that adult stem cells have a protective mechanism to ensure their genetic integrity over numerous cell divisions with a high DNA replication error rate (Cairns, 1975; Cairns, 2002).

Protecting stem cells from detrimental mutations is critical because stem cells have the responsibility to self-renew and replenish the stem cell niche. The idea of cancers arising from mutated stem cells has existed for over 40 years but has rapidly regained interest in the last 5 years (reviewed by Reya et al., 2001; Cairns, 2002; Presnell et al., 2002; Potten and Booth, 2002; Pardal et al., 2003; Smalley et al., 2003). Tumors are made of cells that are both differentiated and that have the ability to renew themselves, much like stem cells. Mutations that accumulate in long-lived stem cells would be at risk for initiating tumors. Stem cells make up a small population of each organ (0.1 to 0.001%), and therefore constitute a low risk for tumor formation (Cairns, 1975). However, if a mutagenic lesion did occur in a stem cell and this stem cell produced new mutant stem cell, as well as early progenitors and differentiated progeny, a cancer or tumor could arise. A mutation occurring in a differentiating cell would not remain in the tissue for long, as newly made differentiated cells would replace it (Potten and Booth, 2002; Presnell et al., 2002). Cairns' hypothesis for selective retention of immortal DNA strands provides a way for an adult stem cell to protect itself from

mutations due to replication errors over many generations and pass on mutations to differentiated progeny that are eliminated before tumor formation.

If immortal DNA strands are retained by a stem cell over a long life span and many cellular divisions, these strands may accumulate mutations from endogenous sources of damage such as oxidative damage (Cairns, 2002). Over time, tissues are known to accumulate oxidative damage (Hamilton et al., 2001) and their proliferative capability decreases (Lesher et al., 1961; Rubin, 1997; Rubin, 2002). If stem cells are not subject to the same DNA repair pathways as other cells and their main anti-cancer protective mechanism is to retain immortal DNA strands, perhaps the immortal strand mechanism loses its integrity in old age when stem cells have accumulated DNA damage in immortal DNA strands and can no longer replenish a mutation-free stem cell niche. Because stem cells are susceptible to mutations over time, Cairns' hypothesis becomes important in understanding how stem cells protect themselves from mutations. Elucidation of the mechanism of immortal DNA strand retention could provide a clue to how aging occurs.

Cairns proposed that the mechanism for immortal strand co-segregation was a uniform marking of the chromosomes for selection or cell division along a specific division plane so that a complete set of immortal strand containing chromosomes is inherited with each division. A molecular tag may exist on the DNA that allows for their selection during chromosome segregation. Cairns hypothesized that a tag to the centromeres must be present and that this identification must be uniform to all retained immortal DNA strands. The centromere is a complex structure in which special histone proteins (e.g., CENP-A) bind specifically to distinguish it from the rest of the chromosome (Shelby et al., 2000). It is possible that the centromeric DNA or

specialized proteins exist specifically on immortal DNA strands to distinguish them from non-immortal DNA strands. A modification to the centromere could either take place on the centromeric DNA itself or the kinetochore proteins which associate with the centromeric (Shelby et al., 2000; Cleveland et al., 2003) DNA after DNA replication is completed (Ahmad and Henikoff, 2001). Kinetochore proteins directly attach to the plus-ends of microtubules, sense bipolar spindle attachment, and participate in a cell cycle checkpoint to ensure correct chromosome segregation (Cleveland et al., 2003). The properties of these proteins make them potentially appealing mechanistic players for immortal strand co-segregation.

In addition, Cairns argued that an adult stem cell must undergo mitosis with all chromosomes positioned correctly along the cell division plane so that the stem cell will always inherit the older parental template strands. Cell division planes are biologically important in generating cellular diversity in an organism. For many organisms, such as *Drosophila melanogaster* and *C. elegans*, spindle pole assemblies are asymmetric in microtubule length or are oriented in a way to asymmetrically segregate proteins involved in cell fate determination. (Kaltschmidt et al., 2000; Kaltschmidt and Brand, 2002). In a recent report, Drosophila male germline stem cells were found to localize Adenomatous Polyposis Coli tumor suppressor protein to position mitotic spindles perpendicularly to the stem cell in order to give rise to a new stem cell. The new stem cell retained the same orientation as the parent stem cell, but the differentiated daughter cell was in a position removed from the stem cell niche (Yamashita et al., 2003). It is possible that *in vivo*, immortal DNA strands are selected using a predetermined cell division axis as well as a molecular tag on the DNA for specific

retention of immortal DNA strands. This idea would provide a mechanistic explanation for how an entire set of chromosomes is non-randomly inherited.

Several researchers attempted to demonstrate the presence of immortal strands in different systems. Non-random segregation of chromosomes was suggested by analyzing cells that retained 3H-thymidine, or bromodeoxyuridine in their DNA. Lark et al., 1966 and 1967, performed the first compelling studies suggesting non-random chromosome segregation of label retaining of cells. Studies supporting the immortal strand hypothesis were performed in various models such as primary cultures of mouse embryo fibroblasts (Lark et al., 1966), plant root tip cells (Lark et al., 1967), mouse intestinal crypt cells, and tongue papillae (Potten et al., 1978). Label-retaining cells in the basal keritinocytes of mice were observed after a chase of 15-90 days and were thought to be slowly cycling stem cells (Bickenback et al., 1986). One study in mouse epidermal basal cells that were labeled with 3H-thymidine for one cell cycle and then chased for 50 days, failed to support the immortal strand hypothesis (Kuroki et al., 1989). Thought not definitive, the label retaining cells observed in these studies provide evidence that support the immortal strand hypothesis because they could in fact represent cells non-randomly retaining immortal DNA strands over long times.

Most recently, a report by Potten et al., 2002, provided evidence for the immortal strand hypothesis in juvenile mouse intestinal crypt cells as well as regenerating crypt cells. Juvenile mice were given 3H-thymidine from 11-21 days post-natum or 21-37 days post-natum, in order to label stem cells in the gut. At week 12 they were treated with BrdU from 40 minutes to 8 days and the number of label retaining cells was quantified. Using this double-labeling strategy, parental template strands are labeled with 3H-thymidine and newly replicated DNA strands are labeled with BrdU. If stem cells

located in the Paneth cell region retain 3H-thymidine label after 11 weeks of cycling in the absence of label, and no BrdU after 2 generations post- BrdU labeling, the data would suggest that stem cells preferentially retain immortal DNA strands. The results do in fact support this hypothesis. The label retaining cells were observed at a frequency of 11.1% ±1.7 % at 8 days after the initial BrdU labeling. BrdU positive cells were observed at 2.8% ± 2.8 %. After 8 days post-BrdU label, the cells containing 3H-thymidine label were not co-labeled with BrdU. All of the BrdU label was cleared from the 3H-thymidine label retaining cells within 2 days, which is what is expected if 3H-labeled immortal DNA strands are retained and newly replicated BrdU labeled strands are segregated to non-stem cell daughter cells.

The same double-labeling experiment was performed when intestinal crypt cells were treated with gamma-irradiation. There is evidence that adult stem cells are more sensitive to irradiation than other cell types and that exposure to gamma-irradiation induces the symmetric renewal of stem cells (Potten et al., 1978). Treatment of mice with 8 Gy gamma-irradiation, induced increased divisions in the intestinal crypt. 3H-thymidine was then given to the mice 6-48 hours post-irradiation with the goal of labeling immortal strands. Mice were given BrdU at 8 days post-irradiation to label all newly replicated DNA strands. Label retaining cells were quantified at 40 minutes and out to 10 days after BrdU labeling. It was observed that after 10 days post-BrdU label, 16.7 % of the cells retained 3H-thymidine label. No BrdU positive cells were found. The presence of label retaining cells found in both the juvenile mouse labeling experiment and the post-irradiation experiment in the gut, provide evidence for immortal DNA strand retention *in vivo*.

The results of these studies provide strong evidence for the immortal strand hypothesis, but have several shortcomings. The population of cells examined in these experiments contain not only stem cells, but also differentiated cells and early progenitor cells, making the data difficult to interpret. Some or all of the observed label retaining cells could be cells arrested in the cell cycle due to radiation toxicity or differentiation. Since the 3H and BrdU content were not quantified, replicative S-phase DNA synthesis was not confirmed for all cells. Cells that were arrested and retaining label would contain 3H-thymidine but no BrdU; these cells would appear to be label-retaining stem cells although they may actually be cells that incorporated the label early on in the experiment and exited the cell cycle because of a toxic response.

In earlier *in vivo* studies by other researchers testing the immortal strand hypothesis, the cell populations were mixed, with a very small population of stem cells and a much larger population of differentiated cells. Therefore, it is possible that non-random segregation of DNA strands was not observed because of a low frequency of the immortal strands amongst newly replicated DNA strands. Our clonally derived cell lines with inducible stem cell kinetics, give us a system that can be manipulated to test the immortal strand hypothesis.

There are several advantages to using these model cells. The cells behave like adult stem cells with self-renewal kinetics by giving rise to a cycling stem-like cell and a non-dividing cell. In this system, the stem -like cells can be identified. Stem cells in tissues are difficult to identify, and must be identified using markers or by studying their differentiation properties. The cells can also be labeled with BrdU and their DNA structure analyzed to show S-phase replication. Lastly, immortal DNA strands can be labeled directly in these cells. In tissues, labeling immortal DNA strands specifically is

difficult unless cells are labeled at the time stem cells are created or are cycling symmetrically to generate two new stem cells.

The laboratory demonstrated the immortal strand mechanism *in vitro* in murine embryonic fibroblasts and mammary epithelial cells with adult stem cell asymmetric kinetics (Merok et al., 2002). These cells can be induced to divide either symmetrically or asymmetrically like adult stem cells. Several different methods in the lab have demonstrated asymmetric cell kinetics for these cells, among them time lapse microscopy (Sherley, 1991; Sherley et al., 1995; Rambhatla et al., 2001; Merok and Sherley, 2001). The main cells used for the studies were derived from p53-null primary murine embryo-fibroblasts, stably transfected with a wild-type p53 gene under the control of an inducible methallothionein promoter. Upon the addition of $ZnCl_2$ to the cell culture medium, the cells divide asymmetrically to produce a new cycling daughter cell and a non-cycling daughter. The ability of these cells to give rise to two daughters with different division fates (i.e., one daughter with the same division capacity as the parent stem-like cell and the other, without) is a model of adult stem cell asymmetric self-renewal. Because the cycling cell fraction of asymmetrically cycling cultures is about 30% of the total culture at 36 hours of induction of asymmetric cell kinetics (Panchalingam, K. and Noh, M., personal communication), the immortal strand mechanism is easier to investigate in our model cell system and occurs at a detectable frequency than would be observed *in vivo*. Also, a constant exposure to both radiation and BrdU is unnecessary for labeling immortal DNA strands in this model cell line, thus eliminating a potential confounding factor of toxicity.

My thesis work focuses on the molecular and biochemical factors characterizing immortal strand DNA. This dissertation research provides additional confirmation of

the mechanism using physicochemical methods. Specifically, buoyant density-shift experiments in equilibrium CsCl density gradients were used to detect co-segregated "immortal DNA strands" based on incorporation of the thymidine base analogue bromodeoxyuridine. In addition, DNA from cells undergoing non-random mitotic chromosome segregation was analyzed for unique DNA base modifications and global structural modifications. Components of the mitotic chromosome separation apparatus that might play a role in the co-segregation mechanism were also evaluated.

These studies independently confirm the immortal strand mechanism and provide methods for its detection in other cell lines. This dissertation research may provide new insights towards understanding an important mechanism relevant to stem cell biology, cancer, biomedicine, and aging. Elucidation of the immortal strand mechanism may also yield potential protein markers for the adult stem cell and may shed light on mechanisms distinguishing differentiated cells from pluri- or multi- potent stem cells.

**References:**


Ahmad K, Henikoff S, *Centromeres are specialized replication domains in heterochromatin.* J Cell Biol, 2001. **153**:p. 101-10.

Bickenbach, J.R., McCutecheon, J., Mackenzie, I.C., *Rate of Loss of Tritiated Thymidine Label in Basal Cells in Mouse Epithelial Tissues.* Cell Tissue Kinet., 1986. **19**: p. 325-333.

Cairns, J., *Mutation Selection and the Natural History of Cancer.* Nature, 1975. **255**: p. 197-200.

Cairns J., *Somatic stem cells and the kinetics of mutagenesis and carcinogenesis.* Proc Natl Acad Sci U S A, 2002. **99**:p.10567-70.

Cleveland DW, Mao Y, Sullivan KF, *Centromeres and kinetochores: from epigenetics to mitotic checkpoint signaling.* Cell, 2003. 112:p. 407-21. Review.

Hamilton ML, Van Remmen H, Drake JA, Yang H, Guo ZM, Kewitt K, Walter CA, Richardson A, *Does oxidative damage to DNA increase with age?* Proc Natl Acad Sci USA, 2001. **98**:p. 10469-74.

Henikoff S, Ahmad K, Malik HS. *The centromere paradox: stable inheritance with rapidly evolving DNA.* Science, 2001. **293**:p. 1098-102. Review.

Kaltschmidt JA, Davidson CM, Brown NH, Brand AH, Rotation and asymmetry of the mitotic spindle direct asymmetric cell division in the developing central nervous system. Nat Cell Biol. 2000. 2:p. 7-12.

Kaltschmidt JA, Brand AH, Asymmetric cell division: microtubule dynamics and spindle asymmetry. J Cell Sci., 2002. 115:p. 2257-64. Review.

Kuroki, T., Murakami, Y., *Random Segregation of DNA Strands in Epidermal Basal Cells.* Jpn. J. Cancer Res., 1989. **80**: p. 637-642.

Lark, K.G., Consigli, R.A., Minocha, H.C., *Segregation of Sister Chromatids in Mammalian Cells.* Science, 1966. **154**:p. 1202-05.

Lark, K.G., *Nonrandom Segregation of Sister Chromatids in Vicia Faba and Triticum Boeoticum.* PNAS, 1967. **58**: p. 352-359.

Lesher S, Fry RJ, Kohn HI, *Age and the generation time of the mouse duodenal epithelial cell.* Exp Cell Res, 1961. **24**:p. 334-43.

Liu, Y., Riley, L.B., Bohn S.A., Boice, J.A., Stadler, P.B., Sherley, J.L., *Comparison of Bax, Waf1, IMP Dehydrogenase Regulation in Response to Wild-type p53 Expression Under Normal Growth Conditions.* J. Cellular Physiology, 1998. **177**: p. 364-376.

Merok, J.R., Sherley, J.L., *Breaching the kinetic barrier to in vitro somatic stem cell propagation.* J. Biomedicine and Biotechnology, 2001. **1**: p. 25-27.

Merok, JR, Lansita, JA, Tunstead, JR, Sherley, JL, *Cosegregation of Chromosomes Containing Immortal DNA Strands in Cells that Cycle with Asymmetric Stem Cell Kinetics.* Cancer Res., 2002. **62**: p. 6791-6795.

Pardal R, Clarke MF, Morrison SJ, *Applying the principles of stem-cell biology to cancer.* Nat Rev Cancer, 2003. **3**:p. 895-902. Review.

Potten, C.S., Hume, W.J., Reid, P., Cairns, J., *The Segregation of DNA in Epithelial Stem Cells.* Cell, 1978. **15**: p. 899-906.

Potten CS, Owen G, Booth D, *Intestinal stem cells protect their genome by selective segregation of template DNA strands.* J Cell Sci, 2002. **115**: p. 2381-8.

Potten, CS, and Booth, C, *Keratinocyte stem cells: a commentary.* J Invest Dermatol. 2002. **119**:p. 888-99. Review.

Presnell SC, Petersen B, Heidaran M, *Stem cells in adult tissues.* Semin Cell Dev Biol., 2002 . **13**: p. 369-76. Review.

Rambhatla, L., Bohn, S.A., Stadler, P.B., Boyd, J.T., Coss, R.A., Sherley, J.L., *Cellular Senescence: ex vivo p53-dependent asymmetric cell kinetics.* J. Biomedicine and Biotechnology, 2001. **1**: p. 28-37.

Reya T, Morrison SJ, Clarke MF, Weissman IL, *Stem cells, cancer, and cancer stem cells.* Nature, 2001. **414**:p. 105-11. Review.

Rubin, H., *Cell aging in vivo and in vitro.* Mech Ageing Dev., 1997. **98**:p. 1-35. Review.

Rubin, H., *The disparity between human cell senescence in vitro and lifelong replication in vivo.* Nat Biotechnol., 2002. **20**:p. 675-81. Review.

Shelby RD, Monier K, Sullivan KF, *Chromatin assembly at kinetochores is uncoupled from DNA replication.* J Cell Biol, 2000. **151**:p. 1113-8.

Sherley, J., *Guanine nucleotide biosynthesis is regulated by the cellular p53 concentration.* J. Biol. Chem., 1991. **266**: p. 24815-24828.

Sherley, J.L., Stadler, P.B., Johnson, D.R., *Expression of wild-type p53 antioncogene induces guanine nucleotide-dependent stem cell division kinetics.* PNAS, 1995. **92**: p. 136-140.

Smalley M, Ashworth A, *Stem cells and breast cancer: A field in transit.* Nat Rev Cancer, 2003. **3**:p. 832-44. Review.

Yamashita YM, Jones DL, Fuller MT, *Orientation of asymmetric stem cell division by the APC tumor suppressor and centrosome.* Science, 2003. **301**:p. 1547-50.

## Chapter 1: Confirmation of Asymmetric Cell Kinetics and Demonstration of Semi-Conservative DNA Replication in Cells that Cycle with Asymmetric Cell Kinetics using CsCl Density gradients

**Rationale:**

CsCl density gradients have commonly been used to purify DNA from proteins, RNA, and other cellular components. In CsCl density gradients, after equilibrium centrifugation at high gravitational force, DNA was separated from other macromolecules based on its buoyant density. This method was effective for demonstrating semi-conservative DNA replication using the method of Meselson and Stahl (1958).

The CsCl gradient density shift method allowed for the study of DNA replication and BrdU retention in asymmetrically cycling cells. Semi-conservative DNA replication was demonstrated using CsCl density gradients by analyzing DNA from cells cycling asymmetrically and comparing it with DNA from cells cycling symmetrically. Using the method of Meselson and Stahl (1958), cells growing asymmetrically in the presence of BrdU incorporated the BrdU label into newly replicated DNA strands, distinguishing them from unlabeled parental template DNA strands. Double-stranded DNA with newly replicated BrdU-containing DNA strands could then be separated from DNA containing non-immortal unlabeled strands using CsCl density gradients. After ultracentrifugation of DNAs to their equilibrium buoyant density, DNA that was hemi-substituted with BrdU (i.e., one strand fully labeled with BrdU) was found at a position corresponding to an increase in buoyant density by 0.05 g/cm$^3$ (Luk and Bick, 1968). This density shift

was sufficient to completely separate unlabeled (1.70 g/cm$^3$), from hemi- (1.75 g/cm$^3$), and fully substituted (1.79 g/cm$^3$) DNA.

The major goal of this work was to use CsCl density gradients to independently confirm the existence of immortal DNA strands in asymmetrically cycling cells and define their physicochemical properties. First, it was important to determine whether or not cells cycling with asymmetric cell kinetics replicate their DNA semi-conservatively, so that immortal DNA strands could be identified on CsCl density gradients. If cells retaining immortal DNA strands replicated their DNA semi-conservatively, immortal DNA strands would be found in the HL peak after one round of replication in the presence of BrdU. Unlabeled immortal DNA strands would be paired with newly replicated DNA strands fully substituted with BrdU to create HL DNA. If cells did not replicate their DNA semi-conservatively and instead underwent conservative DNA replication, HL DNA would not be made in asymmetrically cycling cells. The immortal strand would be paired with an unsubstituted DNA strand and immortal DNA strands would be contained in the LL DNA peak on CsCl density gradients, not the HL peak as expected if semi-conservative DNA replication took place. Understanding the way in which asymmetrically cycling cells replicate their DNA, was essential for the interpretation of all future immortal DNA strand experiments.

In the process of demonstrating semi-conservative DNA replication, it became clear that CsCl gradient analyses also independently validated asymmetric cell kinetics as previously observed using time-lapse microscopy and growth curve analyses (Sherley, 1991; Sherley, et al., 1995; Rambhatla, et al., 2001).

## Experimental Method

## Cell Culture and BrdU Labeling

Murine embryo fibroblast cell lines with a spontaneous null p53 mutation transfected with wild-type p53 under the control of a metallothionein promotor have been described (Sherley, 1991; Sherley, et al., 1995; Rambhatla, et al., 2001). Upon the induction of p53 expression using $ZnCl_2$, the cells divided asymmetrically (designated Ind-8). The control cells (designated Con-3) were derived with an empty vector containing the metallothionein promotor. The control cells do not express p53 and divide symmetrically in the presence or absence of $ZnCl_2$ (Sherley *et al.*, 1991, Sherley *et al.*, 1995, Rambhatla *et al.*, 2001). To examine DNA replication in cells cycling with asymmetric cell kinetics, cells were plated at $2x10^4$ cells/75 $cm^2$/15 mls of culture medium. Twenty-four hours after plating, the cells were induced to divide asymmetrically in 75μM $ZnCl_2$ as described previously (Sherley *et al.*, 1991, Sherley *et al.*, 1995, Rambhatla *et al.*, 2001). $ZnCl_2$ was supplied by Sigma Aldrich (St. Louis, MO). Twenty-four hours after the induction of asymmetric cell kinetics, a 15-μl aliquot of 20mM BrdU (supplied by Sigma Aldrich) stock solution was added to each flask to make a final BrdU concentration of 20 μM BrdU. Thereafter, the cells were cultured continuously in BrdU for supplemented media for 24, 48, 72, and 96 hours. Cells were harvested by trypsinization with EDTA. Cells were washed with ice cold PBS at each time point, and cell pellets were made by centrifuging cells at 1500 rpm (500 x *g*) for 5 minutes.

## DNA Extraction

DNA was extracted by lysing $0.5 \times 10^6$ - $1 \times 10^6$ cells in 0.5 mls of a hypotonic lysis buffer containing 100mM NaCl, 10mM Tris pH 8.0, 1mM EDTA, and 1% SDS. Five μl of

a 20 mg/ml stock solution of proteinase K was added to a final concentration of 200 μg/ml. The cell lysate was incubated for 3 hours at 50 °C and extracted with an equal volume of 1:1 phenol:$CHCl_3$ equilibrated with 10mM Tris pH 8.0. The supernatant containing DNA was transferred to a new tube and extracted with an equal volume of $CHCl_3$. The supernatant was then treated with DNAse free RNAase A supplied by Sigma-Aldrich (final concentration = 100 μg/ml) for one hour. The RNAse A-treated sample was extracted two times more with phenol:$CHCl_3$ and once more with chloroform. Two volumes of ice cold ethanol and 1/10 the aqueous volume of 0.5M sodium acetate was added to the final sample to precipitate the DNA. Samples were held overnight at -20°C and then spun in a microcentrifuge at 13,200 rpm (16,110 x *g*) for 30 minutes at 4°C. The ethanol was poured off and 1 ml of 70% ethanol was added to wash the pellet. The sample was spun for 15 minutes at 13,200 rpm (16,110 x *g)* at4°C. The air-dried DNA pellets were dissolved in TE, pH 8.0 (typical volume range = 50-100 μl).

**CsCl Gradient Fractionation**

The DNA concentration of each sample was determined using a UV spectrophotometer (Pharmacia LKB Ultrospec Plus Spectraphotometer) or using Picogreen™ dye (supplied by Molecular Probes), which emits UV fluorescence upon binding to DNA and has picogram sensitivity. The manufacturer's protocol was used to determine DNA concentrations by Picogreen™. Beckman Opti-Seal™ ultracentrifugation tubes were filled with 8.9 mls of a filtered solution of CsCl dissolved in TE pH 8.0 (260 g CsCl in 200ml TE). Solutions with a refractive index (RI) = 1.4015 were used (Milton Roy Co. Refractometer). Ten micrograms of DNA was loaded onto

each gradient. An additional volume of TE pH 8.0 was added to bring the total loading volume to 100 µl. Samples were sealed using the Beckman Opti-Seal System™.

$^{3}$H-thymidine labeled control DNA (0.1 µg; approximately 200,000 cpm) was included as an internal standard for each sample to control for peak position and gradient quality. The $^{3}$H-thymidine DNA internal standard was prepared by plating symmetrically cycling control cells at 2X10$^{4}$ cells/75 cm$^{2}$/15 mls. After 24 hours of culture, 0.3 mls of 1 mCi/ml $^{3}$H-thymidine, specific activity = 72 Ci/mmol (supplied by ICN Biomedicals, Inc., Irvine, CA), was added to the culture to make a final labeling concentration of 20 µCi/ml. The cells were grown in $^{3}$H-thymidine for 24 hours, trypsinized, and their DNA extracted as described above. A concentration of $^{3}$H-thymidine labeled DNA was determined to load approximately 2X10$^{5}$ cpm/0.1 -0.2 µg/gradient of internal standard DNA per gradient.

Gradients were centrifuged for 20 hours at 40,000 rpm (110,000x g), T = 25°C using a Beckman Ti70.1 rotor and a Beckman L8-70M ultracentrifuge. After centrifugation to equilibrium, the gradients were dripped using a 21-gauge needle punctured through the bottom of the tube. Dripping was done immediately after centrifugation. The vacuum seal on the tube was broken using another 21-gauge needle punctured at the top of the tube. Three drops per fraction were collected, 140 ul-160 ul each, into a 96 well, 0.5 ml volume/well, microplate. Approximately 62-64 fractions were collected per gradient. Seals provided specifically for the microplate were used to prevent evaporation of the fractions.

Each gradient fraction was evaluated for DNA content, refractive index, and 3H cpm. DNA content was measured in duplicate assays using Picogreen® as described previously. The density of each fraction was estimated by refractometry. The R.I.

reading was converted to density using the following formula: $\rho^{25C} = 10.8601x - 13.4974$, x = refractive index (n D, the optical density), ρ= density (g/cm$^3$) (Meselson, *et al.*, 1957, Schildkraut, et al, 1962). 3H counts were measured by taking a 5µl aliquot from each fraction adding 5mls of EcoScint (National Diagnostics, Atlanta, GA) scintillation fluid and determining counts per minute (cpm) using a Beckman LS 1801scintillation counter set to determine the average cpm for 5 minutes (count error < 10%) .

**Results and Discussion:**

DNA molecules substituted with distinct amounts of BrdU can be fully separated and resolved by buoyant density. The mean density of unsubstituted DNA, light-light (LL) DNA was 1.700 ± 0.009 g/cm$^3$ (n=4) ; the density of hemi-labeled, heavy-light (HL) DNA was 1.746 ± 0.004 g/cm$^3$ (n=8) ; the density of fully labeled DNA, heavy-heavy (HH), was determined to be 1.788 ± 0.008 g/cm$^3$ (n=9). These three forms were well-resolved by CsCl density gradients and are in agreement with Luk and Bick's (1968) determinations for BrdU containing DNA which are equal to 1.70 g/cm$^3$ (LL), 1.75 g/cm$^3$ (HL), and 1.80 g/cm$^3$ (HH). % BrdU substitution can be calculated from density by using the following calculation: % BrdU substitution = $(\rho_{\text{Brdu subst}} - \rho_{\text{no BrdU}})/((\%dT/50) - 0.1730)$ (Luk and Bick, 1968). A value of 29% 2'-deoxythymidine, dT was used according to determined values for mouse genomic DNA (Waterston, et al., 2002).

After 24-48 hours of BrdU labeling, cells cycling symmetrically show three peaks of DNA corresponding to LL DNA, HL DNA, and HH DNA (Figure 1). Mainly two distinct peaks are observed at 24 hours, one peak at the position of LL DNA, and one peak at the position of HL DNA. The HL peak is indicative of semi-conservative DNA replication as defined by Meselson and Stahl (1958). The observation of a large HL

fraction in the absence of significant amounts of HH DNA, effectively excludes the possibility of a conservative DNA replication mechanism. The LL DNA peak represents DNA from cells that were non-cycling before the BrdU label was added and would, therefore, not incorporate the label. When asymmetric cell kinetics are induced, time-lapse microscopy results show that approximately half of the cells immediately become non-cycling. The LL peak at 24 hours is consistent with this observation. If this interpretation is correct, then the ratio of HL:LL DNA should approach 2:1 before the appearance of HH DNA. Given the generation times for the cycling cells, a 2:1 ratio of HL:LL should occur at about 20-24 hours. This relationship has been shown previously (Merok, et al., 2002).

From 24 hours to 96 hours, the CsCl gradient profiles show that the DNA species are incorporating more BrdU label as expected and producing an increasing fraction of HH DNA. At 48 hours, the asymmetrically cycling cells show production of HH DNA as predicted, this peak of HH DNA continues to increase out to 96 hours. The creation of HH DNA at >1 generation time is further evidence that semi-conservative DNA replication is occurring during asymmetric cell kinetics. This observation is consistent with the expectation from our modeling of DNA replication in cells cycling with asymmetric stem cell kinetics. The data show that both symmetrically cycling and asymmetrically cycling cells replicate their DNA semi-conservatively.

A peak area ratio analysis was performed to evaluate the quality of the cell kinetics during the DNA replication study. The peak area ratios can be determined from the area under the curve for the HH, HL, or LL DNA peak. The peak area ratios normalized to the HL DNA peak were evaluated across all time points. These peak area ratios were compared to the expected values for the two-respective predicted cell kinetics types,

asymmetric vs. symmetric. Peak areas were quantified by choosing gradient points at which there would be the least possible peak overlap. The points of area determination are noted with dotted lines in Figure 1.

By comparing the observed area ratios of the three DNA species to model expectations, cell kinetics during the replication study could be internally evaluated. In Table 1, the asymmetric cycling cells' peak area ratios do not differ significantly from their expected values, $X^2 = 0.60$, $p = 0.99$ (7 degrees of freedom), thus supporting our model of asymmetric cell kinetics. The symmetric cycling cells' peak area ratios also agree with their expected values, $X^2 = 2.75$, $p = 0.91$ (7 degrees of freedom), though not to the same extent as the asymmetrically cycling cells. This may be due to a poorer peak resolution in the gradients at later labeling times.

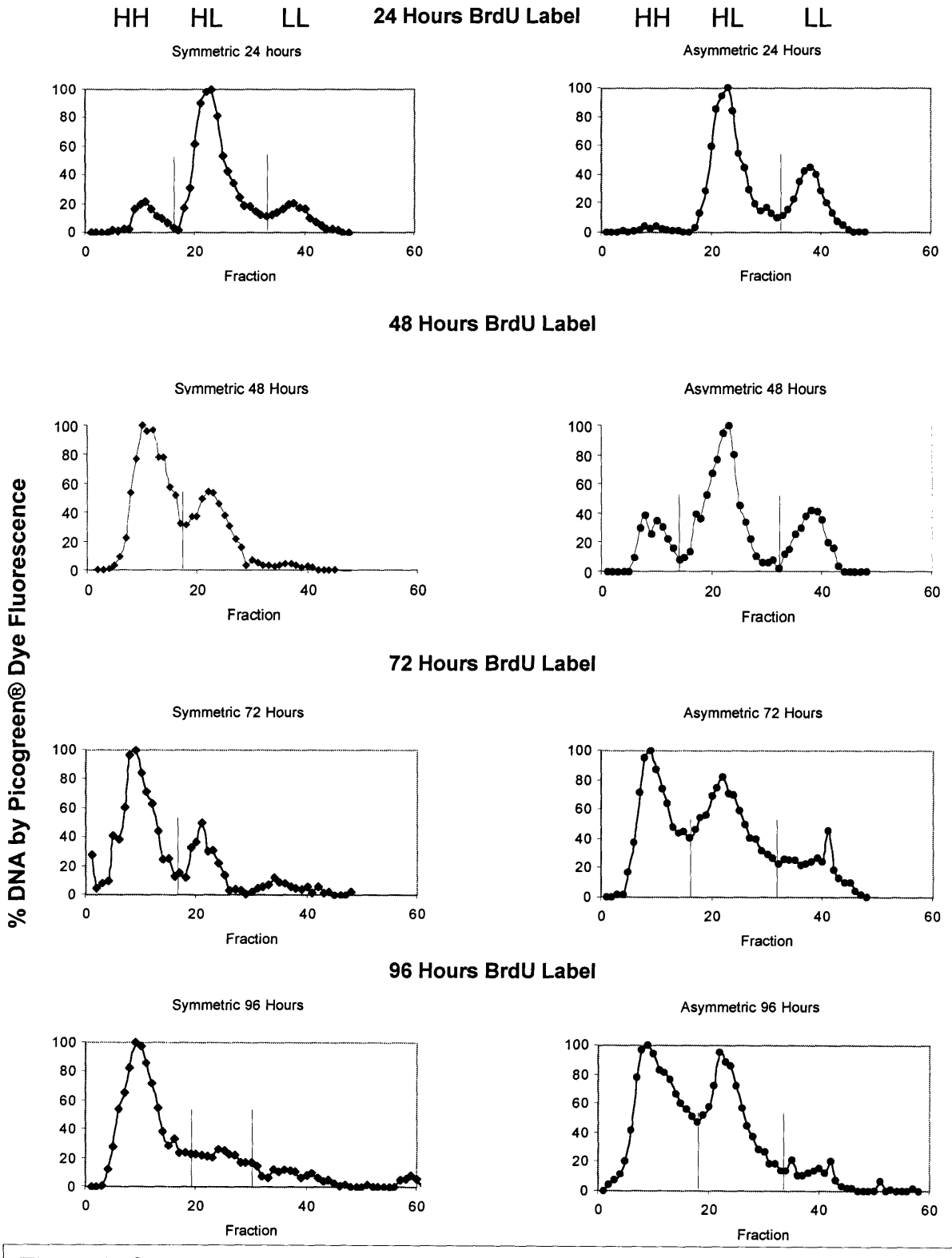


**Figure 1. Semi-conservative DNA Replication in Asymmetrically Cycling Cells.** Symmetrically and asymmetrically cycling cells were labeled continuously with BrdU for 24, 48, 72, and 96 hours. The cells were harvested, and their DNA extracted and purified. 10 µg DNA was analyzed using equilibrium CsCl density gradients. The gradients were fractionated and each fraction was evaluated for DNA content by Picogreen® fluorescence. All data are scaled to the percentage (%) of the peak fraction.

## Results for Symmetrically Cycling Cells

| | Observed Ratios | | | | Expected Ratios for Symmetric Cell Kinetics | | |
|---|---|---|---|---|---|---|---|
| BrdU Label (hours) | HH | HL | LL | | HH | HL | LL |
| 24 | 0.2 | 1 | 0.2 | | 0 | 1 | 0 |
| 48 | 2 | 1 | 0 | | 1 | 1 | 0 |
| 72 | 3 | 1 | 0.3 | | 3 | 1 | 0 |
| 96 | 4 | 1 | 0.3 | | 7 | 1 | 0 |

Chi-Squared Value, $X^2 = 2.75$, (7 degrees of freedom), $p = 0.91$

## Results for Asymmetrically Cycling Cells

| | Observed Ratios | | | | Expected Ratios for Asymmetric Cell Kinetics | | |
|---|---|---|---|---|---|---|---|
| BrdU Label (hours) | HH | HL | LL | | HH | HL | LL |
| 24 | 0 | 1 | 0.4 | | 0 | 1 | 0.5 |
| 48 | 0.3 | 1 | 0.4 | | 0.5 | 1 | 0.5 |
| 72 | 0.8 | 1 | 0.3 | | 1 | 1 | 0.5 |
| 96 | 1.2 | 1 | 0.2 | | 1.5 | 1 | 0.5 |

Chi-Squared Value, $X^2 = 0.60$, (7 degrees of freedom), $p = 0.99$

**Table 1. Evaluation of Quality of Cell Kinetics During CsCl Gradient DNA Replication Study by the Method of Calculating Peak Area Ratios.**
Areas for the HH, HL, and LL peaks were determined from CsCl gradient DNA profiles by summing the DNA/fraction for each peak from Ch. 1,Fig. 1. These areas were normalized to the HL peak area to generate a peak area ratio. The $X^2$ values for good ness of fit to idealized models for respective asymmetric and symmetric cell kinetics are shown.

The LL DNA peak is a direct measurement of the non-cycling cell fraction that was not cycling at the time the BrdU label was introduced into asymmetrically cycling cultures. As expected, the LL DNA persists in the asymmetric cycling cell cultures from 24, to 96 hours, showing that the asymmetrically cycling cells were producing non-cycling cells before the BrdU label was introduced. This observation is consistent with a stable division arrest as reported previously for these cell lines (Merok, *et al.*, 2002, Sherley *et al.*, 1991, Sherley *et al.*, 1995, Rambhatla *et al.*, 2001). In the asymmetrically cycling cell cultures, the LL DNA peak is stable from 24 hours to 48 hours and represents 29% of the total DNA on the gradient at 24 hours and 23% of total DNA at 48 hours. The LL peak then goes down by about half at 72 hours (12% of total DNA). By 96 hours, it is reduced to 5% of the total DNA which is equivalent to background levels observed in symmetrically cycling cells. Some of the decreases in the LL DNA fraction reflect continued cell division by cycling cells. As the total number increases, a stable LL DNA containing cell fraction is predicted to decrease to 25%, 20% and 17% of the total DNA at 48 hours, 72 hours and 96 hours, respectively (Ch.1, Table 1). This observation could explain earlier observations (Sherley et al, 1995; Liu et al., 1998) that non-cycling cells are found in G1 and S phase. Cells initially arrested in G1 may progress through to S-phase for final arrest there or in G2. Non-cycling cells do not divide for out to 15 days. In symmetrically cycling cells, after 24 hours no consistently well-resolved peak is found in the region corresponding to LL DNA.

The CsCl gradient profiles of DNA from asynchronous cultures show that the DNA forms in cells cycling asymmetrically are the same as those found in cells cycling symmetrically, even though they appear in different proportions over time. By 96 hours, symmetrically cycling cells have almost entirely BrdU substituted DNA. In

contrast, asymmetrically cycling cells show a significant amount of HL DNA. The HL and HH peak both contain DNA from non-cycling cells produced from divisions of stem-like cells after S-phase and BrdU incorporation. If immortal DNA strands are retained, only the HL peak will contain DNA from cycling cells with immortal DNA strands, since the immortal strand is predicted to be unlabeled in the continuous BrdU labeling scheme.

**Conclusions:**

CsCl density gradients were used to evaluate aspects of asymmetrically cycling cells important for planned immortal DNA strand investigations. Prior to these studies, it was not known how cells cycling asymmetrically and retaining immortal DNA strands replicated their DNA or whether the basic physical properties of DNA in these cells were different than those found in symmetrically cycling cells.

These studies reveal that CsCl gradient analysis of BrdU-labeling kinetics can be used to confirm and quantify asymmetric cell kinetics. The cell population of asymmetrically cycling cultures never became fully labeled and instead maintained both LL DNA and HL DNA forms for at least 96 hours (4-5 generations). The persistence of the LL DNA peak from asymmetrically cycling cells is a key indication of asymmetric cell kinetics. The symmetrically cycling cells show early loss of well-resolved LL and HL peaks demonstrating that most of the DNA is fully substituted with BrdU in actively dividing cells. The LL DNA peak does appear to exhibit a slow rate of instability. This property illuminates the previous observation that asymmetrically produced non-cycling cells also arrest in later phases of the cell cycle (S and G2). It was observed that the peak area ratios of the asymmetrically cycling cells has an excellent fit to the

idealized model for asymmetric cell kinetics determined by other sampling methods (e.g. time lapse, Rambathla, *et al.*, 2001). This population approach provides greater confidence that average behavior of individual cells is as prescribed by earlier analyses.

In addition to confirming asymmetric cell kinetics, the CsCl gradient studies demonstrated semi-conservative replication. The way in which asymmetrically cycling cells replicate their DNA was important to establish, because subsequent immortal DNA strand experiments are predicated on semi-conservative DNA replication. The step-wise progression of DNA from LL→ HL → HH over time in the asymmetrically cycling cells is consistent with semi-conservative DNA replication. In addition, the DNA structure of DNAs found in asymmetric cells was not unlike the typical DNA species observed in symmetrically cycling cells. This was previously unknown and allows subsequent studies of immortal strand retention to be interpreted using prevailing ideas on DNA structure and strand inheritance.

The continuous labeling studies of total asynchronous cultures confirm asymmetric cell kinetics by CsCl density gradients and also demonstrate semi-conservative DNA replication in asymmetrically cycling cells. These experiments are consistent with asymmetric cell kinetic data from flow cytometry, time-lapse photomicroscopy, and growth curve analyses (Sherley *et al.*, 1991, Sherley *et al.*, 1995, Rambhatla *et al.*, 2001)).

These studies set the stage for investigations of the physical chemical nature of immortal DNA strands and the molecular basis for their non-random segregation to cycling stem-like cells.

**Discussion:**

These first studies show that the CsCl gradient profiles of asymmetric cycling cells' DNA are different than the profiles of DNA from symmetrically cycling cells and are indicative of the asymmetric cell kinetics occurring in the cells induced to divide with asymmetric self-renewal like adult stem cells. As such, the CsCl method also provides a new application for the detection of non-symmetric cell kinetics in other cultured cell lines. By following BrdU labeling kinetics, one can determine whether a culture is cycling asymmetrically or symmetrically.

Using CsCl density gradients, DNA species can be fully separated by their BrdU content. This experimental approach allows for the detection of retained immortal DNA strands in subsequent experiments (Chapter 2). If immortal DNA strands are retained, they are located in the HL peak of total DNA in CsCl gradient profiles, since the immortal strand is unlabeled at the time asymmetric cell kinetics is induced. These initial studies provide a system by which immortal DNA strands can be fully resolved, detected, and isolated for further analyses and characterization.

**References:**

Liu Y, Bohn SA, Sherley JL, Inosine-5'-monophosphate dehydrogenase is a rate-determining factor for p53-dependent growth regulation. Mol Biol Cell, 1998. **9**: p. 15-28.

Luk, D.C.,and Bick, M.D., *Determination of 5'-Bromodeoxyuridine in DNA by Buoyant Density. Analytical Biochem.*, 1968. 77:p.346-349.

Merok, JR, Lansita, JA, Tunstead, JR, Sherley, JL, *Cosegregation of Chromosomes Containing Immortal DNA Strands in Cells that Cycle with Asymmetric Stem Cell Kinetics.* Cancer Res., 2002. **62**: p. 6791-6795.

Meselson, M., Stahl, F., Vinograd, J., *Equilibrium Sedimentation of Macromolecules in Density Gradients.* PNAS, 1957. **43**: p. 581-588.

Meselson, M., Stahl, F.W., *The Replication of DNA in Escherichia coli.* PNAS, 1958. **44**: p. 671-682.

Rambhatla, L., Bohn, S.A., Stadler, P.B., Boyd, J.T., Coss, R.A., Sherley, J.L., *Cellular Senescence: ex vivo p53-dependent asymmetric cell kinetics.* J. Biomedicine and Biotechnology, 2001. **1**: p. 28-37.

Schildkraut CL, Marmur J, Doty P, Determination of the base composition of deoxyribonucleic acid from its buoyant density in CsCl. J Mol Biol, 1962. **4**:p. 430-43.

Sherley, J., *Guanine nucleotide biosynthesis is regulated by the cellular p53 concentration.* J. Biol. Chem., 1991. **266**: p. 24815-24828.

Sherley, J.L., Stadler, P.B., Johnson, D.R., *Expression of wild-type p53 antioncogene induces guanine nucleotide-dependent stem cell division kinetics.* PNAS, 1995. **92**: p. 136-140.

## Chapter 2. Demonstration of the Immortal DNA Strand Mechanism Using CsCl Density Gradients

### Section A: Label Retention Studies – Pulse Label without Chase

**Rationale:**

In Chapter 1, asymmetrically cycling cells continuously labeled with BrdU, display asymmetric cell kinetics in CsCl density gradient analyses. In these studies, it is predicted that retained immortal DNA strands are unlabeled with BrdU because asymmetric cell kinetics was initiated prior to the addition of BrdU. Immortal DNA strands can also be selectively labeled with BrdU by inducing asymmetric cell kinetics after the DNA has been hemi-labeled with BrdU for one generation of symmetric cell kinetics. This label retention strategy was used for one of the first demonstrations of the immortal DNA strand mechanism in asymmetrically cycling cells using *in situ* cytology methods (Merok, et al., 2002). An advantage to using the label retention strategy over the continuous labeling strategy for *in situ* detection of immortal strands is that the end result will be a "plus-minus" interpretation of the results. Cells co-segregating immortal DNA strands will have BrdU present in their nuclei whereas cells randomly segregating their chromsomes will have no BrdU in their DNA. Nuclei stained with anti-BrdU antibodies are predicted to show a 100% difference in BrdU content between nuclei retaining HL immortal DNA strands and LL non-immortal DNA strands. A 100% difference between two nuclei is easier to interpret than a 50% difference in BrdU content between HL (immortal DNA strand is unlabeled) immortal DNA strands and HH non-immortal DNA strands.

Once the cellular DNA is hemi-labeled with BrdU during symmetric cell kinetics, the BrdU is removed from the system and the culture is induced to cycle asymmetrically in the absence of BrdU for 4 to 6 generations. In order to look specifically at the BrdU retention properties of cycling cells, mitotic cells were selected by mitotic shake-off. The expected DNA content of mitotic cells retaining immortal DNA strands is 1:1 HL:LL DNA after 4-6 generations. The mitotic control cells cycling symmetrically will dilute their BrdU label as more LL DNA is created with each generation and are expected to have a DNA content of 1:63 HL:LL DNA. The expected results for symmetrically and asymmetrically cycling cells are shown in Figure 1.

**Expectation for Symmetrically Cycling Cells with Random Chromosome Segregation and Dilution of Hemi-Labeled BrdU-containing HL DNA Strands**

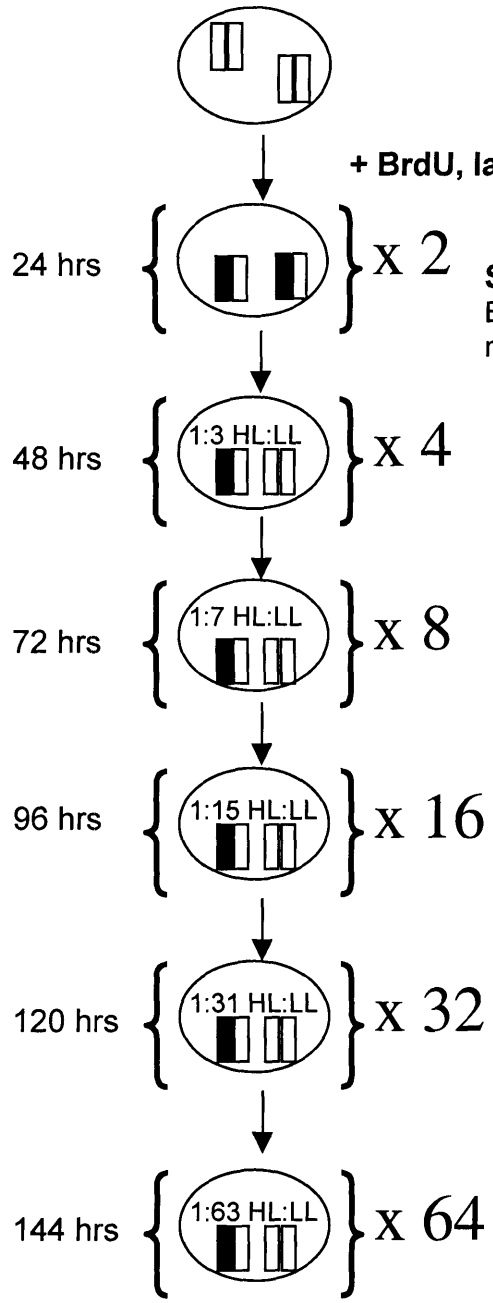


*100% HL DNA.*
**Symmetric cell kinetics**
Exponential dilution of HL DNA strands by newly replicated LL DNA strands

***Random Chromosome Segregation***

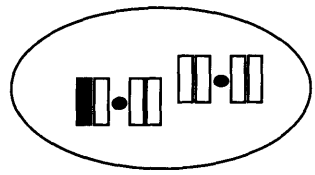

Mitotic Cells with chromosomes containing Randomly Assorted DNA Strands

**1:63 ratio of HL :LL DNA**

**Expectation for Asymmetrically Cycling Cells with Non-random Chromosome Segregation and Retention of Labeled Immortal DNA Strands**

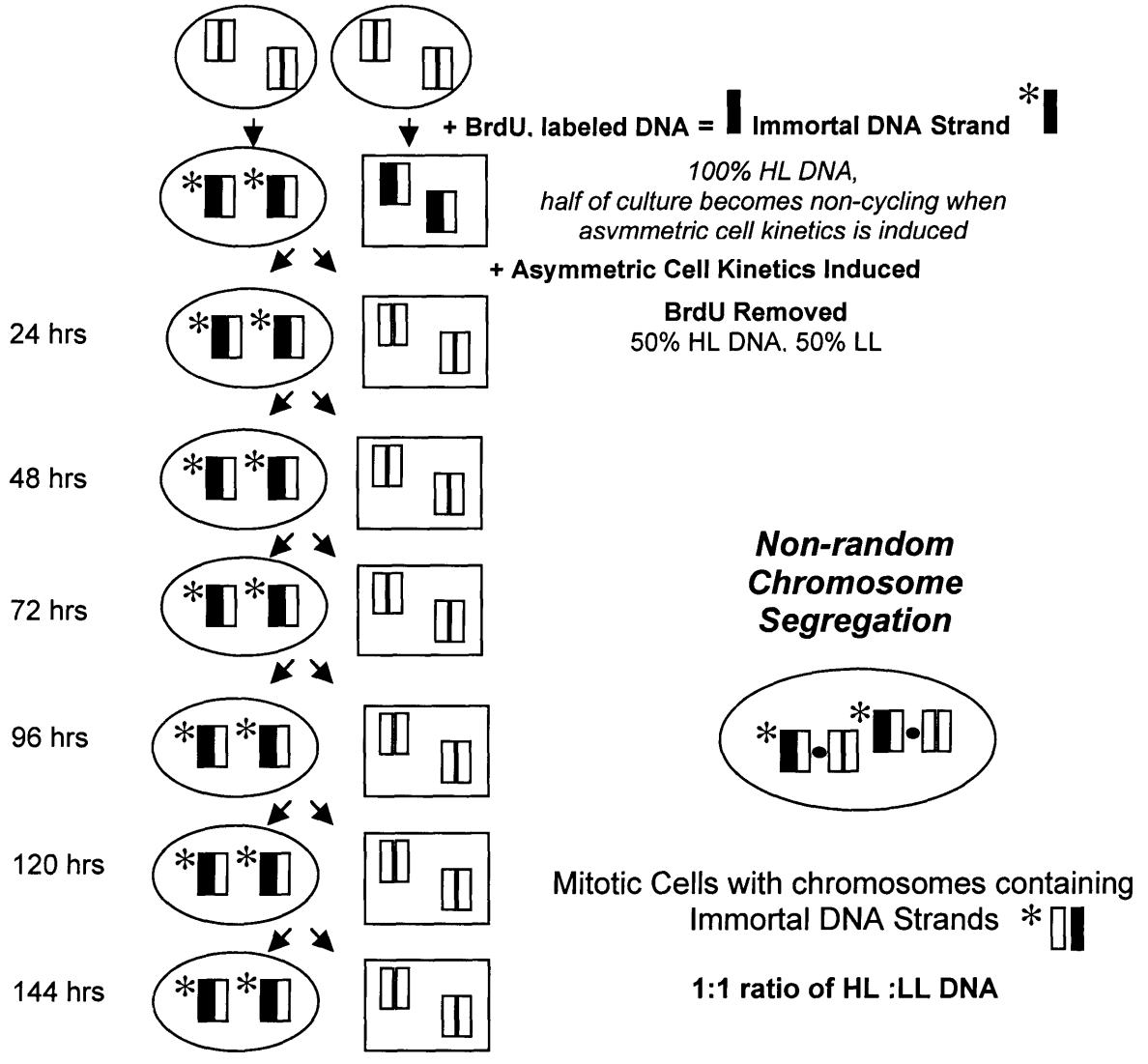


**Figure 1. Schematic of Predicted Outcome for Symmetrically and Asymmetrically Cycling Cells Retaining BrdU Labeled Immortal DNA Strands**

DNA is uniformly labeled with BrdU during the first 24 hours of symmetric growth. Symmetrically cycling cells not retaining immortal DNA strands will synthesize new LL DNA with each division after the BrdU is removed. Chromosomes are randomly assorted between daughter cells. The expected ratio of HL:LL DNA in mitotic symmetrically cycling cells after 6 symmetric divisions is 1:63 (Figure 1A). Uninduced asymmetric cell cultures uniformly label immortal DNA strands with BrdU during the first 24 hours of symmetric growth. Half of the culture will arrest at the time asymmetric kinetics is induced. The BrdU label is removed after 24 hours and cells are induced to cycle asymmetrically. All newly replicated DNA will incorporate no BrdU. The BrdU label is non-randomly segregated to cycling cells and the non-cycling cells created with each asymmetric division will inherit unlabeled non-immortal DNA strands. After 144 hours (6 generations) of growth, mitotic asymmetrically cycling cells retaining immortal DNA strands will have a 1:1, HL:LL DNA content.

▮◧ = HL duplex DNA, * ▮ = Immortal Strand DNA, ◫ = LL duplex DNA,O= cycling cell, □ = non-cycling cell.

## Experimental Methods:

Cells were plated at 1.7X10$^3$ cells/30 mls /150 cm$^2$. 24 hours later, all cells for the study were labeled with 20μM BrdU for 24 hours under conditions of asymmetric cell kinetics. After 24 hours (approximately 1 generation time), the DNA was hemi-labeled with BrdU. The BrdU containing medium was then removed and replaced with medium containing 65 μM $ZnCl_2$ to induce cells to cycle asymmetrically. Cells were grown in the absence of BrdU for 4-6 generations.

### Mitotic Selection

Mitotic cells were isolated by mitotic selection. Mitotic cells are not attached to the flask surface as tightly as cells in other phases of the cell cycle and can removed by firmly shaking the tissue culture flask. Cellular debris was removed from the cultures by discarding the first two mitotic shake-off collections before harvesting mitotic cells. Half of the media containing cellular debris was removed and spun down for 5 minutes at 1500 rpm (500 x g) at 25° C to pellet dead cells and debris. The cleaned media was poured off from the pellet and warmed to 37°C in the water bath. The pellet was discarded. The remaining half of the media in the flask was cleaned in the same way. After the second half of the media was removed from the flask, it was replaced with the cleaned, warm media from the first half. By cleaning half of the media at a time, the cells were constantly exposed to the same media to minimize any cell kinetic changes. The flasks were checked for residual debris after the first two debris removal shake-offs. Mitotic cells were collected by shaking each T150 cm$^2$ flask 8-10 times to detach mitotic cells from the flask and collecting the media containing the mitotic cells from each flask. After all of the media containing the harvested mitotic cells was pooled on ice, the warm

cleaned media from the second debris removal procedure was used to replace the media from the first mitotic shake-off. This procedure was repeated for 4-8 shake-offs to ensure the collection of at least one million cells so that a minimum of 10 μg of DNA could be harvested for CsCl gradient analysis. The collected mitotic cells were spun down for 5 minutes at 1000 rpm (300 x g), a low g-force spin to keep mitotic cells intact. The percentage of mitotic cells recovered ranged from 3%-6% based on cell counts at the end of the mitotic shake-offs. 50,000 to 100,000 cells were also fixed in 70% ethanol and stained in 0.5 μg/ml propidium iodide to determine the quality of the mitotic cell preparation by flow cytometry. Based on flow cytometry analyses (n = 3), the preparations contained > 87 % mitotic cells. DNA was extracted from mitotic cells and analyzed by CsCl gradients as described in the Experimental Methods section of Chapter 1.

**Results:**

Label retention studies were performed for 96 hours and 144 hours after the initial BrdU labeling. The 96 hour results were comparable to the 144 hour results (data not shown). DNA isolated from mitotic symmetrically cycling cells shows one peak of LL DNA ($\rho$=1.690 g/cm$^3$ ± 0.014) as predicted for the dilution of labeled DNA due to randomization with newly synthesized unlabeled DNA. The asymmetrically cycling mitotic cells exhibited one peak close to the position of HL DNA ($\rho$=1.723 g/cm$^3$ ± 0.008) which indicated BrdU labeled DNA strand retention but not at the expected 1:1 ratio of HL:LL. Instead, the CsCl gradient profile for DNA from asymmetric mitotic cells showed one peak centered at HL DNA with no resolved LL DNA peak. This result indicated that the asymmetric cells were retaining the BrdU label, consistent with the

immortal strand hypothesis, but not exactly as expected. Using the method of Luk and Bick (1968), the % BrdU substitution of the DNA can be determined from the densities listed above. The % BrdU content for symmetrically cycling cells was determined to be 11%. Asymmetrically cycling cells have a predicted BrdU content of 53%, if the DNA position in the gradient is determined solely by BrdU content. The difference in BrdU content between symmetrically cycling and asymmetrically cycling cells is 42%. The difference in density between the two types of DNA confirms that the asymmetric cells are retaining BrdU label to a greater extent than the symmetrically cycling cells. The gradient profiles of control and asymmetric cells are shown in Figure 2.

These results suggest that the asymmetric cycling cells are retaining immortal DNA strands because they retained the BrdU label at a 4.8-fold higher % BrdU substitution rate than the symmetrically cycling cells. However, the predicted 1:1, HL:LL expected outcome was not observed.

The arrested, non-cycling cells were analyzed to determine whether or not their DNA was modified as this might account for the failure to observe LL DNA. Either the immortal or non-immortal strand might contain a DNA modification. DNA from cells left attached to the tissue culture flask after the mitotic shake-off was analyzed by CsCl gradients. These "attached" cells left after the mitotic shake-off are mostly arrested cells.

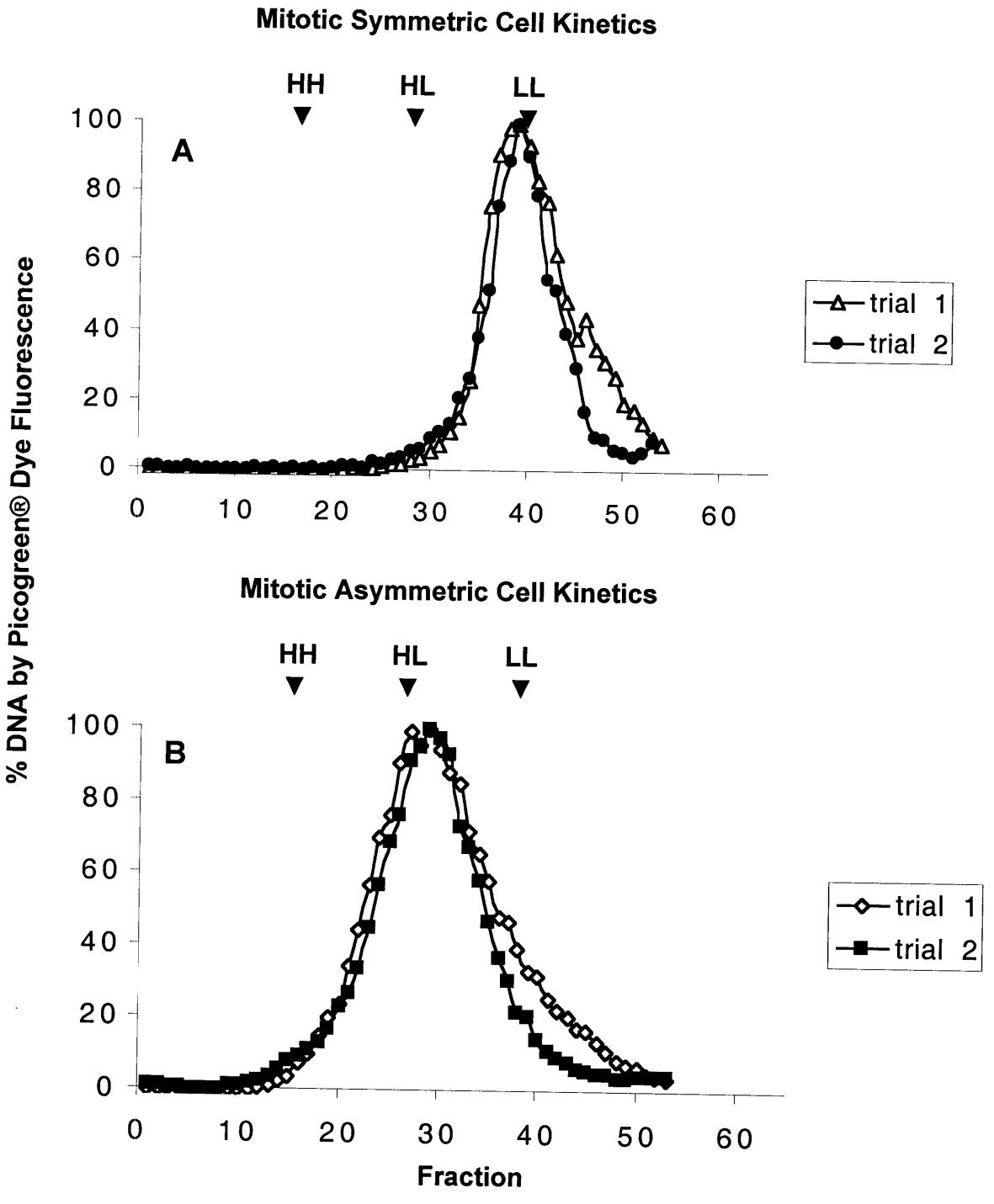


**Figure 2. Evidence for BrdU DNA Strand Retention in Cells Cycling Asymmetrically**
Cells were labeled for 24 hours in BrdU while cycling symmetrically. Cells were induced to cycle asymmetrically as described, and the BrdU label was chased for 144 hours (6 generations). Mitotic cells were collected by mitotic shake-off, their DNA extracted, and run on a CsCl gradient. The summary of two trials is shown above. Symmetrically cycling cells have a mean peak density of $\rho$ = 1.690 g/cm$^3$ ± 0.014. Asymmetrically cycling cells have a mean peak density of $\rho$ = 1.723 g/cm$^3$ ± 0.008.

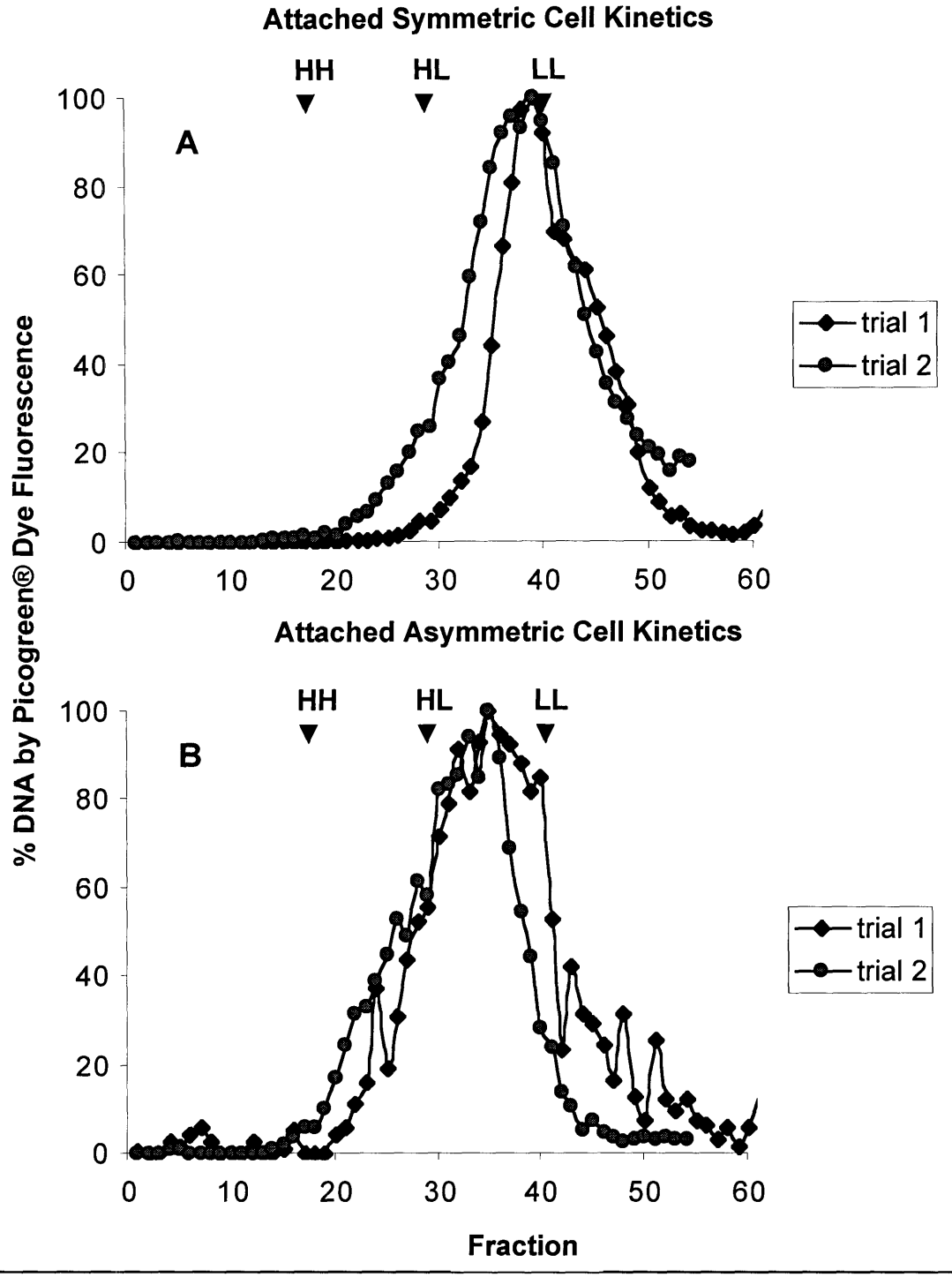


**Figure 3. CsCl Gradient Analysis of Adherent Cells Remaining at End of Mitotic Shake-off**

Cells remaining at the end of the mitotic shake-off were harvested. Cells from cultures cycling asymmetrically that are left at the end of the mitotic shake-off are mainly arrested, non-cycling cells. Their DNA was extracted, purified, and analyzed by CsCl density gradients to look for DNA peak profile differences between cells undergoing symmetric cell kinetics and asymmetric cell kinetics. Symmetrically non-cycling cells have a mean peak density of $\rho = 1.699$ g/cm$^3$ $\pm$ 0.012. Asymmetrically non-cycling cells have a mean peak density of $\rho = 1.722$ g/cm$^3$ $\pm$ 0.014.

The "attached" cells have CsCl gradient profiles similar to the mitotic DNA profiles. DNA from attached symmetric cells have a peak DNA density at the LL position, $\rho$ = 1.699 g/cm$^3$ ± 0.012 g/cm$^3$. For the asymmetric culture, there is a slight shift in density to $\rho$ = 1.722 g/cm$^3$ ± 0.014 g/cm$^3$, corresponding to a BrdU % substitution value of 45% (Luk and Bick, 1977). The CsCl gradient profile for the attached cells' DNA does not show the expected 1:4 ratio of HL:LL, for total cells in culture. This suggests that the BrdU label may not be fully chased from the culture upon removal of the BrdU containing media. If the BrdU were not fully chased, the cells would continue incorporating BrdU to varying degrees throughout the experiment. The attached cells' CsCl profiles are shown in Figure 3.

**Conclusions:**

The CsCl gradient results for DNA from mitotic cells cycling asymmetrically show that the cells retained BrdU at a 4.8 fold higher % BrdU content when compared with the control cells cycling symmetrically. This result supports the hypothesis of immortal strand retention in these cells. However the gradient profile is not consistent with the expected outcome of an equal amount of HL:LL DNA in a 1:1 ratio. The LL DNA is not resolved in these studies. The LL DNA could be modified causing it to run at a heavier density or it could contain residual amounts of BrdU, leftover from the initial pulse labeling. This will be addressed in Chapter 2B.

It is unknown whether a modification to the DNA exists in the immortal or the non-immortal strand DNA. By analyzing cells that remained after the mitotic shake-off, which are enriched for arrested cells, it can be concluded that no major modification is

evident in the arrested cells. A modification of the LL DNA is not responsible for the unresolved HL and LL peaks found in DNA from mitotic cells.

The fact that the non-cycling cells did not show the expected ratio of 1:6 HL:LL peak area ratio but instead exhibited a broad peak similar to that found in the mitotic cells suggests that the BrdU label is not being fully chased in these studies or that a modification is causing the observed shift in density. This observation is consistent with what was found in the mitotic cells. The studies discussed in Chapter 2B will attempt to address this issue.

**Discussion:**

The DNA from asymmetric cells did not yield the predicted 1:1 ratio of HL:LL for ideal non-random segregation. One possibility to explain this result is that the BrdU label was not fully chased when asymmetric cell kinetics was induced. If intracellular pools of BrdU were remaining, then a small amount of BrdU would continue to be incorporated in newly made non-immortal DNA strands. Symmetrically cycling cells did not show this effect because the BrdU label was sufficiently diluted after 6 symmetric divisions, the total ratio of HL:LL DNA would be 1:63. A 1:63 dilution of HL DNA by newly replicated LL DNA would result in a BrdU content of about 1.6% which would run at the LL position on a CsCl density gradient (Luk and Bick, 1977).

If residual BrdU remains in the system, the selection and retention of BrdU containing immortal DNA strands would still occur. However, some of the DNA paired with immortal strands would also contain BrdU. If non-immortal strands were labeled with BrdU, then cells would contain a mixture of retained BrdU immortal strands and labeled non-immortal strands. Over the course of the 6 generation BrdU chase, the

DNA would be slowly diluted but small amounts of BrdU would continue to be incorporated in the newly replicated DNA. The resulting CsCl gradient profile from such an outcome would be a broad distribution of DNA labeled with BrdU to varying degrees. This is in fact what is observed in the label retention CsCl gradient studies suggesting this is a likely hypothesis.

It is possible that these studies could explain parallel (done at different points in time) experiments done *in situ* which demonstrated immortal strand retention but at a lower frequency than expected. In these studies, cells were uniformly hemi-labeled with BrdU. Asymmetric kinetics was induced and the BrdU label was removed. Instead of using a mitotic shake-off and CsCl gradients to evaluate immortal DNA strand retention, cells were treated with cytochalasin D, an actin inhibitor that prevents cytokinesis. This chemical treatment resulted in the creation of binucleates; two nuclei contained in one cytoplasm. Binucleates were then stained with fluorescent anti-BrdU antibodies to evaluate nuclei side-by-side for the non-random segregation of BrdU containing immortal DNA strands. In these studies, 22% of the cells (Merok, et al., 2002) fully segregated BrdU containing chromosomes to one nuclei and not the other. In CsCl density gradient evaluations of the same experiment, cells not completely retaining immortal DNA strands would be observed as intermediates of HL and LL DNA and would mask the complete resolution of the HL and LL DNA peaks. This experimental caveat, which is problematic for CsCl density gradients, is not a problem for detecting non-random immortal strand co-segregation *in situ* as observed previously (Merok, et al., 2002).

## Chapter 2. Demonstration of the Immortal Strand Mechanism Using CsCl Gradients

## Section B: Label Retention with Chase (2'-deoxythymidine and 2'-deoxycytidine) Studies

**Rationale:**

The label retention experiments did not yield the expected 1:1 ratio of HL:LL DNA in mitotic cells cycling with asymmetric cell kinetics. A LL DNA peak was not resolved in the label retention studies. One possible explanation for this result is that the BrdU label was not fully chased from cultures before asymmetric cell kinetics were induced. Residual BrdU in cultures would cause non-immortal strands to be labeled with varying amounts of BrdU, resulting from DNA strand synthesis when there was BrdU remaining in the system. This would provide an explanation for the missing LL DNA peak in CsCl gradient profiles of DNA from asymmetrically cycling mitotic cells. To address this issue, a 2'-deoxythymidine (dT), 2'-deoxycytidine (dC) chase was incorporated into the label retention studies to see if LL DNA could be resolved from HL DNA.

**Experiment:**

Cells were plated at 5 X $10^5$ cells/150 $cm^2$ /30mls media. 20 hours later, cultures were labeled with BrdU for 24 or 72 hours (for the HH pulse chase experiment), under the conditions of symmetric kinetics, to hemi-label (24 hours) or fully label (72 hours) the DNA with BrdU. The BrdU containing media was then removed and replaced with medium containing 65 μM $ZnCl_2$ to induce p53 expressing cells to cycle asymmetrically,

and 100μM dT and 100μM dC to chase the residual BrdU. Cells were grown in the $ZnCl_2$-chase media for 4-6 generations (96-144 hours). Mitotic cells were harvested by mitotic shake off as described in Chapter 2A. Approximately 1 x $10^6$ mitotics were collected. The mitotic cell collections were combined and washed with ice cold PBS. DNA was extracted and analyzed using CsCl gradients as described previously in pulse-label experiments in Chapter 2A. Cells were counted before $ZnCl_2$ addition and at the end of the experiment to determine the number of population division cycles (PDC). For asymmetrically cycling cultures, PDC is the number of times the initial population of cycling cells divides, PDC = $(N_t-N_o)/0.5\ N_o$. For symmetrically cycling cells, PDC is the number of population doublings, PDC = $\ln(N_t/N_o)/\ln 2$ (Merok et al., 2002).

**Results:**

The dT/dC chase was included in order to prevent incorporation of BrdU into DNA synthesized after the induction of asymmetric cell kinetics. A combination of pyrimidines dT/dC was used in order to avoid the adverse effects of nucleotide pool imbalances (Thilly, W., personal communication). Chromosomal cross-overs occur more frequently in cells labeled with BrdU and chased with dT alone (Davidson and Kaufman, 1978; Ashman, et al., 1981). In the dT and dC chase studies, the profiles for the mitotic asymmetric and symmetric cells show complete resolution of the HL and LL peaks from one another. The LL peak observed for symmetrically cycling mitotic cells showed improved peak resolution than was observed in the pulse, no chase studies. This experiment was performed two times. The gradient profiles for each trial are shown in Figure 1.

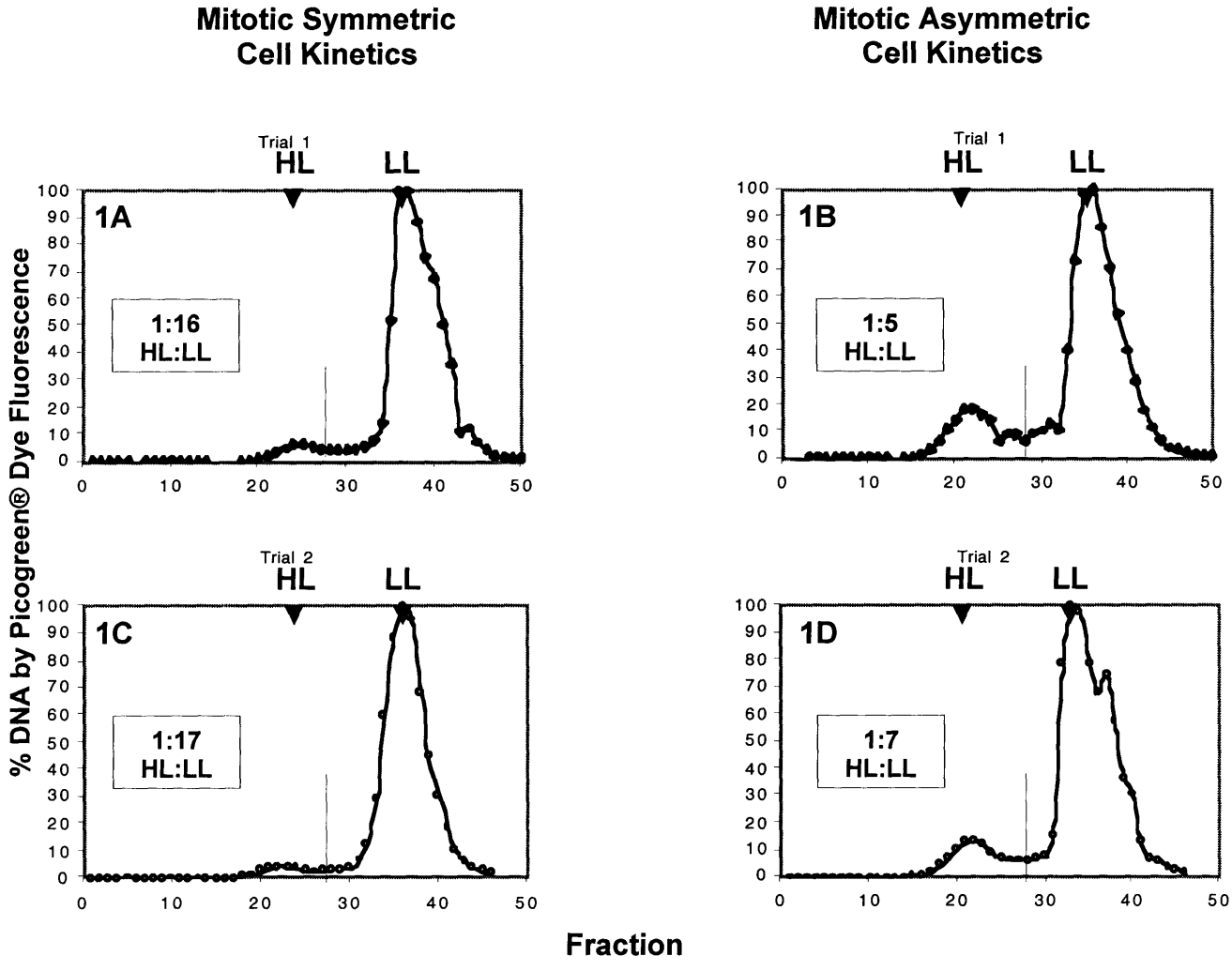


**Figure 1. The dT, dC Chase Resolves DNA from Asymmetrically Cycling Cells Retaining Immortal DNA Strands into HL and LL DNA**

Cells cycling symmetrically were pulse labeled with BrdU. After 24 hours of growth, the BrdU label was removed and cells were induced to divide asymmetrically in a medium containing 100μM dT/dC to fully chase residual BrdU from intracellular pools. Mitotic cells were harvested and their DNA extracted. Purified DNA was analyzed by CsCl density gradients and DNA profiles determined using Picogreen® DNA quantitation dye. Two experiments were performed. Trial 1 (1A and 1B) and Trial 2 (1C and 1D) both show distinct HL peak and LL peaks. The symmetrically cycling cells are shown in panels 1A (Trial 1) and 1C (Trial 2). The asymmetrically cycling cells are shown in 1B (Trial 1) and 1D (Trial 2). The observed peak area ratios are included for each trial. The predicted peak area ratios for symmetrically cycling cells is 1:15. The predicted peak area ratios for asymmetrically cycling cells is 1:1. The indicated lines separating HL and LL DNA peaks show where peak area ratios were determined..

The symmetrically cycling mitotic cells show a small peak at the HL position (density = 1.743 g/cm$^3$ ± 0.002 g/cm$^3$, n=2) and a major peak at the LL position (density = 1.704 g/cm$^3$ ± 0.003 g/cm$^3$, n=2). The mitotic asymmetrically cycling cells also show a larger peak at the HL position (density = 1.749 g/cm$^3$ ± 0.000 g/cm$^3$) than the symmetric cells and a major peak at the LL position (density = 1.713 g/cm$^3$ ± 0.005 g/cm$^3$). This result indicates that the dT, dC chase was able to resolve the broad heterogeneous peak found in the label retention studies into well resolved HL and LL peaks.

In the label retention studies without a chase, a broad peak, spanning the positions of HL and LL DNA and centered near the HL position was observed. Using the dT/dC chase conditions, two well-resolved peaks at the HL and LL positions were observed and were the expected DNAs species to be found in this experiment. However, the peak area ratios of each DNA type recovered were different than predicted. Asymmetrically cycling cells have a predicted peak area ratio of 1:1 ratio of HL:LL DNA. The observed peak area ratio for the asymmetrically cycling mitotic cells of 1:6 ± 2 (average of Trials 1 and 2) is significantly different than the predicted area ratio of 1:1, HL:LL. The peak area ratio for the symmetrically cycling mitotic cells was 1:17 ± 0.6(average of Trials 1 and 2), which closely matches the predicted peak area ratio of 1:15, HL:LL. However, the asymmetrically cycling mitotic cells have a 2.8-fold higher amount of HL DNA than the symmetrically cycling mitotic cells indicating there is in fact immortal DNA strand retention occurring in the asymmetric cells.

The 1:6 observed HL:LL peak area ratio in asymmetrically cycling mitotic cells was not expected. Previously, it was hypothesized that the most recently replicated strand was chosen for immortal strand retention (Merok, et al., 2002). In these studies, the BrdU labeled strand is the most recently replicated. If this hypothesis is not correct

and a cell chooses at random either the most recently replicated BrdU-containing strand or an unlabeled strand, than the cell will retain a mixture of HL and LL immortal DNA strands. The peak area ratio if a cell chooses randomly should be 1:3, HL:LL. This value does not match the observed 1:6 result. However, if cells preferred to select unlabeled immortal DNA strands, this hypothesis may explain the data. Another explanation for the observed 1:6 ratio in mitotic asymmetrically cycling cells may be a loss of asymmetric cell kinetics due to the dT/dC chase conditions. If cells were not cycling asymmetrically or changed from asymmetric to symmetric kinetics over time under these conditions, immortal strands would no longer be retained and the ratio of HL:LL DNA would decrease. To address these possible explanations, a second dT/dC pulse chase experiment was performed.

### 72 Hour BrdU Label with dT/dC Chase Experiment

The same pulse chase experiment was performed except that the initial BrdU labeling time was changed from 24 hours to 72 hours. This was done to uniformly label DNA strands with BrdU so that at the time immortal DNA strand selection occurs 75% of the total DNA is HH DNA. By making the majority of the strands fully labeled with BrdU, a cell's choice for selecting a labeled immortal DNA strand will be enriched from 50% to 75%, compared with previous 24 hour BrdU label studies.

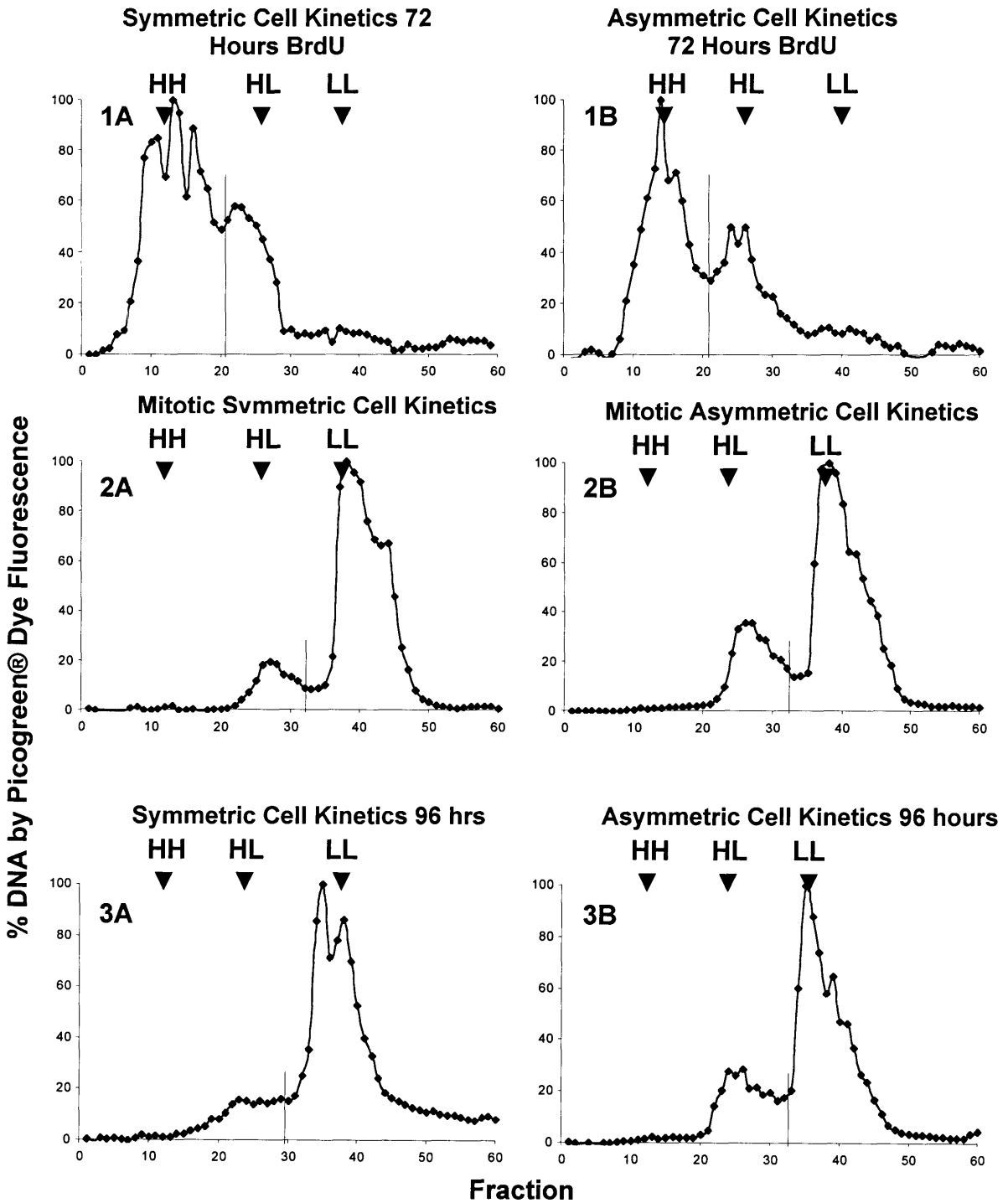


**Figure 2. Evidence for Disruption of Asymmetric Cell Kinetics after 72 hour BrdU Label plus 96 hour dT/dC Chase**

Cells cycling symmetrically were labeled with BrdU to create HH DNA. After 72 hours of growth, the BrdU label was removed and cells were induced to divide asymmetrically in medium containing 100μM dT/dC to chase any residual BrdU. Asynchronous cells were harvested by trypsinization and mitotic cells were selected by mitotic shake-off. The DNA was purified and analyzed by CsCl density gradients. DNA profiles were determined using Picogreen® DNA quantitation dye. One experiment was performed. Asynchronous cells were harvested at time (t) = 0 hours (1A and 1B) and 96 hours (3A and 3B). Mitotic cells were selected by mitotic shake-off. (2A and 2B). Gradients at t = 0, represent cells after the 72 hour BrdU labeling and before asymmetric cell kinetics is induced (1A and 1B). Lines indicate where peak areas were determined.

Cells fully labeled with BrdU for 72 hours and then chased with the dT, dC chase conditions did not show the expected ratio of strand retention. At time (t) = 0 hours, after the 72 hour BrdU labeling and before asymmetric cell kinetics was induced, the DNA of symmetrically cycling cells consisted of 79% HH DNA from peak area calculations. The asymmetric cells' DNA had a 72% HH DNA content. These values agree with the expected value of 75% HH DNA after 3 generations of BrdU labeling during symmetric divisions. Mitotic cells collected should have a 1:1 ratio of HL:LL DNA and the asymmetric cells a 1:7 ratio of HL:LL DNA in the symmetric cells. Instead, a 1:3 HL:LL ratio was observed for asymmetrically cycling mitotic cells. A 1:6 ratio was observed for symmetric mitotic cells in close agreement with the expected 1:7 ratio determined from modeling. The observed results for mitotic asymmetrically cycling cells, do not agree with the expected results for immortal strand retention. Explanations for this data will be further analyzed in the Discussion.

**Conclusions:**

The addition of the dT, dC chase to the label retention studies resolved the missing LL DNA peak from the HL DNA peak. These results suggest that the BrdU label was not fully chased in past label retention studies and provide an explanation for the single broad peak of DNA centered between HL and LL DNA.

The observed experimental results showed a higher amount of HL DNA in asymmetrically cycling cells vs. symmetrically cycling cells and presumably a higher rate of retained immortal DNA strands in asymmetric cells.

The observed peak area ratios for the symmetric cells 1:17 ± 0.58 matched the expected result of 1:15 (p-value = 0.52). However, the observed peak area ratio for the

asymmetric mitotic cells of 1:6 ± 1.8 HL:LL DNA is significantly different than the 1:1 expected ratio.

The 72 hour BrdU pulse chase experiment did not yield the expected results for immortal strand retention. The asymmetrically cycling cells did show a greater retention of immortal strands than the symmetrically cycling cells (1:3 vs. 1:6) but not to the expected degree of 1:1 HL:LL.

The experiment also indicated that a significant number of chromosomal cross-overs did not occur in the system. Otherwise, fully resolved peaks of HL and LL DNA would not be observed after long BrdU labeling times.

**Discussion:**

Although immortal strands are resolved from non-immortal strands using the dT, dC chase, the ratio of HL:LL DNA was not the predicted result for immortal DNA strand retention. The 72 hour BrdU pulse chase experiment attempted to address the issue of random selection of immortal strands at the time asymmetric kinetics is induced. However, the experiment did not yield the expected results for immortal strand retention. The asymmetrically cycling cells showed a greater retention of HL DNA containing immortal strands than the symmetrically cycling cells but not at the expected ratios. If cells were selecting the most recently replicated strand for retention, the HL:LL peak area ratio in asymmetrically cylcling mitotic cells would be 1:1. If cells randomly chose either the labeled or the unlabeled strand for retention the ratio would be 2:3. If the ratio is less than these ratios, a loss of asymmetric cell kinetics under these experimental conditions is the most likely explanation.

When HH DNA is created before asymmetric cell kinetics is induced, non-dividing cells should be made at that time that will contain HH DNA, just as shown in Chapter 1. This peak of HH DNA should remain stable over time and be observed in gradients of DNA from asymmetrically cycling asynchronous cultures at 96 hours. The lack of the HH DNA peak, is strong evidence supporting the idea that asymmetric cell kinetics is lost under these experimental conditions. The faulty kinetics may be attributed to two possible experimental factors: the 72 hour BrdU labeling time or the dT, dC chase conditions or a combination of the two. The 72 hour BrdU labeling is time is probably not the reason the ideal DNA retention was not observed. Gradients at t=0, showed the expected HH:HL DNA peak ratios, indicating that cells were dividing symmetrically as expected until the chase medium was added. The ideal experimental conditions for the pulse chase experiment remain to be optimized in order to maintain asymmetric cell kinetics and immortal strand retention.

Whether or not random selection of BrdU labeled vs. unlabeled immortal DNA strands occurs after asymmetric kinetics is induced, was not determined in these experiments because of factors affecting asymmetric cell kinetics. These issues can be avoided by performing the inverse BrdU labeling experiment. As shown in Chapter 1, asymmetrically cycling cells continuously labeled with BrdU not only exhibit asymmetric cell kinetics using CsCl density gradient analyses but also show that these studies can be used to detect immortal DNA strands. If asymmetric cell kinetics was induced prior to BrdU labeling, immortal DNA strands would remain unlabeled. As asymmetrically cycling cells continue to grow in the presence of BrdU, retained immortal DNA strands are predicted to remain unlabeled. The selection of mitotic cells from these cultures should yield a 1:1 ratio of HH:HL DNA, where the HL DNA contains

the unlabeled immortal DNA strand. If immortal DNA strand selection occurs prior to asymmetric kinetics induction, than using this experimental strategy will help elucidate non-random chromosome co-segregation in model cell lines this will be discussed in Chapter 2, Section C.

## Chapter 2. Demonstration of the Immortal DNA Strand Mechanism Using CsCl Density Gradients

## Section C: Continuous Labeling Studies

**Rationale:**

As discussed in Chapter 1, cells that are induced to cycle asymmetrically and then continuously labeled with BrdU, display asymmetric cell kinetics in CsCl density gradient analyses of BrdU labeling kinetics. Because asymmetric cell kinetics are induced before BrdU is added in these studies, it is predicted that immortal DNA strands will be unlabeled at the time of "strand selection" and therefore, will appear in the HL peak of DNA from asymmetrically cycling cells. In CsCl gradient profiles, DNA from asynchronous populations will also contain DNA from non-cycling cells produced after the first generation from asymmetrically cycling cells in the presence of BrdU. Analysis of mitotic cells provides a means to eliminate DNA from non-cycling cells in the HL peak and specifically evaluate immortal DNA strands, bearing DNA in this position. The expected ratio of HH DNA to immortal strand containing HL DNA in mitotic cells is 1:1, since the immortal strands should not incorporate BrdU. This 1:1 ratio of HH:HL DNA in mitotic cells should hold true even after prolonged labeling times. Cells randomly assorting DNA will have a mixture of labeled and unlabeled strands, over time with newly replicated BrdU containing strands, the unlabeled strand will be significantly diluted. By selecting mitotic cells at the endpoint of the continuous labeling study, the non-random segregation of immortal DNA strands can be demonstrated.

## A. Symmetric Cell Kinetics

***Random Chromosome Segregation***

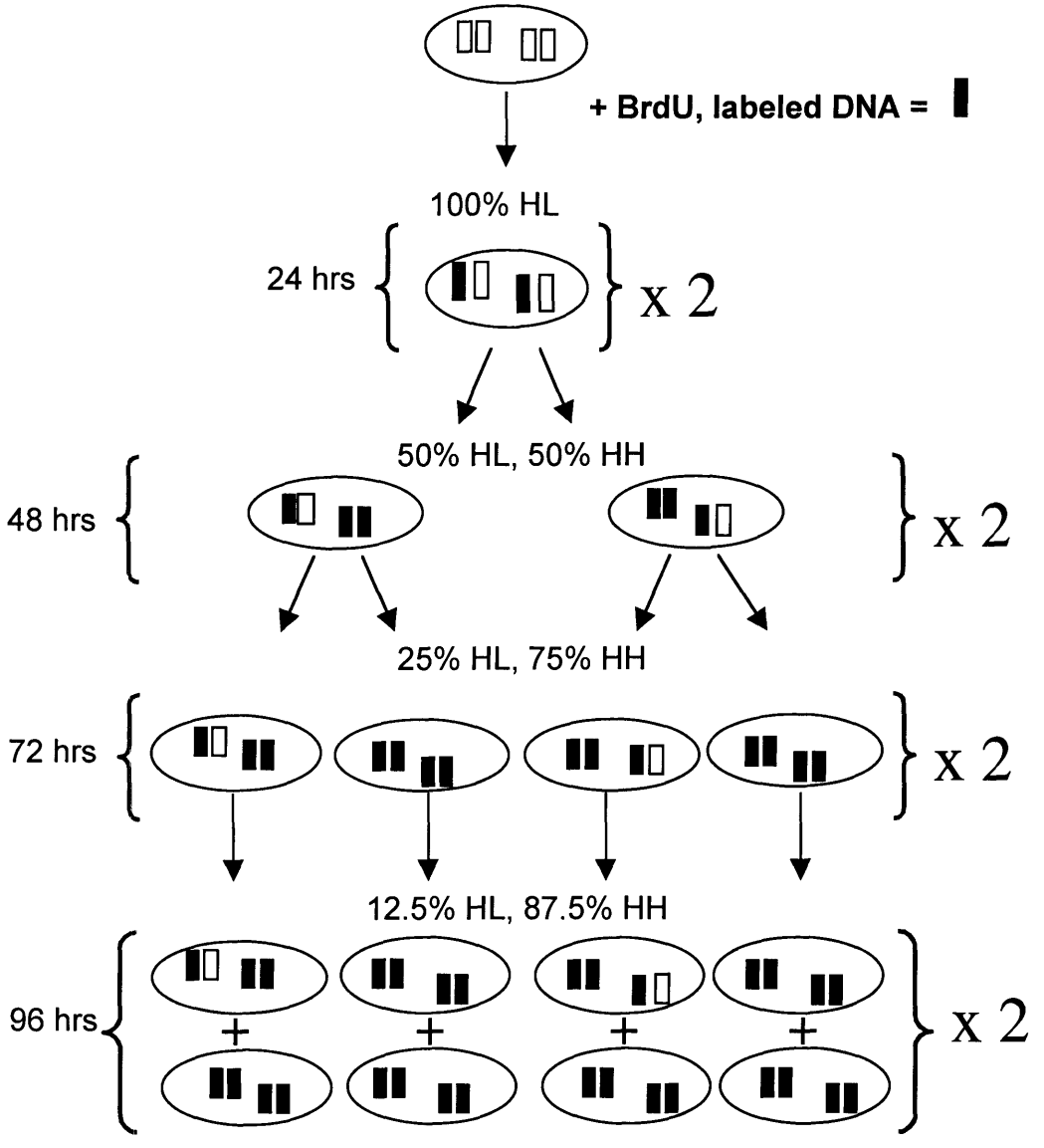


Symmetrically Cycling Cells
1:7 ratio of HL :HH DNA

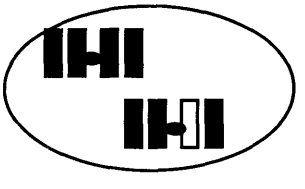

Mitotic Cells with randomly assorted chromosomes, 1:7 HL:HH DNA

## B. Asymmetric Cell Kinetics

***Non-random Co-segregation of Immortal DNA Strands***

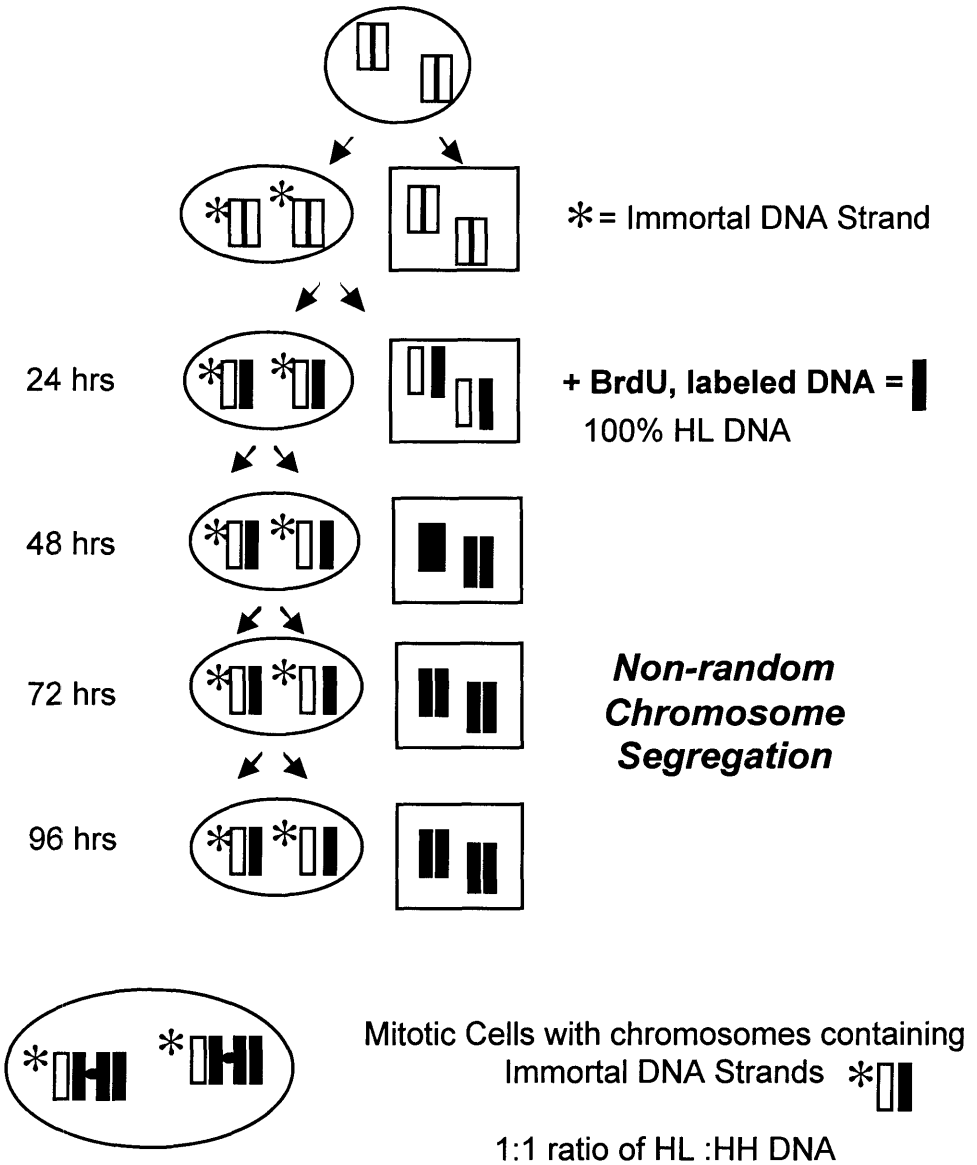


**Figure 1. Predicted Mitotic Cell HL:HH Distributions in Cells with Non-Random Immortal DNA Strand Segregation**

After asymmetric cell kinetics is induced, BrdU is added to label all newly replicated DNA. Symmetrically cycling cells (Figure 1A) randomly assort chromosomes and continuously incorporate BrdU into newly synthesized DNA, to create a majority of HH DNA after 96 hours. In contrast, asymmetrically cycling cells (Figure 1B) retain unlabeled immortal strands with each asymmetric division. After multiple divisions in the presence of BrdU, mitotic asymmetrically cycling cells will non-randomly segregate unlabeled immortal DNA strands to the cycling cell. The collected asymmetrically cycling mitotic cells will contain a DNA content of 1:1, HH:HL DNA, regardless of how long the cells are grown in BrdU.

▮▯ = HL duplex DNA, * ▯= Immortal Strand DNA, ▮▮= HH duplex DNA, O = cycling cell, □ = non-cycling cell.

**Experimental Methods:**

Cells were plated at 2 X $10^4$ cells/150cm$^2$/30mls and induced to cycle asymmetrically with 75μM $ZnCl_2$. After 24 hours of asymmetric cell kinetics, an aliquot of 20mM BrdU was added to each flask so that the final BrdU concentration was 20μM. The cells were cultured with BrdU for 41 hours (1 experiment) and 96 hours (2 experiments). In experiments performed for 96 hours, cells were counted before $ZnCl_2$ addition and at the end of the experiment to determine the number of population division cycles (PDC) as described in Chapter 2, Section B. DNA was extracted from mitotic cells and analyzed by CsCl gradients as described in the Experimental Methods section of Chapter 1.

**Results:**

A total of three continuous labeling mitotic shake-off experiments were performed. One experiment was done at 41 hours and two were performed at 96 hours. The CsCl gradients for all experiments were analyzed and evaluated by fractionating the gradients, quantifying the DNA per fraction, measuring the CsCl density per fraction, and determining the internal standard position as described in Chapter 1. Peak areas were calculated for all experiments. Experiment 1 at 41 hours is shown below. Though not performed in parallel with this experiment Chapter 1, Fig 1 panels at 48 hours provide an approximation of the profiles for asynchronous cells near the same labeling time.

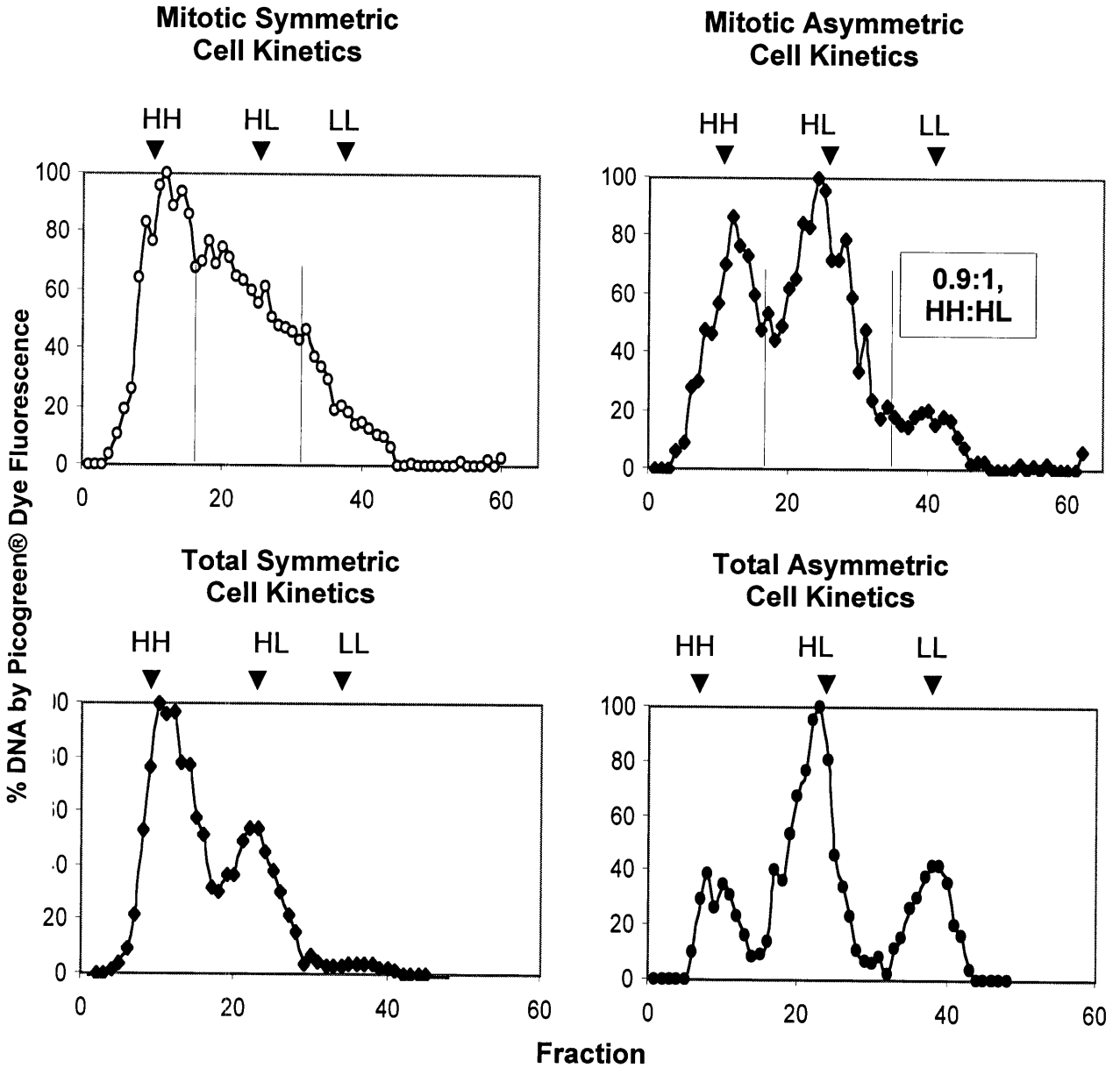


**Figure 2. Evidence for Retention of Unlabeled Immortal DNA in Cells Cycling Asymmetrically in BrdU for 41 hours**

Mitotic cells were collected by mitotic shake off and their DNA extracted and purified. DNA extracted from mitotic cells was analyzed using equilibrium CsCl density gradients. The symmetric mitotic DNA profile has one resolved peak at the position of HH DNA ($\rho$ = 1.784 g/cm$^3$). The DNA from mitotic asymmetrically cycling cells shows two well-resolved peaks at the HH ($\rho$ = 1.786 g/cm$^3$) and HL positions ($\rho$ = 1.750 g/cm$^3$). The ratio of HH:HL was 0.9:1 for asymmetrically cycling mitotic cells. Asynchronous samples grown continuously in BrdU for 48 hours (samples not done in parallel) are shown to compare the difference in the HL:LL ratios between mitotic cells retaining immortal DNA strands, 0.9:1, and asynchronous asymmetrically cycling cells 0.5:1.

The mitotic symmetrically cycling cells have a major peak at the HH position ($\rho$ = 1.784 g/cm$^3$) and a large amount of DNA running in the HL position, though this material is not resolved. This agrees with the expectation that the majority of the DNA will be fully labeled in a 3:1 HH:HL ratio. DNA from symmetrically cycling cells is found at the position of HL DNA, but the peak is not well-resolved. In contrast, the CsCl gradient profile of the mitotic asymmetric cells shows two major peaks, one at the HH position ($\rho$ = 1.786 g/cm$^3$) and one at the HL position ($\rho$ = 1.750 g/cm$^3$). The HH:HL peak area ratio was determined to be 0.9:1. In addition, there is a small peak of DNA at the LL position. Because the DNA contains no BrdU, it most likely comes from non-cycling cells that were detached with the mitotic shake off. The peak area ratio of HH:HL DNA for the symmetrically cycling cells was 1.3:1. In Chapter 1, the CsCl gradient total profiles of asymmetric cells at 48 hours (Chapter 1, Figure 1) show a different profile than the mitotic cells. The HH:HL:LL peak area ratios were 0.5:1:0.5 and closely match the expected ratios for asynchronous cells growing with asymmetric stem cell kinetics for 48 hours. It is important to note that the mitotic cells at 41 hours have the expected 1:1 ratio of HH:HL DNA but the total DNA at 48 hours has a 0.5:1 ratio. At 48 hours, it is expected that there would be more HH DNA created in the asynchronous cultures than the 41 hour mitotic cultures. The asynchronous profile for symmetrically cycling cells at 48 hours closely matches the profile for the related mitotic cells. The results for DNA from asymmetrically cycling mitotic cells labeled with BrdU for 41 hours supports the immortal strand hypothesis.

For the 96 hour mitotic shake off continuous label experiment, the essential method used in the 41 hour experiment was repeated. The immortal strand hypothesis predicts that the 1:1 HL:HH ratio in mitotic cells should be stable for many cell

generations. The CsCl gradient profiles of mitotic cells selected after 96 hours of asymmetric and symmetric growth in the presence of BrdU are shown below in Figure 3.

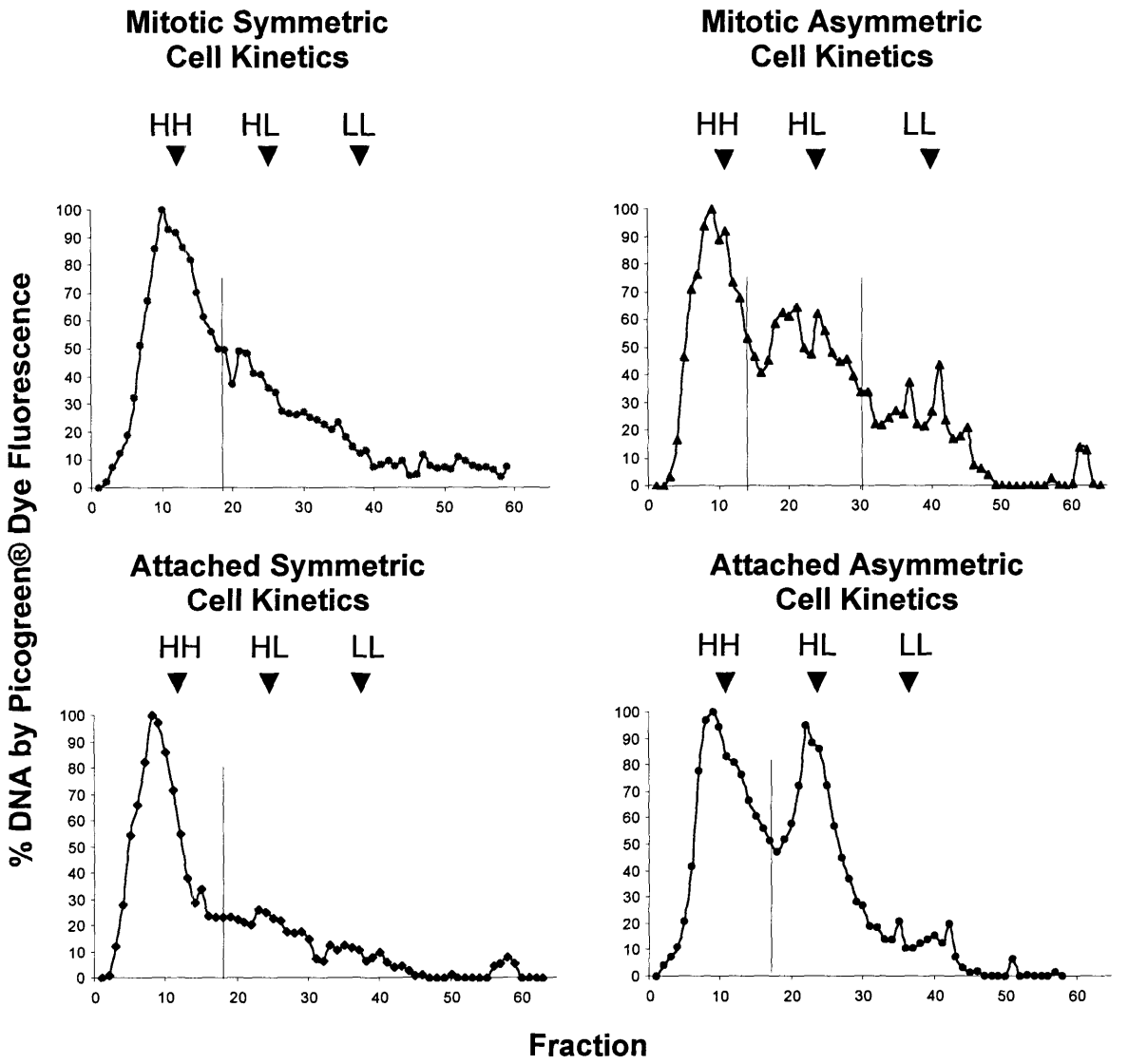


**Figure 3. Evidence for Stable Inheritance of Unlabeled Immortal DNA in Asymmetrically Cycling Cells Labeled with BrdU for 96 hours**

DNA extracted from mitotic cells was analyzed on CsCl density gradients after continuous labeling in BrdU for 96 hours. The DNA was quantified using Picogreen®. The symmetric mitotic DNA profile has one major resolved peak at the position of HH DNA ($\rho$ = 1.780 g/cm$^3$) and a smaller peak at the HL position. The DNA from mitotic asymmetrically cycling cells has two well-resolved peaks at the HH ($\rho$ = 1.796 g/cm$^3$) and HL($\rho$ = 1.750 g/cm$^3$) positions. The cells remaining after the mitotic shake off were also analyzed and showed one major peak a t the HH position for symmetrically cycling cells and two peaks at HH and HL for asymmetrically cycling cells.

The CsCl gradient profiles for the cells at 96 hours are different between asymmetrically and symmetrically cycling cells. The DNA from asymmetrically cycling cells on CsCl density gradients display similar peak areas at the positions of HH and HL. Although the resolution differs, the areas are very similar. The symmetric cells show a major peak at HH, with a small DNA peak at the HL position. The relative areas of the peaks are summarized in Table 1.

**Results for Mitotic Symmetrically Cycling Cells**

| | Observed Ratios | | | | Expected Ratios | | |
|---|---|---|---|---|---|---|---|
| BrdU Label (hours) | HH | HL | LL | | HH | HL | LL |
| 41 | 1.3 | 1 | 0.2 | | 3 | 1 | 0 |
| 96 | 3 | 1 | 0.1 | | 7 | 1 | 0 |
| 96 | 2.4 | 1 | 0.3 | | 7 | 1 | 0 |

HH Peak Chi-Squared Value, $X^2 = 6.8$ (5 degrees of freedom), p-value = 0.24

**Results for Mitotic Asymmetrically Cycling Cells**

| | Observed Ratios | | | | Expected Ratios | | |
|---|---|---|---|---|---|---|---|
| BrdU Label (hours) | HH | HL | LL | | HH | HL | LL |
| 41 | 0.9 | 1 | 0.2 | | 1 | 1 | 0 |
| 96 | 1.1 | 1 | 0.2 | | 1 | 1 | 0 |
| 96 | 1 | 1 | 0.5 | | 1 | 1 | 0 |

HH Peak Chi-Squared Value, $X^2 = 0.58$ (5 degrees of freedom), p-value = 0.99

**Table 1. Comparison of Observed vs. Expected Peak Area Ratios for Mitotic Cells Continuously Labeled in BrdU**

Observed peak area ratios were determined from CsCl gradients and compared with expected peak area ratios calculated from modeling asymmetric and symmetric cell kinetics. Chi-squared values were determined by comparing the observed and expected peak area ratio values for the HH and LL peaks.

At 96 hours, the observed HL:LL peak area ratio for the asymmetrically cycling cells is 1:1 (average, n=2), whereas the observed HL:LL peak area ratio for the symmetric cells is 3:1 (average, n=2). The peak area ratios for the asymmetrically cycling mitotic cells agrees with the expected 1:1 HL:LL ratio and matches the modeled expectation for immortal strand retention in mitotic cells. The peak area ratio of 2:1 HH:HL for the symmetric cells does not match the expected 7:1 ratio. This is probably due to the symmetric cells either running out of Brdu label or the cells in the flask becoming confluent so that cells cannot completely label their DNA out to 96 hours.

The continuous labeling study with mitotic shake off at 41 hours and 96 hours show retention of immortal strands based on the peak area ratio of the HH DNA peak to the immortal strand containing, HL peak. The structure of immortal strand DNA found in mitotic cells confirms that our modeling for immortal strand retention is correct. The DNA in mitotic cells appears to be HL or HH with no novel forms of DNA detected using this method.

**Conclusions:**

In continuous BrdU label studies, asymmetric cell kinetics are induced prior to the addition of BrdU, therefore the immortal strand remains unlabeled and is found in the HL peak of CsCl gradients. In cycling mitotic cells retaining unlabeled immortal strands, their 4N DNA content should be a mixture of HL:HH DNA in a 1:1 ratio. This ratio should be constant for multiple generations of BrdU labeling, if an immortal strand mechanism is taking place. Experiments at 41 hours and 96 hours show that the 1:1 ratio of HL:HH DNA is maintained from 41 hours out to 96 hours, providing independent physical confirmation that an immortal strand mechanism is present.

These results confirm a previous observation *in situ* using anti-BrdU antibodies to detect immortal strand retention (Merok et al., 2002). The continuous labeling studies also show that the structure of retained immortal strand DNA exists in a typical DNA form.

**Discussion:**

The continuous labeling studies with mitotic selection allow for the detection of DNA bearing immortal DNA strands. In these studies, the immortal strands are sequestered in the HL peak of CsCl gradients. The peak area ratio for mitotic cells retaining unlabeled immortal DNA strands is expected to be 1:1, HH:HL. A 1:1 ratio was in fact observed for asymmetric cells both at 41 hours and 96 hours, confirming the immortal strand mechanism in model cells.

An important question to address was whether or not retained immortal DNA strands had a different DNA structure than non-immortal DNA. According to the observed results of immortal strand containing DNA on CsCl gradients, there is no detectable structural modification to the DNA that resulted in a significant or measurable density shift or peak character difference. It is interesting to note that the mitotic DNAs did have more heterogeneity in their gradient profiles. This may be a result of lower yields of DNA with peaks that are closer to the signal to noise threshold. This heterogeneity is not consistently observed in other experiments where mitotic cells are harvested.

The continuous label studies not only confirm immortal strand retention, but also prove to be a useful assay for resolving immortal strand containing DNA molecules. This assay could potentially be used for other stem cell lines to study their kinetics and

evaluate immortal DNA strand retention. In addition, because the HL immortal strand containing DNA peak is purified from the LL and HL non-immortal strand DNA peaks, the HL DNA peak can be further evaluated for any unique properties of immortal strands. These ideas will be addressed further in Chapter 3.

**References:**

Ashman CR, Kaufman ER, Davidson RL, *Bromodeoxyuridine mutagenesis and deoxyribonucleotide pool imbalance in mammalian cells.* Basic Life Sci, 1985. **31**:p.391-408. Review.

Davidson RL, Kaufman ER, *Bromodeoxyuridine mutagenesis in mammalian cells is stimulated by thymidine and suppressed by deoxycytidine.* Nature, 1978. **276**: p.722-3.

Luk, D.C.,and Bick, M.D., *Determination of 5'-Bromodeoxyuridine in DNA by Buoyant Density. Analytical Biochem.*, 1968. 77:p.346-349.

Merok, JR, Lansita, JA, Tunstead, JR, Sherley, JL, *Cosegregation of Chromosomes Containing Immortal DNA Strands in Cells that Cycle with Asymmetric Stem Cell Kinetics.* Cancer Res., 2002. **62**: p. 6791-6795.

# Chapter 3. Physicochemical Characterization of DNA from Cells Undergoing Immortal Strand Co-Segregation

## Section A: DNA Base Composition Analyses

**Rationale:**

If model cells with asymmetric stem cell kinetics retain immortal DNA strands, it is possible that cells are able to distinguish immortal from non-immortal DNA by a molecular tag that allows a cell to preferentially select immortal DNA strands. One hypothesis evaluated in this research is that immortal DNA strands are globally modified in a way that distinguishes them from non-immortal DNA. If this were true, the chemical structure of DNA bases of immortal strands could differ from non-immortal DNA strands.

As more non-immortal DNA strands are made with each generation, the ratio of immortal to non-immortal DNA will decrease (Figure 1).

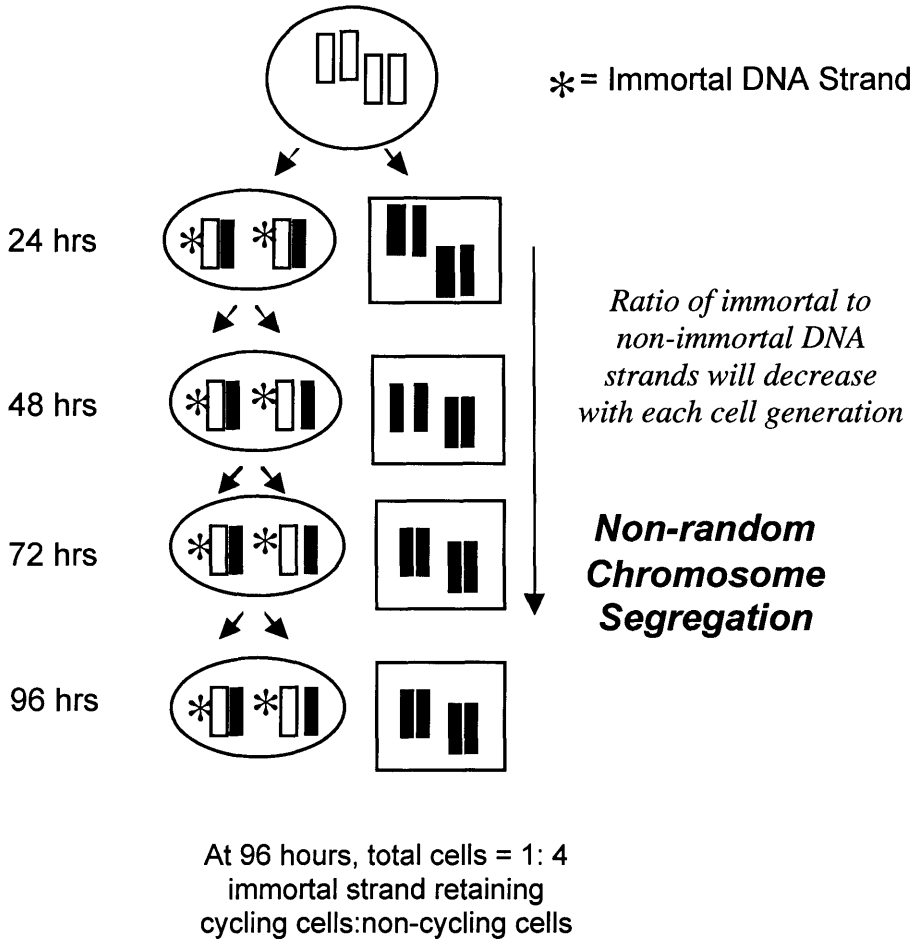


**Figure 1. Respective Dilution and Accumulation Kinetics of Immortal and Non-Immortal DNA Strands in Asymmetrically Cycling Cell Cultures**

As cells divide asymmetrically, non-cycling cells are produced with each generation. If the immortal strand contained in the cycling cell is modified, a change in DNA base composition will be diluted over time as the ratio of cycling to non-cycling cells decreases. If the non-immortal strands are modified, the base modification is expected to increase over time, as more non-cycling cells are produced. If there is no modification, there will be no change in DNA base composition over time.

* ▯ = immortal strand, ▮ = non-immortal strands, O = cycling cell, □ = non-cycling cell.

A DNA modification could occur on either the immortal DNA strand or the non-immortal DNA strand. If the modification occurs on the immortal DNA strand, its frequency will decrease as more non-cycling cells with unmodified DNA are made. If the modification occurs on the non-immortal strand, the modification will increase over time. And if there is no modification, there will be no change in the DNA base composition. A global analysis of the DNA was performed to determine whether an overall modification to the DNA could be detected. Using reverse-phase high performance liquid chromatography (HPLC), a chemical modification such as a DNA base modification, could be detected to a level of sensitivity of 10 picomoles, or a 0.2% (1/500 bases) modified base frequency, estimated for mouse genomic DNA . DNA samples from total asynchronous cultures grown in the presence or absence of BrdU were studied in these analyses.

A major assumption of this experiment is that the modification to immortal strands is global and detectable by this HPLC method. This methodology would fail to detect low frequency localized modifications to the DNA at chromosome sites such as the centromere, telomere or specific genes, fall below the system's level of detection, of a 0.2% (1/500 bases) modified base frequency.

**Experimental Method:**

DNA was extracted and quantified as previously described in Chapter 2 Section A. 5 μg of purified DNA in 200μls of TE pH 8.0, was precipitated in a microcentrifuge tube by adding two volumes of 200 proof ethanol, 400μls, and 1/10 of the aqueous volume, 20μls, of sodium acetate. The DNA was pelleted by microcentrifugation for 30 minutes, at 4°C, and maximum speed 13,200 rpm (16,500 x g). The DNA pellet was

washed with 70% ethanol for 15 minutes, at 4°C, and maximum speed (16,500 x g). The ethanol supernatant was poured off and the pellet was air-dried for 30 minutes. Samples were reconstituted in 10mM Tris, pH 7.2. The purified DNA was denatured to single-strands by placing in a heating block (VWR) for 2 minutes at 100°C. Samples were immediately quenched in ice water to prevent reannealing. 15mM Sodium acetate, pH 5.3 was added to the sample and 10mM ZnSO4 was added to a final concentration of 0.5mM. 10 U/mg of nuclease P1 (Roche Diagnostics) was added from a 1 mg/ml stock solution of nuclease P1 in 30mM sodium acetate, pH 5.3. Bacterial alkaline phosphatase (BAP) was used at a concentration of 150 U/ml (supplied by Sigma Aldrich). BAP was treated with coformycin (CalBiochem) by adding 1/10 vol of 1 mg/ml coformycin stock solution diluted in MilliQ H20 before addition of BAP to samples in order to inhibit deoxyadenosine deaminase activity (Aggarwal et al., 1977; Dong, Min, personal communication.). Samples were incubated for 2 hours at 37°C. 0.5M Tris-HCl, pH 8.5 was added to a final concentration of 50mM. Samples were incubated for an additional 2 hours at 37°C. Samples were stored at -20°C until HPLC using the methods of Gehrke et al, 1984.

**HPLC Analysis Method**

The HPLC running buffers used were 2.5% methanol and $KH_2PO_4$ and 8% Methanol in $KH_2PO_4$. All buffers were filtered and diluted using MilliQ purified water. Methanol was HPLC grade and supplied by Sigma-Aldrich.

10mM stock solutions of nucleotide standards were prepared for 2'-deoxyguanosine (dG), 2'-deoxythymidine (dT), 2'-deoxycytidine(dC), 2'-deoxyadenosine (dA), 2'-deoxyuridine (dU) and 2'-deoxyinosine (dI). In addition, 7'-methyl-guanosine

(7-Me-G) was used as an internal standard for both samples and standard mixes. 10mM stock solutions of each standard were prepared in MilliQ water and sterile filtered using a 0.25 μM filter. The peak areas for standards ranging from 10 picomoles to 500 picomoles were determined and standard curves were generated with a linear regression ($R^2$) value of 0.99 or greater for each standard curve. Areas were converted to picomoles using the linear equation determined from each standard curve.

Each sample was spiked with the 7-Me-G internal standard to determine peak positions and identification. 1μl of a 10mM stock of 7-Me-G was added to each 40 μl sample immediately before injection.

HPLC analysis was performed using a Hewlett Packard 1040A system coupled with a UV-diode array detection system, Hewlett Packard Series1050. 20 μl sample volumes were injected using a syringe. A reversed phase column, Supelcosil LC-18-DB, 25 cm x 4.6mm, 5μm (Supelco) was used for nucleotide separation. A guard column Supelguard LC-18-DB (Supelco) was used. Buffer A: 2.5% methanol and 0.05 M $KH_2PO_4$ was run from 0 minutes to 22 minutes. Buffer B: 8.0% methanol in 0.05 M $KH_2PO_4$ was run from 23 minutes to 50 minutes. The total run time per sample was 50 minutes. The column was allowed to equilibrate with buffer A, for 10 minutes before injecting the next sample. Every two samples, a 10 minute wash of 100% methanol was run through the column in order to remove any residual nucleotides or contaminants from the column. The column was re-equilibrated with buffer A before injection of the next sample. The column flow rate was 1ml/min. UV diode array detection was performed at 254nm (4nm bandwidth) and 280 nm (4nm bandwidth), using a reference wavelength of 300 nm (50nm bandwidth). Spectra of all samples were stored from 190 nm - 600 nm.

Sample areas were determined using HPChemStation for LC and LC/MS, peak integration software. Sample quantitation was done by determining the mole % values for dC, dG, dT, dA, and 7-Me-G in each sample. Mole % values were calculated by taking the absolute picomoles calculated from the areas for each base and normalizing to the total picomoles of dT, dG, dC, and dA. The HPLC peak traces showed a consistent pattern for all samples.

**CsCl Peak Analysis**

DNA from CsCl gradients was collected by pooling the fractions corresponding to the HL and LL DNA peaks of the pulse chase CsCl density gradient samples. After the fractions were pooled, a 10X volume of distilled, sterile water was added to substantially dilute the CsCl to the point that it would not be precipitated with the DNA. 1/10 volume of sodium acetate was added to the diluted pooled fractions and 2 volumes of 100% ethanol were added. The samples were spun in 50 ml Nalgene centrifugation tubes on a Sorvall RC5B Plus Centrifuge at 9,000x g at 4°C for 30 minutes. Samples were washed with 70% ethanol for 15 minutes at 4°C and 9,000xg. Pelleted DNA samples were then reconstituted with TE pH 8.0. The TE was carefully washed down the side of the centrifuge tube because the pellet was not visible to the naked eye. Samples were quantified using Picogreen® dye as described.

**Results:**

Asymmetrically and symmetrically cycling samples grown in the presence of BrdU for 24, 30, 48, 72, and 96 hours were harvested and their DNA purified. The BrdU containing DNA samples were prepared for HPLC analysis by enzymatic digestion and

analyzed by HPLC. The mole % values for all BrdU labeled samples are shown in Figure 1. For all four bases, there were no significant diffferences in % mole fraction between asymmetric and symmetric cycling cells. There was a higher degree of variation for dG and dA analyses across all time points. The experiment was repeated in the absence of BrdU in order to evaluate whether BrdU contributed to the observed variation.

A similar experiment was performed for samples grown in the absence of BrdU. Cells were harvested at 0 hours, 36 hours, 72 hours, and 96 hours. All DNA samples were analyzed twice except for the one for the 72 hour time point. The results of this experiment were similar to the results when BrdU was present, but reduced variance was present for replicate enzymatic assays. The overall variance was similar among individual time point determinations. No significant differences were noted in base composition between symmetric and asymmetrically cycling cells as a function of time after induction of asymmetric cell kinetics. More over, no evidence for modified bases was obtained at any time in the analyses, with or without BrdU.

Figure 3 summarizes the results of the mole % determinations for samples across all time points either in the presence, Trial 1, or absence of BrdU, Trial 2. When comparing the results of the two trials summarized in Figure 3 and Table 1., there is no indication of a significant difference in base composition between the symmetric and asymmetric cycling cells. The determined mole % values for dG and dC agree with the expected G+C content of 42% determined in the mouse genome project (Waterston, RH, et al., 2002). The calculated G+C content observed in these experiments ranged from

43% - 49%, somewhat higher than the expected G+C content but well within the range of error for these experiments.

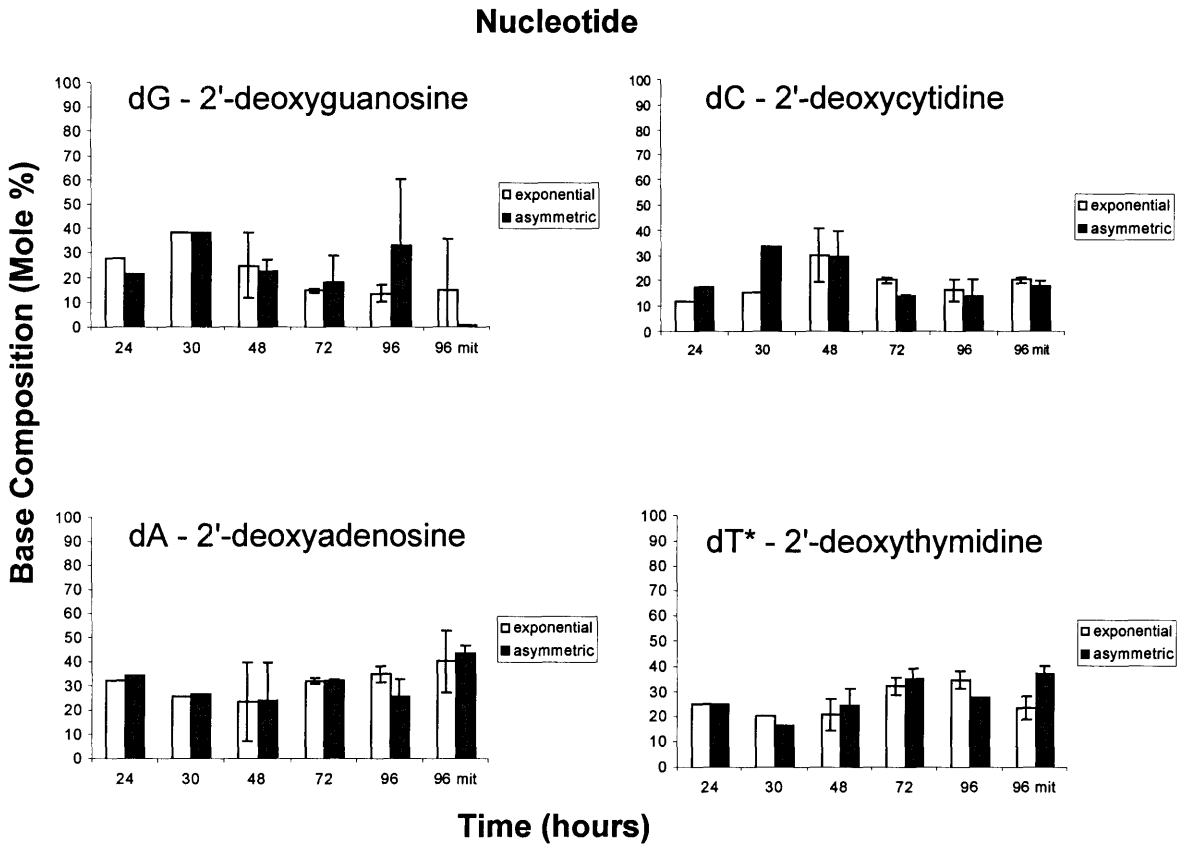


**Figure 2. DNA Base Composition Analysis for Cells Labeled Continuously with BrdU**
Asymmetrically and symmetrically cycling cells were grown in the presence of BrdU for 24, 30, 48, 72, and 96 hours. Total asynchronous cells were harvested, and their DNA extracted. Purified DNA samples were enzymatically digested into nucleotides for HPLC analysis. Each time point represents two samples except for the 24 hour and 30 hour time points, where only 1 nucleotide measurement was made. The average of the enzymatic digestion samples for each DNA preparation is graphed., except for the 24 hour and 36 hour time. Error bars indicate the range of the data. dT* mole % is determined by summing dT and BrdU.

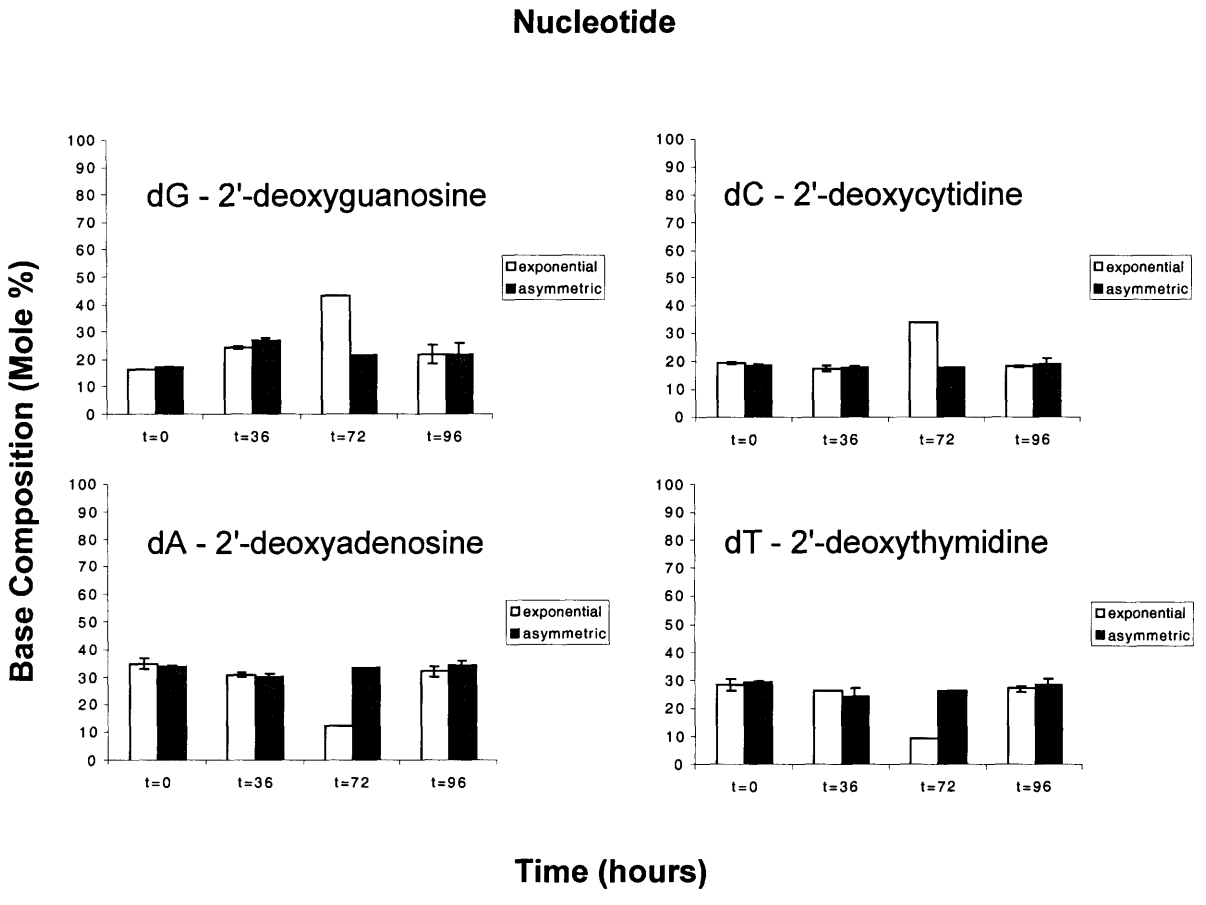


**Figure 3. DNA Base Composition Analysis of Cells Cultured without BrdU**
Asymmetrically and symmetrically cycling cells were cultured for 24, 30, 48, 72 and 96 hours (in the absence of BrdU). Total asynchronous cells were harvested, and their DNA extracted. Purified DNA samples were enzymatically digested into nucleotides for HPLC evaluation. The average of the enzymatic digestion samples for each DNA preparation is graphed, except for the 72 hour time point.

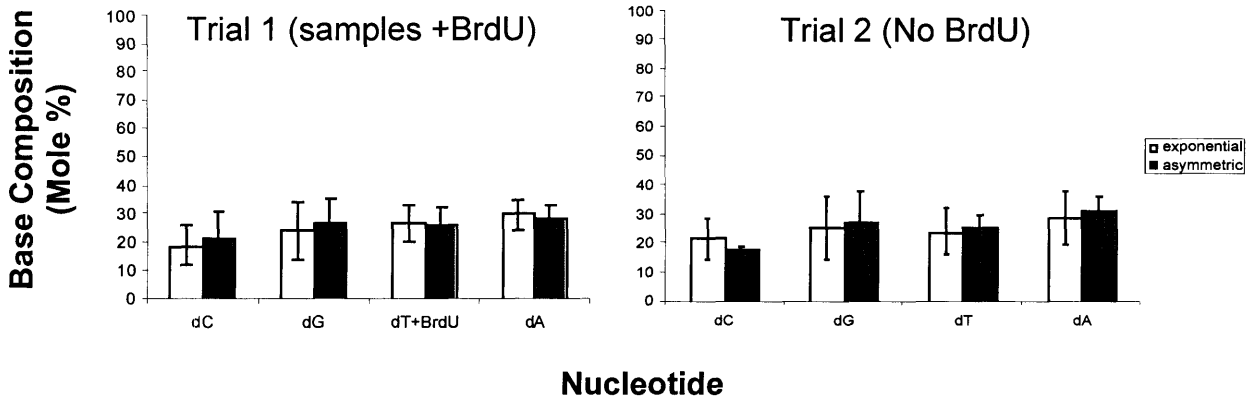


**Figure 4. Summary of Total DNA Base Composition Analyses: Average of BrdU Samples, Trial 1 and non-BrdU Containing Samples, Trial 2**
The mole % values of symmetric and asymmetric cells cultured in the presence, Trial 1, and absence of BrdU, Trial 2, were averaged across all time points.

**HPLC Analysis of Cells Continuously Labeled with BrdU**

| | symmetric, n=10 | asymmetric, n=10 |
|---|---|---|
| dC | 19 ± 6.9 | 22 ± 9.2 |
| dG | 24 ± 10 | 27 ± 8.6 |
| dT* | 27 ± 6.5 | 26 ± 6.6 |
| dA | 30 ± 4.9 | 29 ± 4.7 |

**HPLC Analysis of Cells Grown in the Absence of BrdU**

| | symmetric, n = 7 | asymmetric, n = 7 |
|---|---|---|
| dC | 22 ± 7.0 | 18 ± 1.4 |
| dG | 25 ± 11 | 27 ± 11 |
| dT | 24 ± 8.1 | 26 ± 4.4 |
| dA | 29 ± 9.2 | 31 ± 5.2 |

**Table 1. Summary of Mole % Values from Cells Cycling Asymmetrically or Symmetrically with and without BrdU from 24 hours to 96 hours**
The average mole % values from Trials 1 and 2 are shown.
**dT*** = the mole % value of BrdU + dT.

DNA from CsCl gradients was collected in order to investigate the possibility of immortal strand specific DNA modifications in more specific DNA species. The fractions corresponding to LL and HL DNA peaks were pooled from the pulse chase mitotic shake off experiments. The HL peak, expected to contain immortal DNA strands did not yield sufficient DNA for analysis. The LL DNA peak did yield a substantial amount of DNA for HPLC analysis. In these experiments, the LL DNA peak corresponds to non-immortal DNA in asymmetrically arrested cells. The base composition results are shown in Figure 5.

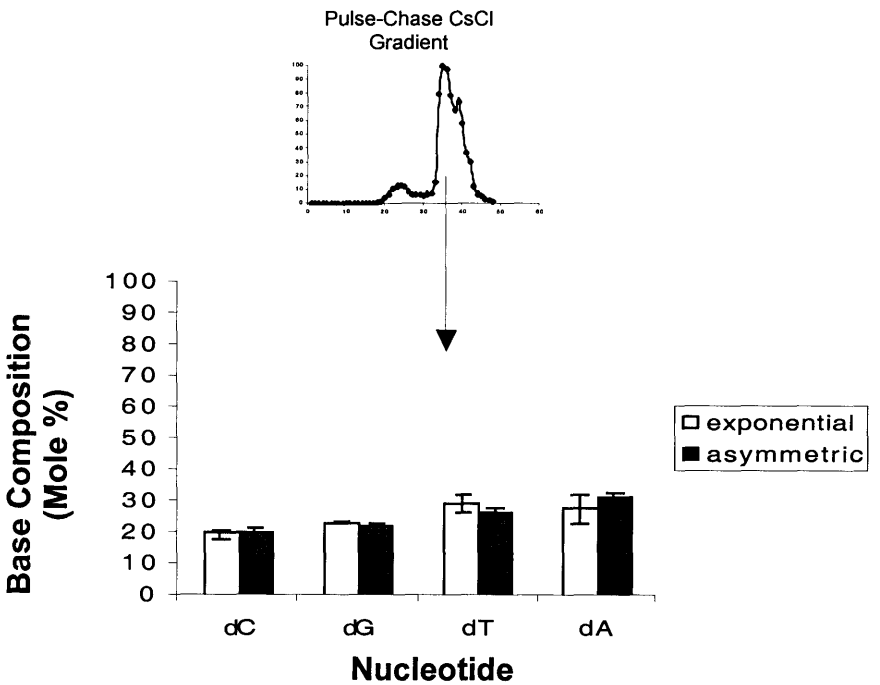


**Figure 5. Base Composition Analysis of Non-Immortal DNA from Asymmetrically Cycling Cells Isolated in CsCl Density Gradients**
CsCl fractions were pooled, diluted, and precipitated using ethanol and sodium acetate. The pooled DNA was enzymatically digested for HPLC analysis. The mole % values of symmetrically cycling and asymmetrically cycling cells DNA from the LL peak of the pulse-chase mitotic shake off studies were determined by HPLC. Graphed are the averages of replicate HPLC analyses. Error bars indicate the range of the data. The absolute values for all determinations are shown in Table 2.

| Mole % | Symmetric, n=2 | Asymmetric, n=3 |
|---|---|---|
| dC | 20 ± 1 | 20 ± 2 |
| dG | 23 ± 0.47 | 22 ± 1 |
| dT | 29 ± 2.70 | 26 ± 1.0 |
| dA | 28 ± 4.5 | 32 ± 0.85 |

**Table 2. Summary of Mole % Determinations of DNA from Mortal DNA Isolated in CsCl Gradient Analysis**
The mole % values were calculated for the LL DNA peak collected from the pulse-chase mitotic shake off CsCl gradient.

Analysis of the LL DNA peak from the pulse chase CsCl gradient analysis showed no significant differences in the mole % values between the asymmetric and symmetric cells. The observed results show that the non-immortal strand has no detectable DNA base modification.

## Conclusions:

The base composition analyses of DNA samples grown asymmetrically and symmetrically in the presence of BrdU showed no significant differences in the nucleotide mole % values. DNA samples from asymmetrically cycling cells grown in the absence of BrdU were also analyzed by HPLC. The observed mole % values for samples without BrdU confirmed the determined mole % values from samples grown in the presence of BrdU by showing no significant nucleotide composition differences. The results from the two HPLC trials provide strong evidence that a global DNA base modification does not exist in the non-immortal strand in total DNA samples over time with asymmetric cell kinetics.

Analysis of DNA samples collected from the LL peak of the pulse-chase CsCl gradient analyses did not show a significant difference in DNA base modification, even though non-immortal strands are enriched for in the LL DNA peak in these gradients. This result supports the conclusion that a global modification most likely does not exist on the non-immortal strand. The G+C content determinations from these studies agree with values found in the literature (Waterston, RH, et al., 2002). Also, no difference in global methylation of the DNA was observed. The methylation of genomic DNA for both the asymmetirc and symmetric cells was determined to be approximately 5% based on studies done by liquid chromatography and mass spectrometry (LC/MS), (M. Dong, data not shown.).

**Discussion:**

It is possible that no DNA modification was observed in these studies because the modification to the DNA is not detectable by this method. The level of sensitivity of this method is on the order of 10 picomoles, or a 0.2% (1/500 bases) modified base frequency. If a global modification to the DNA is at or below the level of detection of this system, a modification may not have been detected. Also, if the modification were localized to a chromosomal region or specific gene loci, unless it was a very abundant change, the modification would not likely be detected by this system.

## Chapter 3. Physicochemical Characterization of DNA from Cells Undergoing Immortal Strand Co-Segregation

## Section B: DNA Melting Temperatures (Tm) Studies

**Rationale:**

The DNA melting temperature (Tm) is the transition temperature at which half of a population of double-stranded DNA molecules becomes single-stranded. A sharp increase in the UV absorbance at 260nm can be detected at the Tm due to the hyperchromic effect caused by the melting of double-stranded DNA to single-stranded DNA. The thermal denaturation of a double-stranded DNA molecule can reveal if DNA is structurally modified, a high G+C content, or has a chemical modification that stabilizes or destabilizes the DNA helix causing the thermodynamic properties of the DNA to be altered (Marmur and Doty, 1959, 1962). A Tm comparison between DNA samples from asymmetrically cycling cells vs. symmetrically cycling cells could reveal a global modification to the DNA, if the DNA is altered to a significant extent.

The DNA analyzed for these studies was isolated from cells cultured asymmetrically or symmetrically for 36 hours. At the 36 hour time in asymmetrically cycling cultures, the number of cycling to non-cycling cells is approximately 1:2. By selecting cells at the 36 hour time point, the culture is optimized to both divide asymmetrically and yield a ratio of cycling cells to non-cycling cells that will not significantly dilute any modified DNA form that might occur in either kinetic cell type. At the 36 hour time, a modification to either the immortal strand or the non-immortal DNA strand would be more easily detected than at later time points when more non-cycling cells containing non-immortal strands are made. The advantage of the Tm

method is the ability to detect global modifications to the DNA without knowledge of the molecular or chemical details of the modification. However, if the modification is not abundant enough to cause a shift in the melting curve, it will go undetected. One advantage of the Tm method is the ability to detect subpopulations of DNA molecules with distinct melting properties. These would appear as discrete melting phases with discrete Tm's.

**Experimental Method:**

DNA was isolated from cell pellets by phenol-chloroform extraction as described in Chapter 1. The DNA was then ethanol precipitated and reconstituted in TE pH 8.0. The DNA was quantified by UV spectrophotometry or by Picogreen® (Molecular Probes Inc.) fluorescence as described in Chapter 1. Isolated DNA was prepared as a 10-15 µg/ml solution in 30mM sodium phosphate buffer (SPB). SPB was an equimolar mixture of mono- and dibasic sodium phosphate (Cullen et al., 1976). Sample volumes of 1.2ml were placed in 10mm path length quartz cuvettes. The UV absorbance of each sample was monitored at 260nm and read at 1°C intervals (from 20°C -93°C) using a Cary UV-Vis Spectrophotometer with a built in temperature probe (Varian, Inc.). The spectrophotometer's temperature probe was placed in DNA free SPB as a temperature control. Thermal denaturation plots of UV absorbance at 260nm versus temperature were generated by Cary WinUV Thermal software and the Tm value was determined from each plot as the midpoint of the transition. Salmon sperm DNA was used as a quality control for each run.

**Results:**

The Tm curves in Figure 1 are representative of the samples analyzed from cells cycling asymmetrically for 36 hours. In four independent Tm determinations with DNA from cells cycling symmetrically or asymmetrically for 36 hours, the Tm values were not significantly different from each other, nor were they significantly different from the salmon sperm DNA quality control sample (see Table 1).

A major transition at Tm = 74°C, is the expected Tm result. Although the Tm curves from symmetric and asymmetric DNA samples are not superimposable and are slightly shifted from one another, the determined Tm values I the same for both samples. The lack of superimposition is most likely to be due to differences in the double-stranded DNA content of such sample preparations. In summary, a significant difference in Tm between DNA from symmetric and asymmetric cells was not observed.

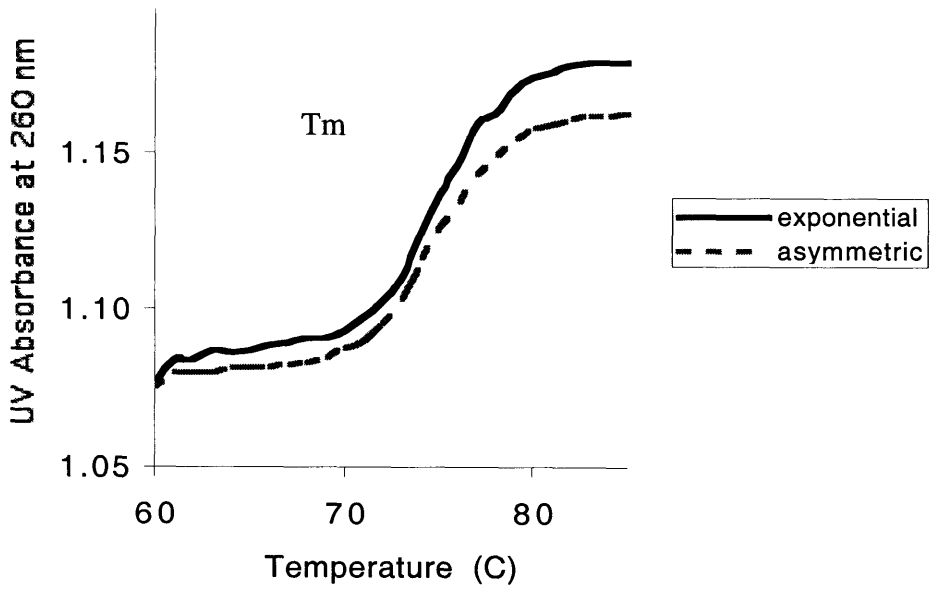


**Figure 1. Thermal Denaturation Curve of DNA from Asymmetrically vs. Symmetrically Cycling Cells**
A 10 - 15 μg/ml solution of DNA from asymmetrically or symmetrically cycling cells was analyzed in a quartz cuvette for UV spectrophotometry analysis. The spectrophotometer's heating block was programmed to increase in temperature by 1°C from 20°C-93°C. The 60°C-80°C of the spectra is shown. The UV absorbance was monitored at each interval. Observed is a major transition at Tm = 74°C in DNA samples for DNA from both asymmetrically cycling and symmetrically cycling cells.

| DNA Type: | Tm (°C) |
|---|---|
| Salmon Sperm DNA | 74.01°C ± 0.41°C(n=8) |
| Asymmetric | 74.0°C ± 0.0°C (n=4) |
| Symmetric | 74.03°C ± 0.77°C (n=4) |

**Table 1. Summary of Tm Determinations from Cells Cycling Asymmetrically or Symmetrically for 36 hours**
Samples of DNA from asymmetric and symmetrically cycling cells were analyzed by determining their Tm values as described in Figure 1. The Tm values for the asymmetric and symmetric cycling cells were not different from one another within the range of error and were not significantly different than the Tm for the salmon sperm DNA quality control.

In four independent Tm determinations for cells cycling symmetrically and asymmetrically for 36 hours, the Tm values were not significantly different from each other nor were they significantly different from the salmon sperm DNA quality control sample.

The Tm curves in Figure 1 are representative of the samples analyzed from cells cycling asymmetrically for 36 hours. The major transition at Tm = 74°C, is the expected Tm result. Although the Tm curves from symmetric and asymmetric DNA samples are not superimposable and are slightly shifted from one another, the determined Tm values are not significantly different.

## Conclusions:

In summary, the Tm studies showed that no detectable global DNA modifications could be determined by conducting thermal denaturation studies of DNA from cells retaining

immortal DNA strands. The Tm for DNA samples cycling asymmetrically and symmetrically was determined to be 74.0°C ± 0°C (n=4) and 74.03°C ± 0.77°C (n=4), respectively in a 30mM sodium phosphate buffer. These values were not significantly different than the determined Tm value for the quality control salmon sperm DNA of 74.01°C ± 0.41°C (n=8), indicating that DNA for cells undergoing asymmetric cell kinetics and immortal DNA strand co-segregation has typical thermodynamic properties.

**Discussion:**

A modification may not have been detected in DNA containing immortal DNA strands by Tm analysis because the modification may not have changed the thermodynamic properties of the DNA to a significant extent or did not effect a significant fraction of DNA molecules. In addition, the modification may not be a global modification to the DNA. A molecular tag to either the immortal or non-immortal strand may be localized to specific genes, or regions of the chromosome such as the centromeres or telomeres. Future experiments to study immortal DNA strands with greater analytical power could use such technology such as mass spectrometry which can detect femtomole changes to the DNA. Also, centromeric or telomeric DNA preparations can be made and analyzed specifically using analytical chemistry combined with molecular biology methods.

**References:**

Marmur, J, Doty, P., *Heterogeneity in deoxyribonucleic acids. I. Dependence on composition of the configurational stability of deoxyribonucleic acids*. Nature, 1959. **183**: p. 1427-9

Marmur, J., Doty, P., *Determination of the base composition of deoxyribonucleic acid from its thermal denaturation temperature.* J. Mol. Biol., 1962. **5**: p. 109-118.

Cullen B, Bick, M., *Thermal denaturation of DNA from bromodeoxyuridine substituted cells*. Nucleic Acids Research, 1976. **3**: p. 49-62.

Gehrke CW, McCune RA, Gama-Sosa MA, Ehrlich M, Kuo KC, *Quantitative reversed-phase high-performance liquid chromatography of major and modified nucleosides in DNA*. J Chromatogr, 1984. **301**:p. 199-219.

R.P. Agarwal, T. Spector and R.E. Parks, Jr.. *Tight-binding inhibitors--IV. Inhibition of adenosine deaminases by various inhibitors*. Biochem. Pharmacol, 1977. **26**:p. 359-67.

Waterston, RH, et al, *Initial sequencing and comparative analysis of the mouse genome*. Nature, 2002. **420**:p. 520-62.

## Chapter 4. Investigation of Proteins Involved in Kinetochore-Microtubule Attachment and Function

### Section A: *In Situ* Immunofluorescence Studies

**Rationale:**

Physicochemical studies of DNA from asymmetrically cycling cells (Chapters 2 and 3) did not reveal a global modification to the DNA that acts as a molecular tag for identifying immortal DNA strands. A DNA modification may still exist that was not detected by our analytical methods. However, it can be concluded that an abundant global modification to the DNA does not exist. It is possible that immortal DNA strands do not have a specific mark on their DNA but are constantly tethered by microtubules so that they are always segregated preferentially to the cycling daughter cell. This mechanism would allow for the co-segregation of all chromosomes with each cycle after immortal strand selection has been initiated. Tanaka, et al., 2002, showed that a mutant form of the Aurora B kinase *S. cerevisiae* homologue IPL1 resulted in monopolar spindle attachment of chromosomes and their co-segregation to one daughter cell. The one qualification of this experiment is that it was performed in cells that were replication defective. From this report, a hypothesis was formed that stable microtubule attachments may account for the non-random chromosome segregation observed in model cells that cycle with asymmetric cell kinetics.

Aurora B kinase is an important protein required for cytokinesis (Terada, et al., 1998), proper chromosome segregation, and sensing tension between microtubules and kinetochores during mitosis (Tanaka et al., 2002; Dewar, et al., 2004). It is a well known chromosome passenger protein that is localized at the centromeres during

metaphase and translocates to the microtubules during the metaphase-anaphase transition localizing at the midbody of cells in anaphase and telophase (Murata-Hori, et al., 2002). If Aurora B is down-regulated or inactivated, a stable microtubule attachment could result in the co-segregation of one full set of chromosomes to one cell as observed by Tanaka, et al., (2002) in *S. cerevisiae*. Aurora B kinase localization and expression were evaluated by immunofluorescence to look for features in the protein that might reflect involvement in the immortal strand mechanism. In addition, the Aurora B kinase paralogue, Aurora A kinase, which localizes to the centrosomes and mitotic spindle during the metaphase to anaphase transition was evaluated (Kufer, et al, 2002). Aurora A kinase has also been shown to be critical for proper chromosome segregation and is emerging as an important cancer marker (Katayama, et al, 2004). A recent study implicates both Aurora A kinase and Aurora B kinase as necessary proteins for proper kinetochore function (Kunitoku, et al, 2003).

**Experimental Method:**

Cells were seeded at $1X10^4$ cells/well in 4-well LabTek chamber slides (Nunc, Inc., Naperville, IL). After 24 hours of plating the cells, medium supplemented to 70μM $ZnCl_2$ was replaced to induce cells on slides to divide asymmetrically. Wells were also left uninduced and changed to fresh media without $ZnCl_2$ as a control. After the 36 hours of culture for asymmetric cell kinetics, the media was aspirated from each well, and the cells were washed with ice cold filtered PBS. Cells were immediately fixed in 3.7% formaldehyde in PBS for 15 minutes at room temperature. After fixation, cells were washed with PBS at room temperature three times for 5 minutes each. Cells were permeablilized and blocked using 0.4% triton-X-100, 0.2% non-fat dry milk ,and 2%

BSA in PBS solution for one hour. Primary antibodies were diluted in the blocking solution. Mouse monoclonal IgG1 Anti-Aurora A kinase and Anti-Aurora B kinase antibodies supplied by BDTransduction Laboratories were used at a concentration of 1:50. Fixed cells were incubated overnight in primary antibody at 4°C. The secondary antibody used was a goat anti-mouse IgG-FITC conjugated antibody supplied by Santa Cruz Biotechnology. The secondary antibody was incubated with the blocking solution at a 1:200 dilution for half an hour before use and microcentrifuged at 6000 rpm for 5 minutes in order to remove any aggregates that could interfere with imaging the cells. The supernatant was taken off and applied to the cells at 37°C for one hour. Counterstaining of nuclei was done with PI or DAPI at 0.1 μg/ml. Slides were mounted using Vectashield® mounting media.

Immunofluorescent images were captured using a Zeiss Axioskop MOT microscope, and a Zeiss Axiocam camera. Images were analyzed using Zeiss KS400 3.0 software. Images were overlayed using Adobe Photoshop software (San Jose, Ca).

**Results:**

Aurora B and Aurora A showed no differences in protein localization between asymmetrically and symmetrically cycling cells. Protein expression level differences were difficult to determine from fluorescent images and so western blotting was done in subsequent experiments (Chapter 4, Section B). In Figure 1, staining for Aurora A kinase in cells cycling symmetrically and asymmetrically, showed no difference in protein localization during mitosis, the only cell-cycle phase in which Aurora A kinase is detectable.

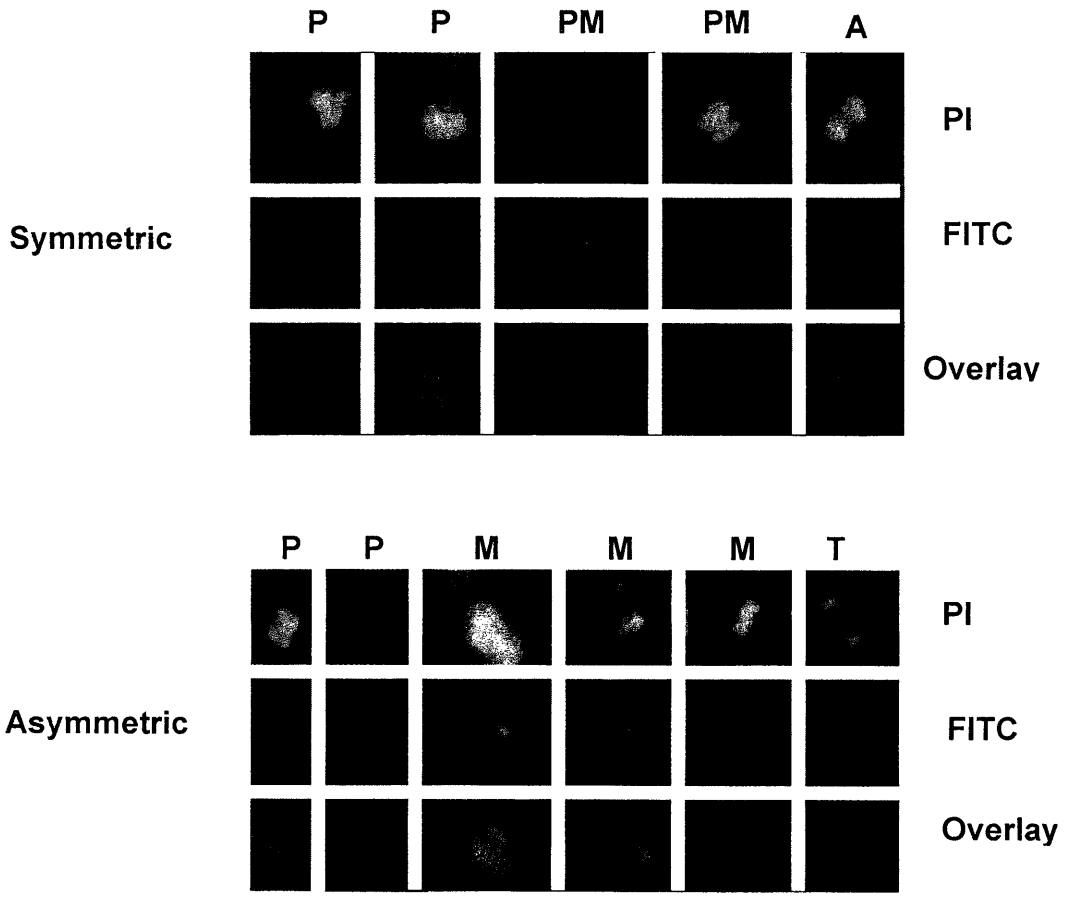


**Figure 1. Aurora A Kinase Localization Studies in Cells Cycling with Asymmetric vs. Symmetric Cell Kinetics**

Cells were plated in 4-well chamber slides and grown for 24 hours before induction of asymmetric cell kinetics. Cells were cultured for an additional 36 hours under asymmetric cell kinetics inducing conditions. Cells were fixed in 3.7% formaldehyde and stained with a monoclonal anti-mouse-Aurora A kinase antibody. Secondary antibody used was a FITC-conjugated goat anti-mouse antibody. Nuclei were counterstained using 0.1$\mu$g/ml PI stain. Cells were imaged and overlayed. Aurora A kinase is localized at the centrosomes and mitotic spindle from prophase through anaphase. 100 X magnification.

**P = Prophase, PM = Prometaphase, M = Metaphase, A = Anaphase, T = Telophase, and I = Interphase.**

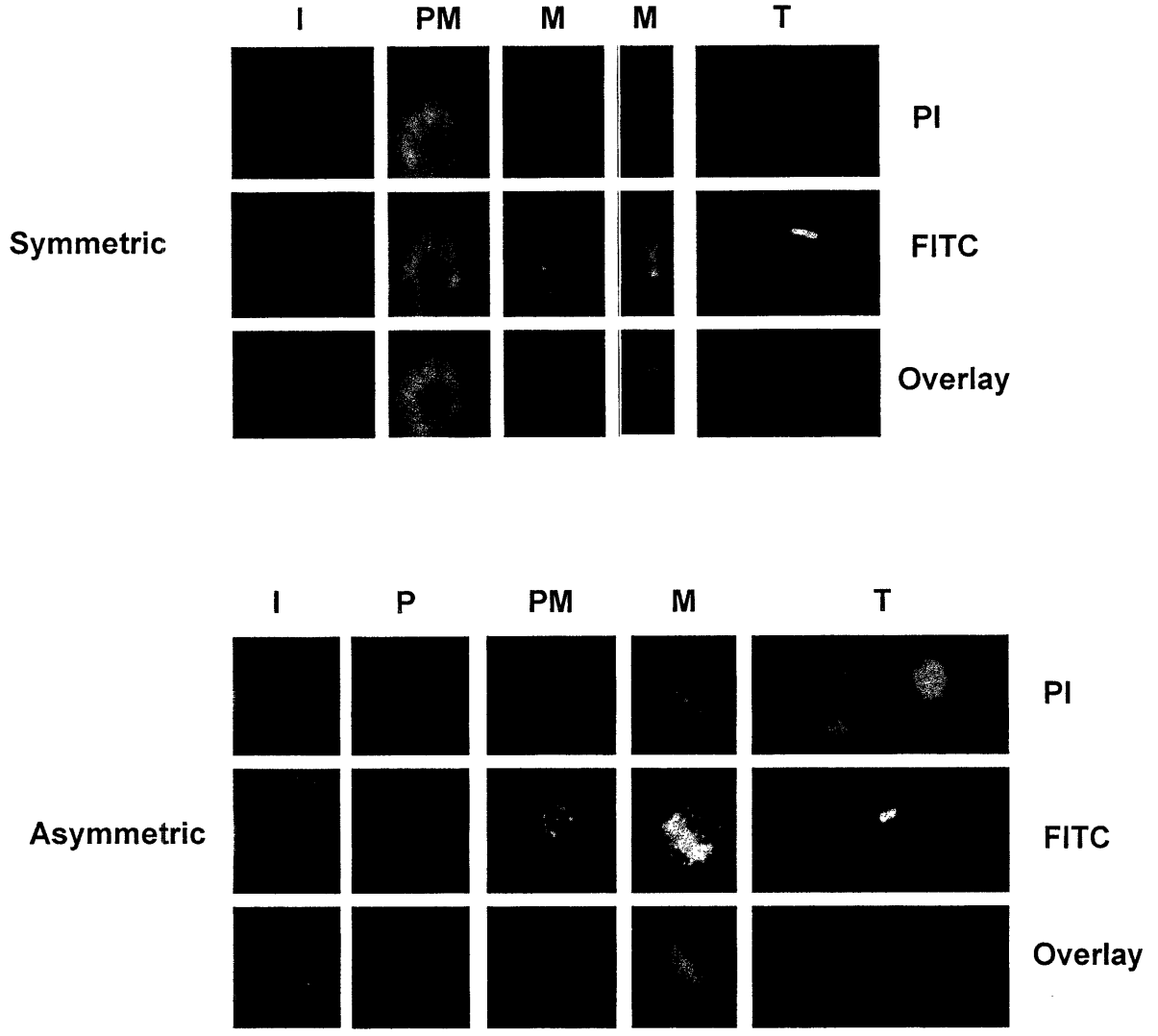


**Figure 2. Aurora B Kinase Localization Studies in Cells Cycling with Asymmetric vs. Symmetric Cell Kinetics**

Cells were plated in 4-well chamber slides and grown for 24 hours before induction of asymmetric cell kinetics. Cells were cultured for an additional 36 hours under asymmetric kinetics inducing conditions. Cells were fixed in 4% formaldehyde and stained with a monoclonal anti-mouse Aurora B kinase. antibody. Secondary antibody used was a FITC-conjugated goat anti-mouse antibody. Nuclei were counterstained using 0.1$\mu$g/ml PI stain. Cells were imaged and overlayed. 100X magnification.

**P = Prophase, PM = Prometaphase, M = Metaphase, A = Anaphase, T = Telophase, and I = Interphase.**

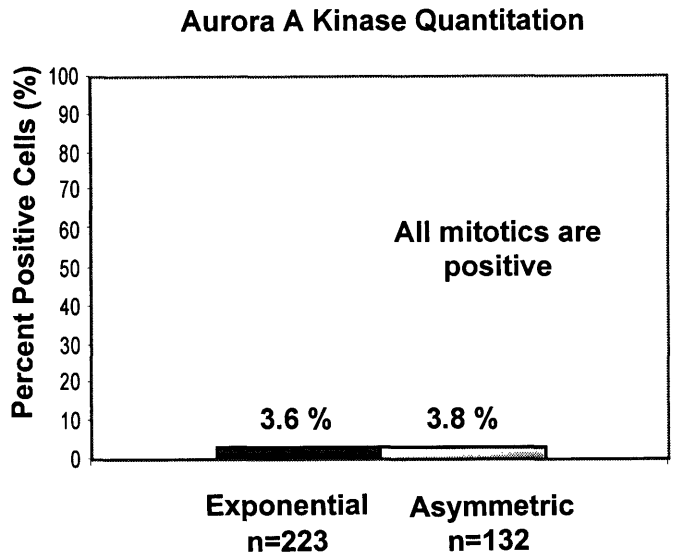


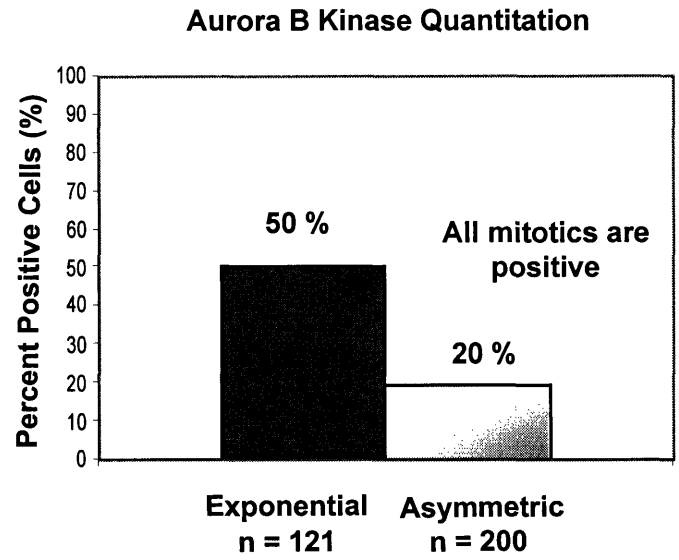


**Figure 3. Quantitation of Aurora A kinase and Aurora B kinase Positive Cells**
FITC positive fluorescent cells were quantified for both Aurora A and Aurora B kinase. Aurora A kinase positive cells were all mitotic cells. The percentage of Aurora A kinase positive cells was equivalent for both symmetrically and asymmetrically dividing cells. The observed value for Aurora A kinase in symmetrically cycling cells was 3.6% and 50% for Aurora B kinase. The observed value for Aurora A kinase in symmetrically cycling cells was 3.8% and 20% for Aurora B kinase. Aurora B kinase positive cells showed a 30% difference between symmetric and asymmetrically dividing cells.

**Results (Continued):**

Aurora A kinase localization and expression appeared the same in both asymmetrically cycling and symmetrically cycling cells. Aurora A kinase was localized at the centrosomes during prophase and metaphase and on the mitotic spindle during metaphase and early anaphase. There was no detected asymmetry in protein localization or expression.

Aurora B kinase localization also appeared normal in both asymmetrically and symmetrically cycling cells as shown in Figure 2. Aurora B kinase was localized on the chromosomes during interphase as indicated by the punctate pattern and is concentrated at the centromeres during prometaphase and metaphase. During anaphase and telophase, Aurora B kinase is present at the midbody of cells undergoing cytokinesis. These observed results were as expected for mitosis and did not show asymmetric protein localization or expression of Aurora B kinase.

The observed values for Aurora A kinase in symmetrically cycling cells was 3.6% and 50% for Aurora B kinase. The observed value for Aurora A kinase in symmetrically cycling cells was 3.8% and 20% for Aurora B kinase. Aurora B kinase positive cells showed a 30% difference between symmetric and asymmetrically dividing cells.

Cells were quantified for whether they expressed Aurora A kinase and Aurora B kinase by counting the numbers of positive nuclei and mitotic cells for cells cycling asymmetrically and symmetrically as shown in Figure 3. Cells expressing Aurora A kinase were all mitotic. Symmetrically cycling cells were 3.6% (n = 223) positive for expression of Aurora A kinase in a total culture. Asymmetrically cycling cells were 3.8% (n = 132) positive for expression of Aurora A kinase. The values are comparable to one another, but this similarity is not expected for cells cycling asymmetrically. For cells

cycling asymmetrically, a 70% lower fraction of mitotic cells should be observed when compared to symmetrically cycling cells, because at this time approximately 70% of asymmetrically cycling cells are non-dividing at the time of culture. This could be explained by the culture losing its asymmetric properties or could reflect slide cultures cycling with less asymmetric renewal than expected based on flask cultures. In highly dense cell culture, asymmetric cell kinetics are prevented. The mitotic index result does approximate the expected mitotic index of about 3-5% for cultures with a 20 hour doubling time.

**Conclusions:**

Localization of Aurora A kinase and Aurora B kinase was normal as reported in the literature (Kufer, et al., 2002; Giet, et al., 2002; Murata-Hori, et al., 2002; Terada, et al., 1998; Terada, et al., 2003 ) for model stem cell lines with asymmetric kinetics. The Aurora kinases show the expected localization and expression patterns through mitosis for both the symmetrically cycling state and the asymmetrically cycling state.

**Discussion:**

If stable microtubule attachments were responsible for the co-segregation of chromosomes in our model system, it was hypothesized that they might be visualized as an alteration in expression or localization. A difference in expression could not be detected in these studies since background fluorescence and fluorescent staining intensity varied from sample to sample and the protein was not completely down-regulated under one condition. The localization of Aurora A kinase and Aurora B kinase was normal. However, the question of Aurora A and B kinase expression levels still

needs to be addressed. If protein levels are reduced, it could signify a difference in how a cells senses tension between the mitotic spindle poles, by preferentially stabilizing one set of chromosomes containing immortal DNA strands. The immunofluorescence studies were able to show that normal localization of the protein was taking place, however, expression levels were not clearly absent from cells cycling with asymmetric cell kinetics. Western blot studies were subsequently done in order to measure protein expression quantitatively (Chapter 4, Section B).

## Chapter 4. Investigation of Proteins Involved in Kinetichore-Microtubule Attachment and Function

## Section B: Aurora A Kinase and Aurora B Kinase Western Blot Studies

### Rationale:

Immunofluorescence studies of the localization of Aurora A and Aurora B kinases did not show a difference in protein localization or segregation between daughter cells during mitosis. The immunofluorescence method was qualitative for expression of the proteins but not quantitative for their level of expression. For a quantitative measurement of protein expression level, Western blots of Aurora A kinase and Aurora B kinase were performed. Protein expression was not only determined from total asynchronous cultures, but also from selected mitotic cells cycling asymmetrically or symmetrically. Since Aurora A and B kinases are highly expressed during mitosis, a difference in expression level may be amplified by studying the protein expression specifically in mitotic cells.

### Experimental Method:

Protein lysates were prepared from cells cycling asymmetrically for 36 hours. Mitotic cells were also harvested as described previously (Chapter 2A) and protein lysates were prepared from them, since Aurora A and B are expressed mainly in mitosis. According to the method of Maniatis et al., the harvested cells were washed in ice cold PBS and lysed in ice cold RIPA buffer, containing 50mM Tris•Cl (pH 7.5), 150mM NaCl, 1% NP-40, 0.1% SDS, 0.5% sodium deoxycholate, and a complete mini-protease inhibitor cocktail tablet, supplied by Roche Diagnostics. After cell lysis, the lysate was

transferred to microcentrifuge tubes and sheared by passing it through a 21-guage needle twenty times. The lysate was incubated on ice at 4°C for 30 minutes and centrifuged at 13,000 rpm (15,682 x *g*) for 20 minutes. The supernatant was removed and used to determine the protein concentration of the extract using the BioRad™ DC protein assay so that an equal amount of protein was loaded for each sample.

A 12% polyacrylamide gel and 5% stacking gel were prepared for Tris-glycine SDS-PAGE using a BioRad Mini-Protean II® system. The 12 % polyacrylamide gel contained 375mM Tris•Cl pH 8.8, 0.1% SDS, 0.1% APS, and0.04% TEMED. The 5% acrylamide stacking gel contained 126mM Tris pH 6.8. as well as 0.1% SDS, 0.1% APS and 0.1% TEMED. Samples were denatured for 5 minutes at 100°C on a heating block using a 6X sample buffer diluted to 1X when added to the sample. The 6x sample buffer contained 300 mM Tris•Cl (pH 6.8), 864 mM beta-mercaptoethanol, 12 mM EDTA, 12% SDS, 0.05% bromophenol blue, and 60% glycerol. 20 μg of protein was loaded in each lane. The gels were run in Tris-glycine electrophoresis buffer containing 25 mM Tris•Cl, 250mM glycine, and 0.1% SDS, for 1 hour at 100V. The samples were then transferred to a Hybond™ ECL™ nitrocellulose membrane (Amersham Biosciences). The protein was transferred in 1XTBS in 20% methanol for 1.5 hours at 100V. The nitrocellulose membrane was then washed with TBS, and stained with Ponceau S (1% Ponceau S and 1% acetic acid) for 5 min to detect transferred proteins and determine if the transfer was done efficiently. The blot was then blocked in 5% nonfat dry milk (Carnation) in TBS-T for 1 hour and incubated with the primary antibody overnight. The primary antibodies used were monoclonal anti-mouse Aurora A kinase and monoclonal anti-mouse Aurora B kinase supplied by BD Transduction Laboratories. Both antibodies were used at a 1:250 dilution in 1% milk. The next day, the membrane was washed three times in TBS-

T for 10 minutes per wash. The membranes were incubated for 2 hours in a sheep anti-mouse IgG horseradish peroxidase linked secondary antibody (Amersham Biosciences) diluted at 1:5000 in 1% milk. The membrane was washed 3 times in TBS-T for 10 minutes per wash. ECL Plus™ horseradish peroxidase chemiluminescent detection system (Amersham Biosciences) was used to visualize the proteins. The blots were exposed to Kodak Biomax MR film and developed manually or using a Kodak (get model) developer.

Western blots were analyzed using Image J (NIH freeware) gel imaging software. Densitometry area calculations were normalized to alpha-tubulin expression. Blots were stripped by incubating membranes in for 2 hours at room temperature. Alpha-tubulin was probed as an internal standard using a monoclonal anti- alpha tubulin antibody supplied by Santa Cruz. The fold difference between Aurora A kinase and Aurora B kinase when compared with alpha-tubulin was averaged for 3-4 independent determinations to calculate the mean difference between random chromosome segregation (symmetrically cycling) and non-random chromosome segregation (asymmetrically cycling) in total cells and mitotic cells.

**Results:**

Western Blots of protein extracts from total asynchronous cultures and selected mitotic cells, were analyzed. Western blots were developed and quantified by densitometry. Aurora A and B kinase densitometry measurements were normalized to alpha-tubulin for each sample. The mean difference in expression between total or mitotic non-random (asymmetric) and random (symmetric) cells was determined.

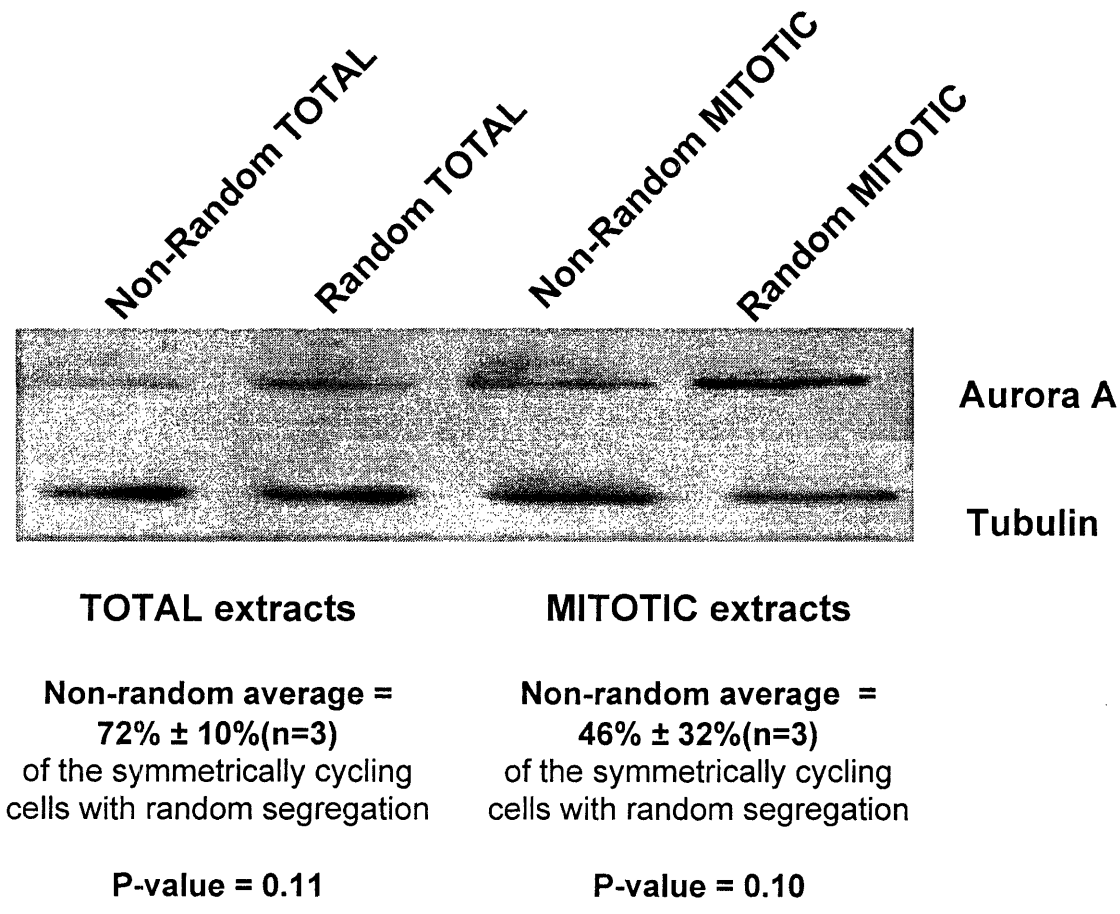


**Figure 1. Aurora A Kinase Western Blot Summary**
Protein extracts from cells cycling symmetrically and asymmetrically were analyzed by Western Blot. 20μg protein wereloaded per lane. Alpha-tubulin was probed as an internal standard. Mitotic and total cell extracts were compared for Aurora A kinase expression. The % difference in expression of the asymmetric cells (non-random chromosome segregation) compared with the symmetric cells (random chromosome segregation), was determined. Alpha-tubulin was probed as an internal standard.

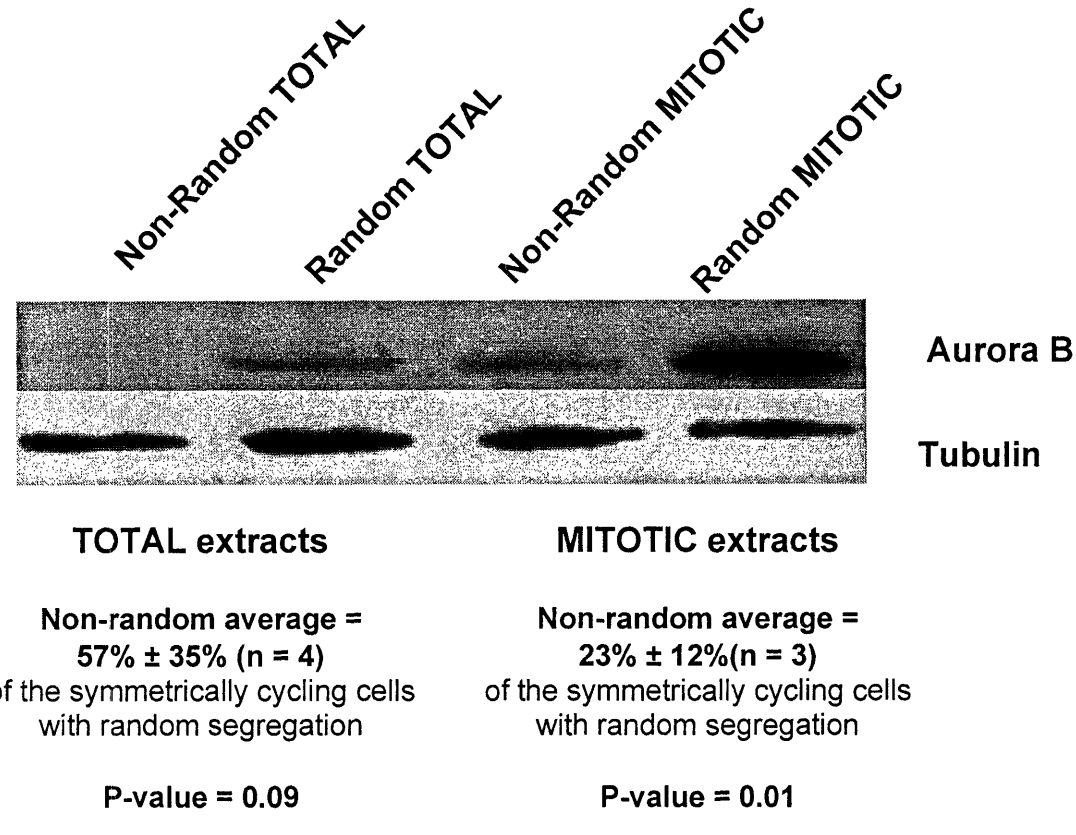


**Figure 2. Aurora B Kinase Western Blot Summary**
Protein extracts from mitotic and total asynchronous cells cycling symmetrically or asymmetrically were prepared and quantified. 20μg protein were loaded per lane. Mitotic and total culture extracts were compared for Aurora B kinase expression. The % difference in expression of the asymmetric cells compared with the symmetric cells was determined. Alpha-tubulin was probed as an internal standard.

Aurora A kinase, Figure 1, showed a difference in expression between protein extracts from asymmetric and symmetric cultures of 72% ±10%, (p-value = 0.11) for asynchronous cultures, and 46% ± 32%, (p-value = 0.10) for mitotic cells. For both asynchronous and mitotic cells, there is a reduction in expression of Aurora A kinase in the asymmetric or non-random chromosome segregation state.

Aurora B kinase, Figure 2, showed a difference in expression between protein extracts from asymmetric and symmetric cultures of 57% ± 35%, (p-value = 0.09) for total cultures, and 23% ± 12%, (p-value = 0.01) for the mitotic cells. Like Aurora A kinase, both mitotic cells and total asynchronous culture cells show a reduced expression of Aurora B kinase.

Whether or not the reduction of these proteins is due to asymmetric cell kinetics or the cell line itself, remains to be determined by measuring the protein expression of Aurora A kinase and Aurora B kinase under the p53-uninduced condition.

**Conclusions:**

Both Aurora A kinase and Aurora B kinase, show on average reduced protein expression in cells cycling with non-random chromosome segregation. This reduction is detectable in both asynchronous cells and isolated mitotic cells. Aurora A kinase showed a 72% ±10%, (p-value= 0.11) for asynchronous cultures, and 46% ± 32%, (p-value =0.10) for mitotic cells level of expression when compared with the symmetrically cycling cells. Aurora B kinase had a protein level expression of 57% ± 35%, (p-value = 0.09) for asynchronous cultures, and 23% ± 12%, (p-value = 0.01) for mitotic cells. Both Aurora A kinase and Aurora B kinase, showed a great reduction in expression in isolated mitotic cells (1.5 to 2-fold). This finding is consistent with the fact that both proteins are

expressed mainly during mitosis. This reduction in protein expression for Aurora A and B kinase, two proteins required for proper chromosome segregation, may be connected to the immortal strand mechanism. However, the proper p53 uninduced control for asymmetric cell kinetics must be evaluated before a connection can be made.

**Discussion:**

Immunofluorescence studies done in Chapter 4, Section A showed normal symmetric localization of both Aurora A and B kinases, however these studies were not able to provide quantitation of protein expression level. Western blotting analyses done on protein extracts of either total cultures or mitotic cells cycling symmetrically or asymmetrically showed an overall reduction of Aurora A kinase and Aurora B kinase in cells cycling with non-random chromosome segregation. Only one of the individual analyses reach statistical significance at the $p < 0.05$ level of confidence (Aurora B kinase expression in mitotic cells). The significant source of variation in Western blot analyses is a limitation in these studies. However, some of the variance in these analyses may indicate a need for better experimental control of the biological process or study.

This reduction in expression of Aurora B kinase, supports the stable microtubule attachment hypothesis documented in Tanaka, et al., 2002. If Aurora B expression is reduced, stable microtubule attachments would be maintained. Immortal strands could be tethered to microtubules throughout the cell cycle providing the cells cycling with immortal DNA strand co-segregation a constant identification mechanism for immortal DNA strands. Whether or not these findings are directly related to asymmetric cell kinetics and the immortal strand mechanism, remain to be addressed.

## Chapter 4. Investigation of Proteins Involved in Kinetochore-Microtubule Attachment and Function

## Section C: Alpha-tubulin Immunofluorescence

**Rationale:**

As discussed in Chapter 4, Section B, if microtubules are stabilized in order for immortal strands to be non-randomly segregated to one cell, then tubulin immunostaining of cells cycling asymmetrically may reveal the mechanism of immortal strand co-segregation. Aurora A and B kinase were both shown to be highly down-regulated in asymmetrically cycling cultures by Western blot (Chapter 4, Section B). According to the hypothesis, if Aurora B is down-regulated, cells with lower Aurora B expression should have more stable kinetochore-microtubule attachments. Whether or not microtubules are invading interphase nuclei, or are just in close proximity to the nucleus is difficult to determine by immunofluorescence techniques alone. However, by treating cells with compounds that disrupt or stabilize microtubules, the localization of microtubules after treatment may reveal features of microtubule function that might play a role in the immortal strand mechanism.

Two chemical cytoskeletal inhibitors used to study microtubule localization in asymmetrically dividing cells were taxol and nocadazole. Taxol arrests cells in mitosis as a result of stabilizing microtubules, thereby preventing microtubule depolymerization (Schiff and Horwitz, 1980; De Brabander et al., 1981). If cells were treated with taxol, and there were more microtubules associated with the nucleus in the asymmetrically cycling cells than the symmetrically cycling cells, this might indicate an association of microtubules within the nuclear envelope in untreated cells. Nocodazole is a known

microtubule depolymerizer and also arrests cells in mitosis at G2/M (DiLeonardo, et al., 1997; Ciciarello, et al., 2001). If microtubules were stably attached to kinetochores, it was postulated that depolymerized tubulin would be more concentrated in the nuclei of asymmetrically cycling cells. In addition to immonofluorescence studies for microtubules in treated cells, transmission electron microscopy (TEM) studies were performed to examine the cytoskeleton and cellular ultrastructure of cells cycling asymmetrically. In addition, actin staining was used to see if microfilament polymerization differences could be detected in asymmetrically vs. symmetrically cycling cells.

**Method:**

Immunofluorescence studies were performed by growing cells as described in Chapter 4, section A. At the end of the 36 hour asymmetric cell kinetics culture period, a 1000 μg/ml nocodazole stock solution was added to each 1 ml of medium per chamber slide well making a final concentration of 0.1 μg/ml nocodazole. For taxol studies, taxol was dissolved in methanol to make a stock solution of 50mM and added at varying concentrations, from 50 nM to 200 nM. Cells were exposed to the mitotic inhibitors for 24 hours before they were fixed and stained for Aurora B kinase and tubulin as described previously. Fluorescent images were taken using a Zeiss Axioskop MOT microscope, and a Zeiss Axiocam. Mouse monoclonal IgG2a anti-alpha-tubulin supplied by Santa Cruz Biotechnology was used at a 1:50 concentration. Secondary antibody used was a goat anti-mouse IgG-FITC conjugated antibody supplied by Santa Cruz Biotechnology at a 1:200 dilution. Antibody staining methods were performed as described previously in Chapter 4, Section A.

For TEM studies, cells were grown asymmetrically or symmetrically for 36 hours. Cells were processed by the WM Keck Microscope Facility at the Whitehead Institute as follows. Cells were fixed in 2.5% gluteraldehyde, 3% paraformaldehyde with 5% sucrose in 0.1M sodium cacodylate buffer (pH 7.4). Cells were then post-fixed in 1% $OsO_4$ in veronal-acetate buffer. Cells were stained in block overnight with 0.5% uranyl acetate in veronal-acetate buffer (pH6.0). Then dehydrated and embedded in epon -812 resin. Sections were cut on a Leica ultra cut UCT microtome at a thickness of 70nm using a diamond knife, stained with 2.0% uranyl acetate followed by 0.1% lead citrate and examined using a Philips EM410 (TEM method provided by Nicki Watson).

**Results:**

Cells grown asymetrically or symmetrically for 36 hours were fixed and stained with alpha-tubulin antibodies to visualize microtubules (Figure 1). The microtubule staining in asymmetrically cycling cells appears more dense than that of the symmetric cycling cells; the staining shows great localization to the nuclei rather than the cytoplasm. For cells cycling symmetrically, there is a dark shadow in the nuclear space where the nuclei is located. This dark nuclear space is not evident in the asymmetrically cycling cells, where the microtubules are concentrated. Immunofluorescent imaging did

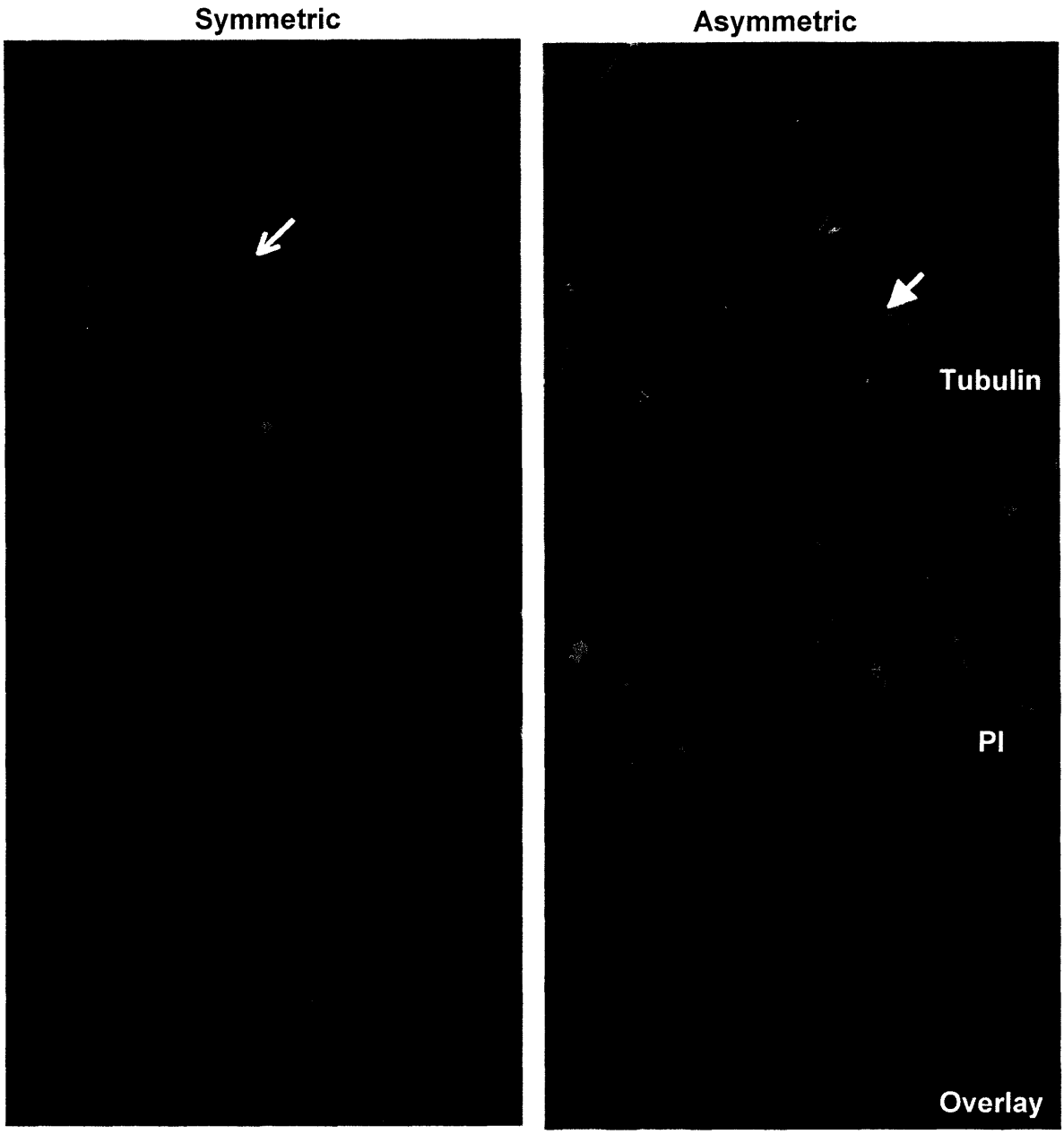


**Figure 1. Alpha-tubulin Staining of Asymmetrically Cycling and Symmetrically Cycling Cells**

Cells were grown in 4-well chamber slides for 24 hours before inducing cells to cycle asymmetrically or symmetrically for 36 hours. At 36 hours, 30% of the culture is made up of cycling cells. Cells were fixed in formaldehyde and stained for alpha-tubulin. Nuclei were counterstained with PI. Cells were imaged using a Zeiss Axioskop. Arrows point to specific cells with intense nuclear staining in the asymmetrically cycling cells and a dark shadow in the nuclear space of the symmetrically cycling cells. 20X magnification.

not give the necessary resolution to see whether microtubules were invading the nucleus or localized at specific regions near the nuclear envelope.

It is important to note that P53 is expressed at normal levels in cells dividing asymmetrically. Non-induced asymmetric cell lines with no p53 expression were also analyzed for tubulin organization and found to have more intensely staining nuclei as well (data not shown). This result indicates that a difference in tubulin organization and localization may be inherent to this cell line and not necessarily related to asymmetric kinetics or p53 expression.

Cells were treated with taxol in order to test whether evidence for stable microtubule attachments would be detected in the presence of the microtubule stabilizer. If cells have stable attachments and these are located in the nuclear space, then treatment of these cells with taxol may allow for the detection of a higher concentration of microtubules in the nuclei. Cells were treated with taxol for 24 hours from 25nM, 50nM, and 200nM taxol.

Ch. 4, Fig 2., shows tubulin staining of cells grown asymmetrically or symmetrically for 36 hours and then treated with 25nM taxol for 24 hours. The alpha tubulin staining reveals intense microtubule bundling in cells with asymmetric cell kinetics. The microtubule bundling is observed as bright dense regions of alpha-tubulin staining concentrated around the nucleus. The symmetrically cycling cells do not show such intense staining for microtubules. This result indicates that there is either a higher microtubule density in the asymmetrically cycling cells or that the microtubule organization is different, creating more intense microtubule bundling.

In Ch. 4, Fig. 3 at a higher concentration of 50nM taxol, a similar observation is made as that at 25nM. The intensity of microtubule staining in the asymmetrically

cycling cells appears to be higher than in cells cycling symmetrically. The PI staining shows that more cycling nuclei are undergoing apoptosis at this concentration for both cell kinetics states.

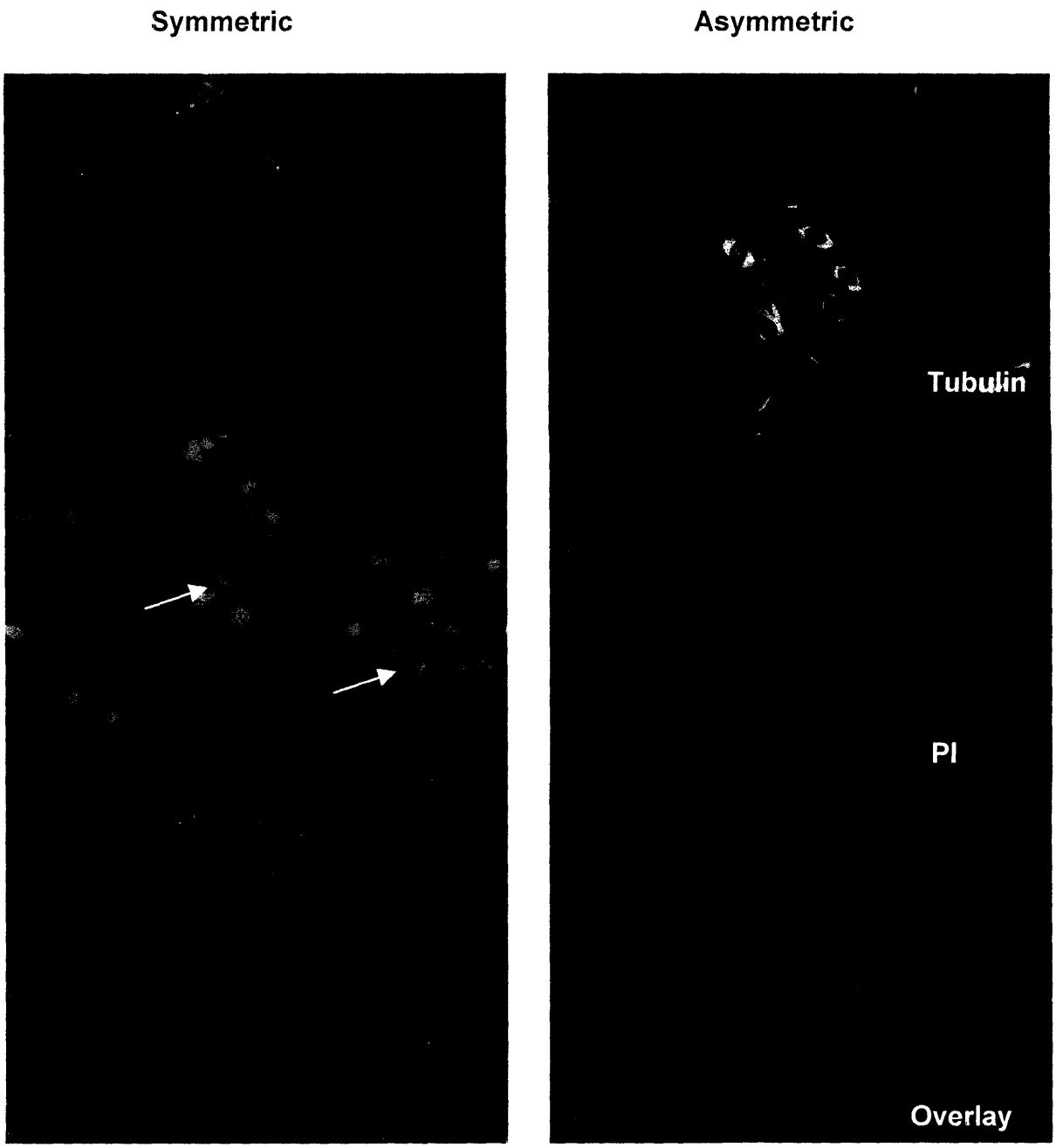


**Figure 2. 25 nM Taxol Treatment of Asymmetric and Symmetric Cycling Cells**
Cells cycling asymmetrically or symmetrically for 36 hours were treated with 25nM taxol for 24 hours. Cells were fixed and stained for alpha-tubulin. Nuclei were counterstained with PI. PI fluorescence shows fragments consistent with apoptotic bodies in symmetrically cycling cells. Apoptotic bodies are marked with arrows. 20X magnification.

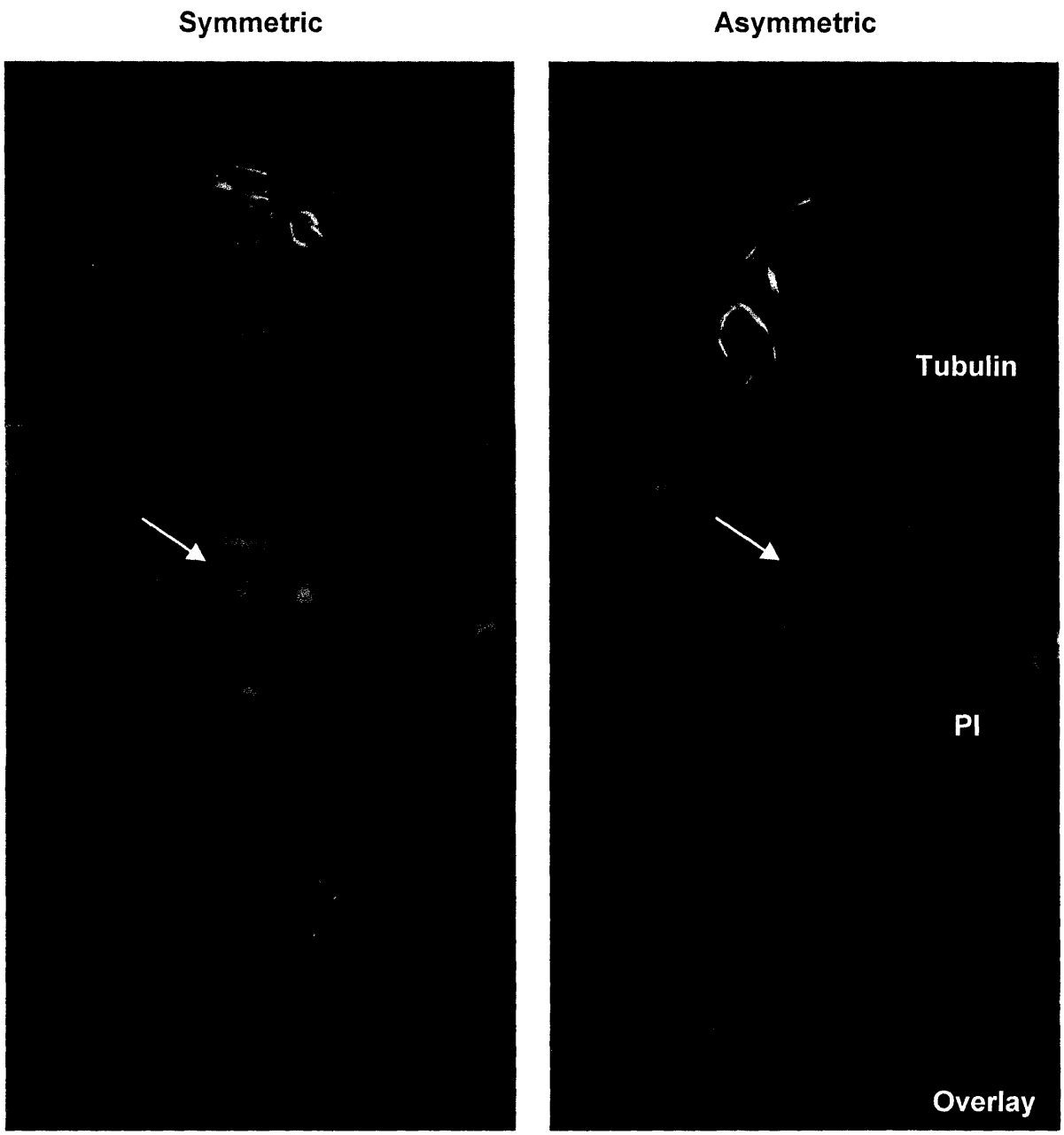


**Figure 3. 50 nM Taxol Treatment of Asymmetric and Symmetric Cycling Cells**
Cells cycling asymmetrically and symmetrically for 36 hours were treated with 50nM taxol for 24 hours. Cells were fixed and stained for alpha-tubulin. Nuclei were counterstained with PI. PI fluorescence shows fragments consistent with apoptotic bodies in symmetrically cycling cells. Arrows indicate nuclear fragmentation detected by PI fluorescence. 20X magnification.

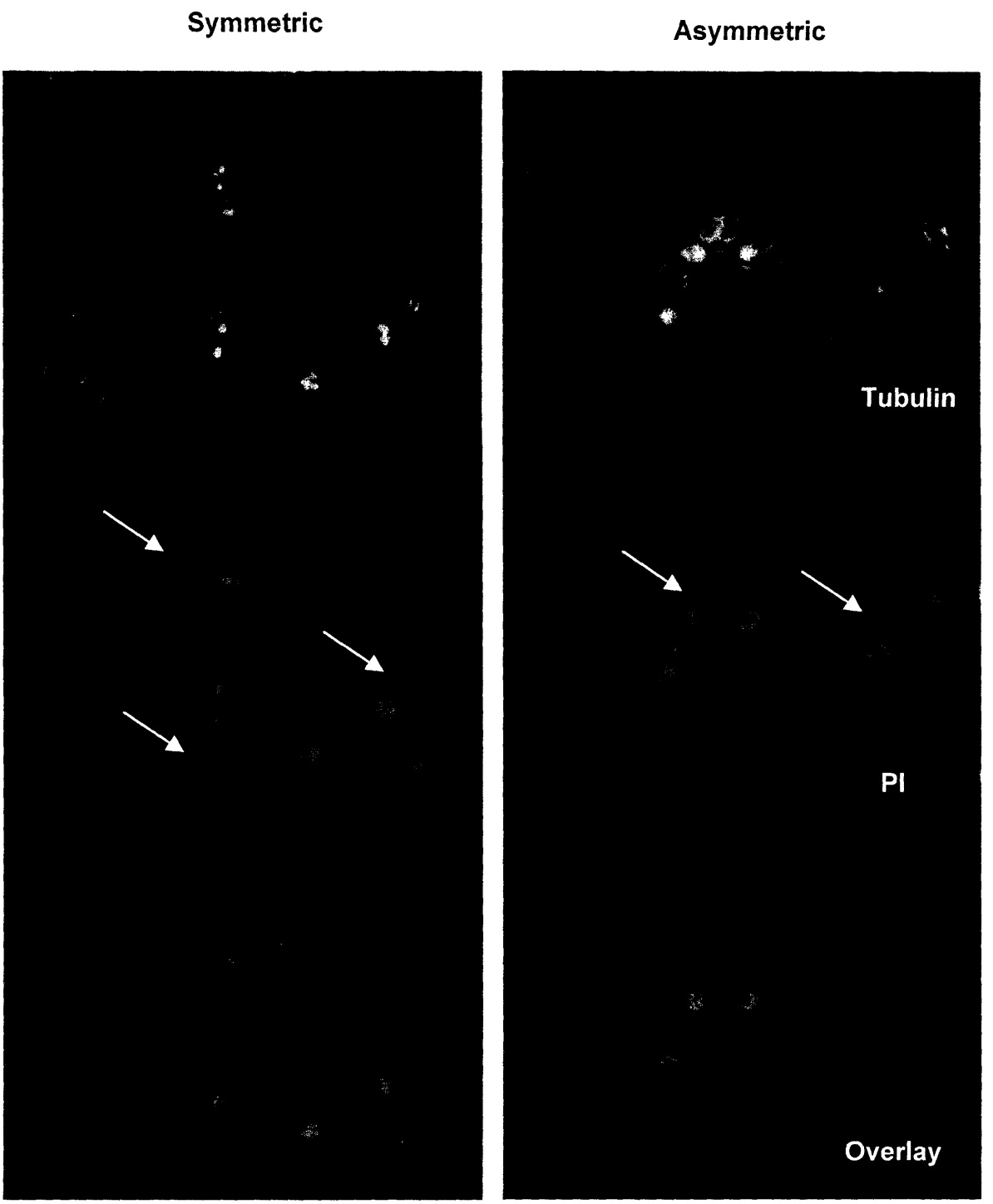


**Figure 4. 200 nM Taxol Treatment of Asymmetric and Symmetric Cycling Cells**
Cells cycling asymmetrically and symmetrically for 36 hours were treated with 200nM taxol for 24 hours. Cells were fixed and stained for alpha-tubulin. Nuclei were counterstained with PI. Apoptotic bodies are marked with arrows. 20X magnification.

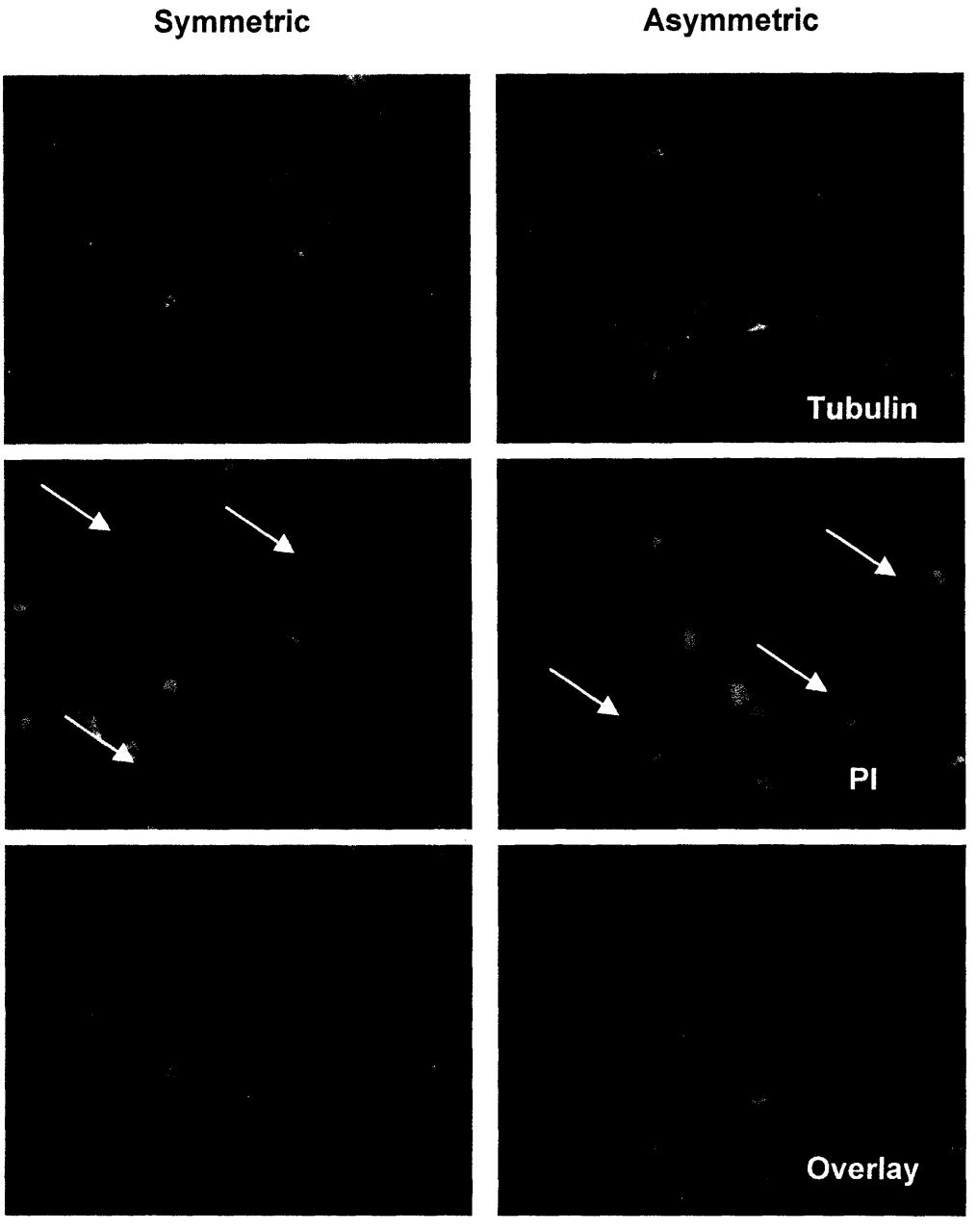


**Figure 5. Nocodazole Treatment of Asymmetric and Symmetric Cycling Cells**
Treatment of asymmetrically or symmetrically cycling cells with 0.1$\mu$g/ml nocodazole causes the depolymerization of microtubules after 24 hours. Arrows indicate nuclear fragmentation.

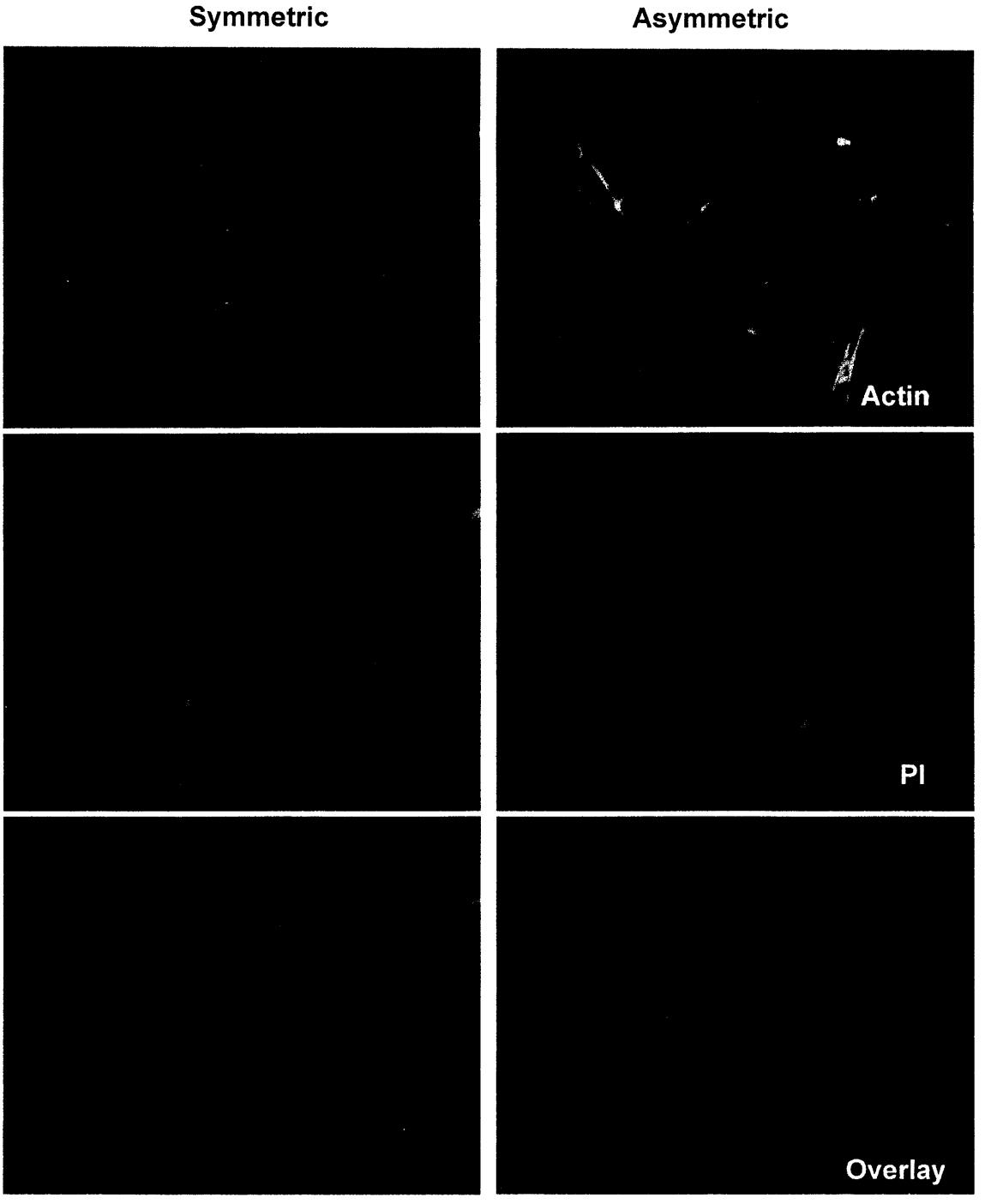


**Figure 6. Actin Staining of Cells Cycling Asymmetrically and Symmetrically**
Cells cycling asymmetrically and symmetrically for 36 hours were fixed and stained with phalloidin, an actin specific dye. Nuclei were counterstained with PI. 20X magnification.

In Ch. 4, Fig. 4 , at 200nM taxol treatment, the symmetric cells appear to have a more similar phenotype as the asymmetric cells. However, the intensity of the microtubule staining is not as intense as it is in the asymmetrically cycling cells. The bundling becomes more equivalent in both asymmetrically and symmetrically cycling cells, although the asymmetric cells still appear to have a higher intensity of staining for tubulin.

Cells treated with 0.1μg/ml nocodazole for 24 hours showed no organized microtubule assembly in either the asymmetric or symmetric cycling cultures as expected (Figure5). After 24 hours of treatment, all of the microtubules are depolymerized. The asymmetrically cycling cultures appear to have more depolymerized microtubules in the cytoplasm, with more intense overall staining than the symmetrically cycling cells. The apoptotic index of cells treated with nocodazole was different for cells cycling asymmetrically than cells cycling symmetrically. At 4 hours, the symmetric and asymmetric cultures had similar apoptotic indices, 8.9% and 7.1%, respectively. At 24 hours, there is a sharp increase in the apoptotic index of the symmetrically cycling cells. A 79.3% apoptotic index was observed for symmetrically cycling cells and a 40% apoptotic index for asymmetrically cycling cells.

The mitotic index of cells treated with nocodazole and taxol increased 2-3 fold for asymmetrically cycling cells, from 3% for untreated cells, to 7% with nocodazole treatment and 9.4% with taxol treatment. The mitotic index of cells cycling symmetrically went from 5.8% for untreated cells, to 6.6% for nocodazole treatment, and 8.3% for taxol treatment.

Cells were stained for actin using the dye phalloidin (Figure 6). Asymmetrically cycling cells appear to have a more complex network of actin than symmetrically cycling cells. EM studies also showed a higher concentration of intermediate filaments in the cytoplasm of asymmetrically cycling cells (Figures 7). Several types of intermediate filaments may be up-regulated in the asymmetrically cycling cells. 2D PAGE studies showed a higher expression of vimentin, a mesenchymal stem cell marker and intermediate filament, in asymmetrically cycling cultures (data not shown).

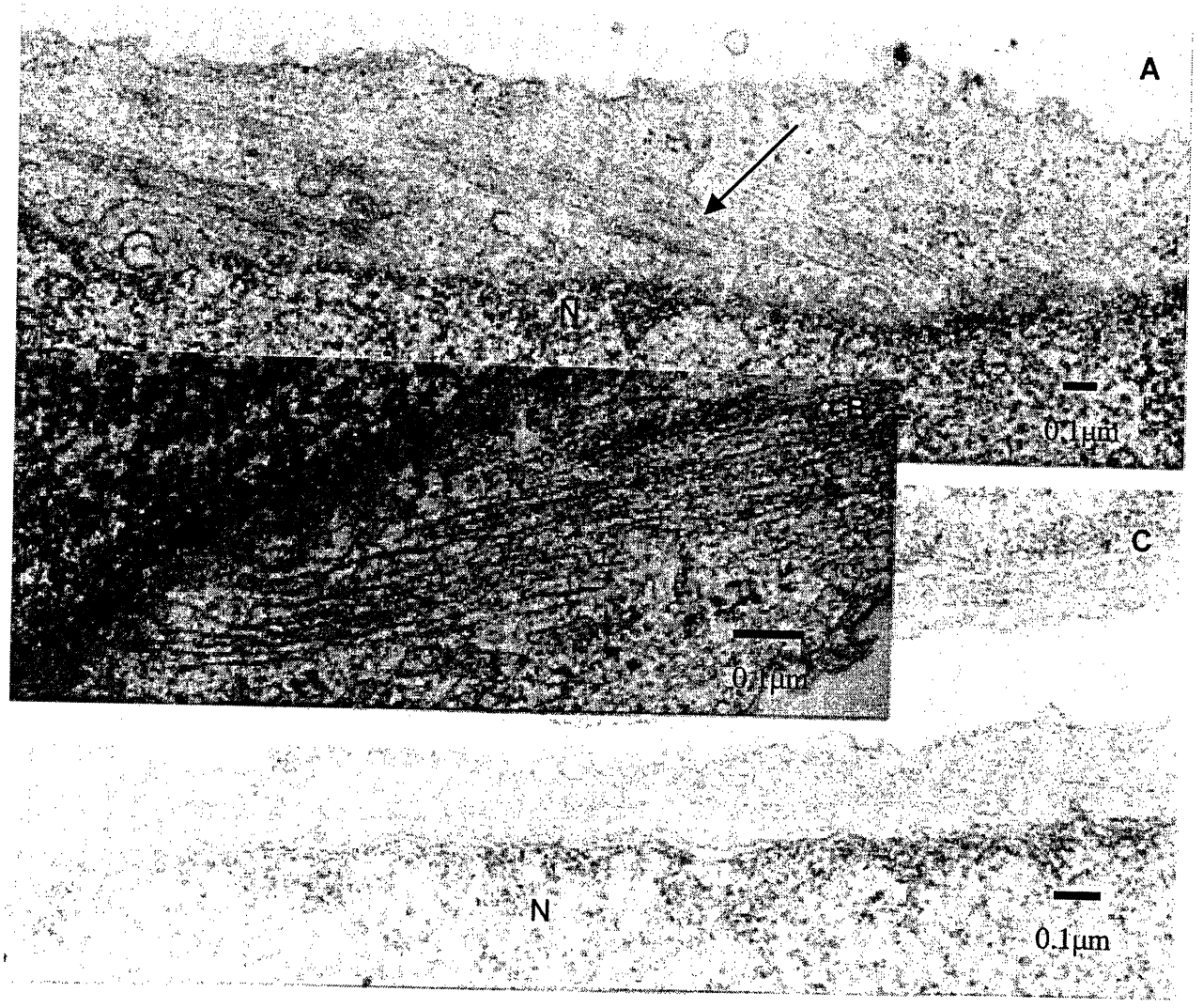


**Figure 7. TEM of Cells Cycling Asymmetrically or Symmetrically**
Cells cycling asymmetrically (Fig. A) or symmetrically (Fig. C) for 36 hours were fixed in 2.5% gluteraldehyde, 3% paraformaldehyde with 5% sucrose in 0.1M sodium cacodylate buffer (pH 7.4). Cells were then post-fixed in 1% $OsO_4$ in veronal-acetate buffer. Cells were stained, dehydrated, and embedded in resin. 70nm sections were cut and stained with 2.0% uranyl acetate followed by 0.1% lead citrate. Scale bars indicate 0.1μm. Inset of Figure A at high magnification is shown in Fig. B. Arrow indicates a high density area of intermediate filaments. N = nucleus.

## Conclusions:

Taxol and nocodazole treatments were performed to see if stabilization or depolymerization of microtubules might affect tubulin localization in asymmetric cultures. More tubulin bundling was observed for asymmetrically cycling from 25nM to 200nM taxol. Nocodazole treatment completely depolymerized microtubules after 24 hours in both asymmetric and symmetric cells. In contrast to the cells' response to taxol, treatment with nocodazole for 24 hours showed that P53-null, symmetrically cycling cells were more sensitive to apoptosis than p53 expressing cells at a level almost 2-fold higher than asymmetric cells.

Actin staining was more intense in asymmetrically cycling cells than symmetrically cycling cells. In addition, TEM studies displayed a high concentration of intermediate filaments in the cytoplasm observed specifically in asymmetrically cycling cells. TEM of symmetrically cycling cells appeared normal. These studies provide evidence for a difference in the cytoskeletal proteins and their organization in asymmetrically cycling cells retaining immortal DNA strands.

## Discussion:

In studies of microtubule staining of asymmetrically and symmetrically cycling cells, the asymmetric cultures have a higher concentration of microtubules localized at the nucleus. The taxol studies support this observation. Taxol treatment of asymmetrically cycling cells showed more microtubule bundling due to taxol induced microtubule stabilization than symmetrically cycling cells at lower concentrations, indicating a difference in tubulin expression or localization in cells cycling asymmetrically. At the highest taxol dose used, 200nM, both asymmetrically and

symmetrically cycling cells responded to taxol similarly, although there appeared to be more tubulin staining intensity in the asymmetric cells. Microtubule bundling sensitivity may or may not be affected by p53 pathways. It was observed that asymmetric cells not induced to express p53 also had an intense nuclear tubulin staining, similar to the microtubule staining observed in the p53-induced cells. The significance of this result to the immortal strand mechanism and asymmetric kinetics remains to be answered in future experiments by evaluating tubulin staining of p53-uninduced cells.

Nocodazole treatment showed the complete loss of polymerized microtubules in symmetric and asymmetric cultures as expected. Whether or not there was more microtubule density evident in the asymmetric cells was difficult to determine because of the range of microtubule density and localization observed in both the asymmetrically cycling and symmetrically cycling cells treated with nocodazole. A 2-fold higher frequency of apoptosis was observed for symmetrically cycling cells in comparison to asymmetrically cycling cells. This result may reflect a p53 dependent sensitivity to nocodazole (DiLeonardo, et al., 1997; Ciciarello, et al., 2001). If p53 arrests cells in G1/S before nocodazole induced apoptosis occurs, cells with normal p53 expression may remain resistant to nocodazole induced killing. It is interesting to note that this difference does not occur with taxol treatment, indicating that nocodazole and taxol affect different pathways of apoptosis and that the asymmetric and symmetric cells do not respond in the same way. If taxol treatment is p53 independent and nocodazole treatment p53 dependent, this may explain the observed results. In a report by Minotti, et al., 1991, it was noted that cells that are resistant to taxol are hypersensitive to destabilizing drugs such as nocodazole. If microtubule bundling were also p53

independent but dependent on asymmetric kinetics, than the observed results may be connected to the immortal strand mechanism.

A higher concentration of intermediate filaments was observed in the EM studies. It had been observed that tubulin organization and intermediate filament organization are linked to one another in mouse fibroblast cells treated with taxol (Geuns, G, et al., 1983). Whether or not this result is related to the immortal strand mechanism, remains to be seen. Differences in the cytoskeleton of cells cycling asymmetrically are clearly observed however more definitive experiments addressing the role of p53 and connections to the immortal strand mechanism must be addressed.

**References:**


Ciciarello M, Mangiacasale R, Casenghi M, Zaira Limongi M, D'Angelo M, Soddu S, Lavia P, Cundari E, *p53 displacement from centrosomes and p53-mediated G1 arrest following transient inhibition of the mitotic spindle.* J Biol Chem, 2001. **276**:p. 19205-13.

De Brabander M, Geuens G, Nuydens R, Willebrords R, De Mey J, *Microtubule assembly in living cells after release from nocodazole block: the effects of metabolic inhibitors, taxol and PH.* Cell Biol Int Rep, 1981. **5**: p.913-20.

Di Leonardo A, Khan SH, Linke SP, Greco V, Seidita G, Wahl GM, *DNA rereplication in the presence of mitotic spindle inhibitors in human and mouse fibroblasts lacking either p53 or pRb function.* Cancer Res, 1997. **57**: p.1013-9.

Geuens G, de Brabander M, Nuydens R, De Mey J, *The interaction between microtubules and intermediate filaments in cultured cells treated with taxol and nocodazole.* Cell Biol Int Rep, 1983. **7**: p.35-47.

Logarinho E, Bousbaa H, Dias JM, Lopes C, Amorim I, Antunes-Martins A, Sunkel CE., *Different spindle checkpoint proteins monitor microtubule attachment and tension at kinetochores in Drosophila cells.* J Cell Sci, 2004. **117**: p. 1757-71.

Dewar H, Tanaka K, Nasmyth K, Tanaka TU, *Tension between two kinetochores suffices for their bi-orientation on the mitotic spindle.* Nature, 2004. **428**: p. 93-7.

Giet R, McLean D, Descamps S, Lee MJ, Raff JW, Prigent C, Glover DM, *Drosophila Aurora A kinase is required to localize D-TACC to centrosomes and to regulate astral microtubules.* J Cell Biol, 2002. **156**: p. 437-51.

Katayama H, Sasai K, Kawai H, Yuan ZM, Bondaruk J, Suzuki F, Fujii S, Arlinghaus RB, Czerniak BA, Sen S, *Phosphorylation by aurora kinase A induces Mdm2-mediated destabilization and inhibition of p53.* Nat Genet, 2004. **36**: p. 55-62.

Kufer TA, Sillje HH, Korner R, Gruss OJ, Meraldi P, Nigg EA, *Human TPX2 is required for targeting Aurora-A kinase to the spindle.* J Cell Biol, 2002. **158**: p. 617-623.

Kunitoku N, Sasayama T, Marumoto T, Zhang D, Honda S, Kobayashi O, Hatakeyama K, Ushio Y, Saya H, Hirota T, *CENP-A phosphorylation by Aurora-A in prophase is required for enrichment of Aurora-B at inner centromeres and for kinetochore function.* Dev Cell, 2003. **5**: p. 853-64.

Murata-Hori M, Tatsuka M, Wang Y, *Probing the dynamics and functions of Aurora B kinase in living cells during mitosis and cytokinesis.* Mol. Biol. Cell, 2002. **13**: p. 1099-1108.

Sambrook J, Fritsch EF, and Maniatis T (1989 a) Molecular Cloning: a laboratory manual, 2nd edition, Cold Spring Harbor Laboratory Press, pp. 18.1 - 18.5 .

Schiff PB, Horwitz SB, Taxol stabilizes microtubules in mouse fibroblast cells. Proc Natl Acad Sci U S A, 1980. **77**: p. 1561-5.

Tanaka TU, Rachidi N, Janke C, Pereira G, Galova M, Schiebel E, Stark MJ, Nasmyth K., *Evidence that the Ipl1-Sli15 (Aurora kinase-INCENP) complex promotes chromosome bi-orientation by altering kinetochore-spindle pole connections.* Cell, 2002. **108**: p. 317-29.

Terada Y, Tatsuka M, Suzuki F, Yasuda Y, Fujita S, Otsu M., *AIM-1: a mammalian midbody-associated protein required for cytokinesis.* EMBO J, 1998. **17**: p. 667-76.

Terada Y, Uetake Y, Kuriyama R, *Interaction of Aurora-A and centrosomin at the microtubule-nucleating site in Drosophila and mammalian cells.* J Cell Biol, 2003. **162**: p. 757-63.

## Summary of Conclusions

Adult stem cells are long-lived and undergo many DNA replication events. Given a significant DNA replication-dependent mutation rate, the immortal strand hypothesis may explain how an adult stem cell protects itself from cancer-causing mutations. Past studies investigating the immortal strand hypothesis are compelling but not definitive (Lark et al., 1966; Lark et al., 1967; Potten et al., 1978; Bickenback et al., 1986; Kuroki et al., 1989; Potten et al., 2002). Because stem cells are rare and cannot be identified morphologically in tissues, these previous studies were unable to provide direct evidence for immortal DNA strand inheritance in cells with demonstrated adult stem cell properties.

This dissertation research investigated the immortal strand hypothesis in a model adult stem cell line that can be manipulated to yield a culture of asymmetrically cycling cells that mimic the division kinetics of adult stem cells. These model cells were used previously to show the asymmetric co-segregation of immortal DNA strands by *in situ* methods (Merok et al., 2002). The model adult stem cell line allows for the detection of immortal strand co-segregation at a significantly higher level than could be observed *in vivo*. Cells that segregate immortal DNA strands are not rare in this culture system, and therefore, also provide a way for studying the underlying mechanism of immortal strand inheritance.

In this dissertation research the existence of immortal DNA strands was independently confirmed, and the molecular basis for their co-segregation was investigated in model cells with asymmetric stem cell kinetics. By developing physicochemical methods to evaluate retention of BrdU-labeled and unlabeled immortal

DNA strands, as well as investigating the presence of a global modification to the DNA, this work provides a novel method for detection of immortal DNA strands in cultured cells.

The main tool developed from this dissertation has three specific applications:

1) Cell kinetics evaluation by BrdU labeling kinetics.
2) Detection of immortal DNA strand inheritance in other cells.
3) Isolation and purification of immortal strands for study.

**CsCl Density Gradient Analyses**

CsCl density gradient studies of cells cycling with asymmetric cell kinetics showed that the density shift method of Meselson and Stahl (1958) could also be used to demonstrate asymmetric cell kinetics by quantifying BrdU labeling kinetics. In addition, the immortal strand mechanism was confirmed in these cell lines using a continuous BrdU labeling method. These studies provide a novel method by which cultured cells can be studied for immortal strand retention.

**Physicochemical Characterization of Immortal Strand DNA**

For chromosomes containing immortal DNA strands to be selectively retained by an adult stem cell, a simple hypothesis to consider is that the chromosomes are uniformly marked in a way that enables an adult stem cell to identify, select, and preferentially segregate a full set of immortal DNA strand containing chromosomes. This hypothesis was investigated using CsCl gradients to separate immortal from non-immortal strand containing DNA. There was no evidence of a structural or chemical DNA modification. Density shift gradients can reveal a chemical or physical

modification to the DNA by studying the peak properties of the sedimented DNA (e.g., variance, position). In addition, using HPLC to determine the base composition of DNA from cells retaining immortal DNA strands did not show any unique base composition differences, nor did these studies identify novel chemical modifications. From these physicochemical studies, one can conclude that a detectable global modification does not mark immortal DNA strands.

It is possible that a modification to specific chromosomal regions such as centromeres, telomeres, or genes could exist on the immortal strand that would not be detected by the methods used in these studies (Luo and Preuss, 2003).

**Chromosome Segregation and Cytoskeletal Protein Studies**

Whether or not immortal DNA strands are chemically distinct, proteins involved in chromosome segregation are prime candidates to play a role in the co-segregation of immortal strand containing chromosomes. In a recent paper by Tanaka et al., 2002, chromosomes were non-randomly segregated in *S. cerevisiae* when the protein Aurora B kinase was mutated. Down-regulation of Aurora B kinase, resulted in monopolar spindle attachments with all of the chromosomes (unreplicated due to a *cdc6* mutant background) preferentially segregated to one cell. In this research, Aurora B kinase and its homologue Aurora A kinase, two proteins involved in proper chromosome segregation and cytokinesis, were found to be highly down-regulated, in asymmetrically cycling cells, by Western blot analysis. It is possible that the significant down-regulation of Aurora B kinase found in mitotic extracts results in preferential stable attachments of immortal DNA strands to microtubules, resulting in their non-random co-segregation to the cycling stem-like cell. Immunofluorescence studies showed no difference in protein

localization of either Aurora B kinase or Aurora A kinase during mitosis. In addition the cytoskeletal proteins, tubulin and actin were observed to have a higher density in asymmetrically vs. symmetrically cycling stem -like cells.

The non-random co-segregation of immortal DNA strands defies the current view of mitotic chromosome segregation as a random segregation event. A highly orchestrated, complex mechanism involving specific DNA sequences, chromosome segregation proteins, kinetochore proteins, as well as the cytoskeleton network may all play a role in the non-random segregation event. Our current understanding suggests that a continued in depth evaluation of the cytoskeleton and chromosome segregation proteins will be important for its complete elucidation.

**Biological Relevance**

The methods used in these studies may be applied to study immortal DNA strands in cultured adult stem cell lines. The immortal strand mechanism, as proposed, is specific to adult stem cells and may provide a way to uniquely identify adult stem cells by the retention of labeled immortal DNA strands in their chromosomes. Currently, there are no universal markers for the adult stem cell, for any tissue type. If proteins specific to the immortal strand mechanism are identified, these unique proteins may be used as specific adult stem cell markers. The identification of adult stem cells across all organs would be a breakthrough in stem cell biology. The identification and further understanding of adult tissue stem cells would further their application to such fields as tissue regeneration, gene therapy, and cell replacement therapy.

It is also possible that inherited immortal DNA strands act as a stem cell fate determinant. Current knowledge from research in Drosophila neuroblasts, indicates

that there are a number of asymmetrically segregated proteins involved in determining cell fate (Giansanti et al., 2001; Bhat and Apsel, 2004). However, immortal DNA strands could also be important for determining cell fate. If immortal DNA strands were constantly segregated to the cycling stem cell, perhaps it is the inheritance of the immortal DNA strand that determines whether or not a stem cell retains its self-renewal capabilities.

Adult stem cells are important for proper tissue function and regeneration, Cairns' hypothesis underlines the importance of preserving their genomic integrity Protecting adult stem cells from mutation is critical for their normal function in tissues. Because stem cells have the ability to self-renew, a cancer causing mutation arising in an adult stem cell, could potentially give rise to a tumor with great efficiency. If proteins specific to the immortal strand mechanism could be identified, then these would not only be markers for stem cells but could also lead to potential therapies for specifically targeting adult stem cells in cancer.

If immortal DNA strands are not subject to the same DNA repair processes as other cells, because strands are continuously retained and selected, then immortal DNA strands presumably accumulate chemical DNA damage over long life spans. It is possible that the mechanism of aging is tied to the integrity of immortal DNA strands. Perhaps as adult stem cells age, immortal DNA strands are no longer in their former mutation free state, and give rise to mutated adult stem cells that could lead to cancer. The immortal strand mechanism provides insight into a possible molecular mechanism for aging and diseases associated with aging such as cancer.

These novel studies attempt to understand a mechanism that has broad ranging implications to the fields of biology and medicine. The goal of identifying the

mechanism behind the non-random chromosome segregation of immortal DNA strands is of ultimate importance to moving the field of stem cell biology forward.

**References:**


Bhat KM, Apsel N, *Upregulation of Mitimere and Nubbin acts through cyclin E to confer self-renewing asymmetric division potential to neural precursor cells.* Development. 2004. **131**:p. 1123-34.

Bickenbach, J.R., McCutecheon, J., Mackenzie, I.C., *Rate of Loss of Tritiated Thymidine Label in Basal Cells in Mouse Epithelial Tissues.* Cell Tissue Kinet., 1986. **19**: p. 325-333.

Giansanti MG, Gatti M, Bonaccorsi S, The role of centrosomes and astral microtubules during asymmetric division of Drosophila neuroblasts. Development. 2001. **128**: p. 1137-45.

Kuroki, T., Murakami, Y., *Random Segregation of DNA Strands in Epidermal Basal Cells.* Jpn. J. Cancer Res., 1989. **80**: p. 637-642.

Lark, K.G., Consigli, R.A., Minocha, H.C., *Segregation of Sister Chromatids in Mammalian Cells.* Science, 1966. **154**:p. 1202-05.

Lark, K.G., *Nonrandom Segregation of Sister Chromatids in Vicia Faba and Triticum Boeoticum.* PNAS, 1967. **58**: p. 352-359.

Luo S, Preuss D, *Strand-biased DNA methylation associated with centromeric regions in Arabidopsis.* Proc Natl Acad Sci U S A, 2003. **100**: p. 11133-8.

Meselson, M., Stahl, F.W., *The Replication of DNA in Escherichia coli.* PNAS, 1958. **44**: p. 671-682.

Potten, C.S., Hume, W.J., Reid, P., Cairns, J., *The Segregation of DNA in Epithelial Stem Cells.* Cell, 1978. **15**: p. 899-906.

Potten CS, Owen G, Booth D, *Intestinal stem cells protect their genome by selective segregation of template DNA strands.* J Cell Sci., 2002. **115**: p. 2381-8.

**Acknowledgments:**

Thank you to James L. Sherley, my advisor, for his unfailing support, creativity, insight, and expertise that contributed to my education and training in my graduate career. His critical review of my research and thesis throughout my time in his laboratory allowed me to produce a higher quality dissertation. In addition, his patience, kindness, and enthusiasm helped foster my growth as a scientist.

The following people directly contributed to this research: Jason Ellis who performed the DNA melting temperature studies (Chapter 2, Section B), Jim Delaney of the Essigmann laboratory who was an excellent resource for the Tm studies, Nicki Watson who performed the TEM studies (Chapter 4, Section C), Thomas Wang who studied methylation rate in asymmetrically cycling cells as well as assisted me in various aspects of the CsCl gradient analyses, Johnathan King who created an ELISA assay for the determination of the BrdU content in purified DNA, Koli Taghizadeh and Elaine Plummer who helped set up the HPLC system and trained me to use it for evaluation of DNA base composition, Min Dong for measuring the global 5-methyl-cytosine content of cells cycling symmetrically and asymmetrically, Elena Gostjeva for instruction and use of her Zeiss Axioskop microscope, Krisha Panchalingam for help formatting the TEM images, and James Tunstead who demonstrated the immortal strand mechanism *in situ* using the continuous labeling experiment. I would especially like to acknowledge Joshua Merok for providing the first demonstration of the immortal strand mechanism using the label retention method *in situ* and laying down the foundation for this research.

I would also like to acknowledge my thesis committee, Peter C. Dedon, Terry Orr-Weaver, William G. Thilly, and Steven R. Tannenbaum for their excellent critical review and support during the course of this work.

The following fellowships provided generous financial support over the years: the Anna Fuller Fund for Molecular Oncology, the Biogen Idec-MIT Fellowship, and the NIH training grant.

Finally, thank you to my friends and family for providing me with the encouragement, hope, and perseverance to continue and complete this dissertation. They include my parents, Linda and Phil Lansita. My friends Aaradhana Prajapati, Keith Santarelli, Amy Engelhart, Joseph Cosgrove, Rouzbeh Taghizadeh, Gracy Crane, and Anu Joshi. C-Entry, for their encouragement every night during the writing of my thesis as well as helping me to remain grounded throughout graduate school. Special thanks to my sister Liza Lansita, my dear friend and lab mate Krisha Panchalingam, my best friend since childhood Tiffanie Treanor, and Michael Berg for always being there for me and believing in my ability to achieve my goals. I could not have completed this thesis without all of your help.

## List of Figures:

## Abbreviations:

**APS** -- Ammonium persulfate
**BrdU** -- 5-bromo-2-deoxyuridine
**BSA** -- Bovine serum albumin
**dA** -- 2'-deoxyadenosine
**DAPI** -- 4',6-diamidino-2-phenylindole
**dC** -- 2'-deoxycytidine
**dG** -- 2'-deoxyguanosine
**dI** -- 2'-deoxyinosine
**DNA** -- Deoxyribonucleic acid
**DNAse** -- Deoxyribonuclease
**dT** -- 2'-deoxythymidine
**dU** -- 2'-deoxyuridine
**EDTA** -- Ethyl diamine tetra-acetic acid
**FITC** -- Fluorescein isothiocyanate
**HH** -- Heavy-heavy DNA
**HL** -- Heavy-light DNA
**HPLC** -- High performance liquid chromatography
**IgG** --Iimmunoglobulin G
**LL** -- Light-light DNA
**M** -- molar
**7-Me-G** -- 7'-methyl-guanosine
**mM** -- millimolar
**NaCl** -- Sodium chloride
**nM** -- nanomolar
**NP-40** -- Nonidet® P40
**PBS** -- Phosphate buffered saline
**PI** -- Propidium iodide
**RIPA** -- Radioimmunoprecipitation buffer
**RNA** -- Ribonucleic acid
**RNAase A** -- Ribonuclease A
**SDS** -- Sodium dodecylsulfate
**TE** -- Tris (hydroxymethyl)-aminomethane and ethyl diamine tetra-acetic acid buffer
**TEM** -- Transmission electron microscopy
**TEMED** -- N,N,N',N'-Tetramethylethylenediamine
**TBS-T** -- Tris-Buffered Saline Tween-20
**Tm** -- DNA melting temperature
**Tris** -- Tris (hydroxymethyl)-aminomethane
**HCl** -- Hydrochloric acid
**UV** -- Ultra-violet